Palaeodrainage evolution of the large rivers of East Asia, and Himalayan-Tibet tectonics

Peng Zhang, Yani Najman, Lianfu Mei, Ian Millar, Edward R Sobel, Andrew Carter, Dan Barfod, Bruno Dhuime, Eduardo Garzanti, Gwladys Govin, et al.

Earth-Science Reviews 192 (2019) 601–630

Contents lists available at ScienceDirect

Earth-Science Reviews

journal homepage: www.elsevier.com/locate/earscirev

Palaeodrainage evolution of the large rivers of East Asia, and Himalayan-Tibet tectonics

Peng Zhang[a,b], Yani Najman[b,*], Lianfu Mei[a,*], Ian Millar[c], Edward R. Sobel[d], Andrew Carter[e], Dan Barfod[f], Bruno Dhuime[g,1], Eduardo Garzanti[h], Gwladys Govin[b,2], Giovanni Vezzoli[h], Xiaolin Hu[i]

[a] Key Laboratory of Tectonics and Petroleum Resources (China University of Geosciences), Ministry of Education, Wuhan 430074, China
[b] Lancaster Environment Centre, Lancaster University, Lancaster LA1 4YQ, United Kingdom
[c] NERC Isotope Geoscience Laboratory, BGS Keyworth, Nottingham NG12 5GG, United Kingdom
[d] Institute of Geosciences, Universität Potsdam, Karl-Liebknecht-Strasse 24-25, 14476 Potsdam-Golm, Germany
[e] Department of Earth & Planetary Sciences, Birkbeck, University of London, Malet Street, Bloomsbury WC1E 7HX, United Kingdom
[f] Argon Isotope Facility, SUERC, Rankine Avenue, East Kilbride G750QF, United Kingdom
[g] Bristol Isotope Group, School of Earth Sciences, University of Bristol, Wills Memorial Building, Queen's Road, Bristol BS8 1RJ, United Kingdom
[h] Department of Earth and Environmental Sciences, University of Milano-Bicocca, 20126 Milano, Italy
[i] Research Institute, China National Offshore Oil Corporation (CNOOC), Beijing 10027, China

ARTICLE INFO

Keywords:
Eastern Tibet
Palaeodrainage
Red River
Irrawaddy River
Yarlung Tsangpo
Central Myanmar Basin

ABSTRACT

Understanding the tectonics that gave rise to the formation of Tibet is critical to our understanding of crustal deformation processes. The unusual geomorphology of the drainage basins of East Asia's major rivers has been proposed to be the result of either (1) distortion and attenuation of antecedent drainages as India indents into Asia, which can therefore be used as passive strain markers of horizontal shear, or (2) due to fragmentation by river captures and flow reversals of an originally continental-scale drainage, in which the major East Asian rivers once flowed into the palaeo-Red River. If the latter hypothesis is correct, then it has been proposed that dating the drainage fragmentation constrains the timing of uplift of Tibet.

A number of sedimentary provenance studies have been undertaken in order to determine whether the palaeo-Red River was once a river of continental proportions into which the upper reaches of the Yangtze, Salween, Mekong, Irrawaddy, and Yarlung drained.

We have assessed the evidence that the Yarlung originally flowed into the palaeo-Red river, and then sequentially into the Irrawaddy and Brahmaputra, connecting to the latter first via the Lohit and then the Siang. For this river system, we have integrated our new data from the Paleogene-Recent Irrawaddy drainage basin (detrital zircon U-Pb with Hf and fission track, rutile U-Pb, mica Ar-Ar, bulk rock Sr-Nd, and petrography) with previously published data, to produce a palaeodrainage model that is consistent with all datasets. In our model, the Yarlung never flowed into the Irrawaddy drainage: during the Paleogene, the Yarlung suture zone was an internally drained basin, and from Neogene times onwards the Yarlung drained into the Brahmaputra in the Bengal Basin. The Central Myanmar Basin, through which the Irrawaddy River flows today, received predominantly locally-derived detritus until the Middle Eocene, the Irrawaddy initiated as a through-going river draining the Mogok Metamorphic Belt and Bomi-Chayu granites to the north sometime in the Late Eocene to Early Oligocene, and the river was dominated by a stable MMB-dominated drainage throughout the Neogene to present day. Existing evidence does not support any connection between the Yarlung and the Red River in the past, but there is a paucity of suitable palaeo-Red River deposits with which to make a robust comparison. We argue that this limitation also precludes a robust assessment of a palaeo-connection between the Yangtze/Salween/Mekong and the Red River; it is difficult to unequivocally interpret the recorded provenance changes as the result of specific drainage reorganisations. We highlight the palaeo-Red River deposits of the Hanoi Basin as a potential location for future research focus in view of the near-complete Cenozoic record of palaeo-Red River deposits at this location.

* Corresponding authors.
E-mail addresses: y.najman@lancaster.ac.uk (Y. Najman), lfmei@cug.edu.cn (L. Mei).
[1] Present address: CNRS-UMR5243, Géosciences Montpellier, Université de Montpellier, 34095 Montpellier Cedex 05, France.
[2] Deceased.

https://doi.org/10.1016/j.earscirev.2019.02.003
Received 18 July 2018; Received in revised form 31 January 2019; Accepted 5 February 2019
Available online 15 February 2019

A majority of previous studies consider that if a major continental-scale drainage ever existed at all, it fragmented early in the Cenozoic. Such a viewpoint would agree with the growing body of evidence from palaeoaltitude studies that large parts of SE Tibet were uplifted by this period. This then leads towards the intriguing question as to the mechanisms which caused the major period of river incision in the Miocene in this region.

1. Introduction

Fluvial systems react rapidly to tectonic events (e.g. Whipple and Tucker, 1999) and therefore palaeodrainage changes are often used to shed light on the tectonic evolution of an area (e.g. Davis et al., 2010; Castelltort et al., 2012). This approach to determination of the tectonic history of a region is especially pertinent where other methods are less successful, for example, where metamorphic rocks which may permit documentation of a chronology of tectonic events, are scarce. SE Tibet provides such a region.

The Himalayan-Tibetan orogen is a type example of crustal deformation processes. Knowledge of the timing and mechanisms responsible for the uplift of SE Tibet is important to models which aim to explain the evolution of the region. Yet the evolution of SE Tibet is still poorly defined. Estimates for the timing of attainment of high elevation range from Paleocene-Eocene to Middle to Late Miocene based on stable isotope palaeo-elevation studies (e.g. Hoke et al., 2014; Li et al., 2015), and low-temperature thermochronological records of river incisions (e.g. Clark et al., 2005; Yang et al., 2016).

An alternative approach to documenting the tectonics of the region involves the interpretation of the palaeodrainage evolution of the main rivers which flow from the SE margin of the plateau. Following from the early work of Brookfield (1998), Hallet and Molnar (2001) proposed that the large river drainages in the region are antecedent, and their unusual geometries are the result of tectonic deformation by horizontal shear. By contrast, Clark et al. (2004) proposed that the drainage configuration is the result of various river captures and drainage reversals away from a previous continental-scale drainage, the timings of which could be used to constrain when surface uplift of Tibet, proposed to occur due to crustal flow, took place.

In order to test these hypotheses, it is necessary to determine whether such drainage reorganisation occurred. In this paper we (1) review the available evidence for the various proposed capture events relating to the upper Yangtze, Mekong, Salween, Red, Yarlung, Irrawaddy headwaters, and Brahmaputra Rivers; (2) add new data to the existing dataset regarding the proposed Yarlung-Irrawaddy-Red river system for which interpretations are currently particularly diverse, and integrate these data to produce a new palaeodrainage model which is consistent with all available material; (3) conclude by assessing the extent to which the river capture model can be used to document east Tibetan Plateau tectonics, with suggestions for how future investigations might consider the hypothesis further.

2. Use of palaeodrainage studies to constrain the tectonics of the eastern Himalayan-Tibet region

Hallet and Molnar (2001) noted that the upper Salween, upper Mekong, and upper Yangtze have unusual drainage basin morphologies in terms of their width:length ratio, close proximity to each other and parallel spacing (Fig. 1A). They proposed that this morphology is the result of extreme attenuation of these antecedent basins, due to their distortion by horizontal shear, subsequent to India-Asia collision. They thus can be used as passive markers of crustal strain (Fig. 2).

By contrast, Clark et al. (2004) proposed that the unusual geometries of these drainage basins can be ascribed to various river captures. The SE margin of Tibet is a gently tilted high-elevation, low relief margin (Fig. 1A and B), commonly interpreted as a relict landscape uplifted by lower crustal flow (cf Yang et al., 2015; Cao et al., 2018). Clark et al. (2004) reconstructed the region's palaeodrainage, such that the headwaters of the upper Yangtze, upper Mekong, upper Salween, and Yarlung Tsangpo were once all tributaries of the palaeo-Red River (Fig. 1B). This reconstructed fluvial network was an integrated “Mississippi-type” continental-scale drainage system, which typically forms in low-relief settings, and that was subsequently fragmented by various drainage captures and flow reversals as uplift commenced (Fig. 1C and D). Clark et al. (2004) therefore proposed that the timings of these river captures constrain the timing of eastern Tibetan uplift, and that the fluvial geomorphologies are a reflection of the surface uplift rather than horizontal shear in the region.

Further interest lies in the case of one of the proposed captures, that of the Yarlung Tsangpo, which Clark et al. (2004) proposed may have successively flowed into the palaeo-Red River, Irrawaddy, Lohit, and finally the Brahmaputra (Fig. 3). It is this final capture of the Brahmaputra that, in the model of Zeitler et al. (2001), may have caused the unusually rapid exhumation of the Eastern Himalayan syntaxis, by rapid incision weakening the crust resulting in a “tectonic aneurism”, thus providing a type example of tectonic-erosion coupling.

The drainage model of Clark et al. (2004) is based largely on an assessment of geomorphic evidence. Yet does the wealth of provenance studies subsequently undertaken in the region support their hypothesis? Our review and assessment of this evidence forms the focus of this paper, bringing together various published work with previously unpublished material to form new palaeodrainage models where the data permit.

3. Documenting river captures within the eastern Asian large river basins from their sedimentary repositories

Much work to test the integrated drainage model of Clark et al. (2004) has focused on provenance analyses in the major rivers' sedimentary repositories, with the assumption that observed changes in provenance within a sedimentary succession reflect river captures, when headwaters flowing through rocks of a different geochemical or isotopic signature to rocks of the downstream reaches were removed from or added to the drainage basin. A caveat to this approach is that there must be distinct differences in the characteristics of the rocks that comprise the regions making up the drainage basins above and below the proposed point of capture, in order for any river capture to be detectable in the sedimentary record. Furthermore, if analyses from modern river sediments are being used to provide source region characterisation, potential changes between the modern and ancient river's signature should be taken into account. Additionally, changes in provenance may reflect upstream tectonism, unrelated to river captures.

3.1. Sedimentary records in the Red, Salween, Mekong, and Yangtze drainage basins and their offshore repositories

Today the Red River, Mekong, and Salween drain overall southeastward from the gently sloping high-elevation low-relief interpreted “relict landscape” of eastern Tibet, to the South China Sea and Andaman Sea, respectively (Fig. 1A). The studies summarised below focus around the region of the continental-scale drainage model that suggests that the upper reaches of the Yangtze, Mekong, and Salween originally connected to the Red River at the “First Bend” (Fig. 1A and B). Early provenance work (Clift et al., 2004, 2006a,b; Hoang et al., 2009; Yan et al., 2011, 2012) predominantly used bulk rock Sm-Nd and

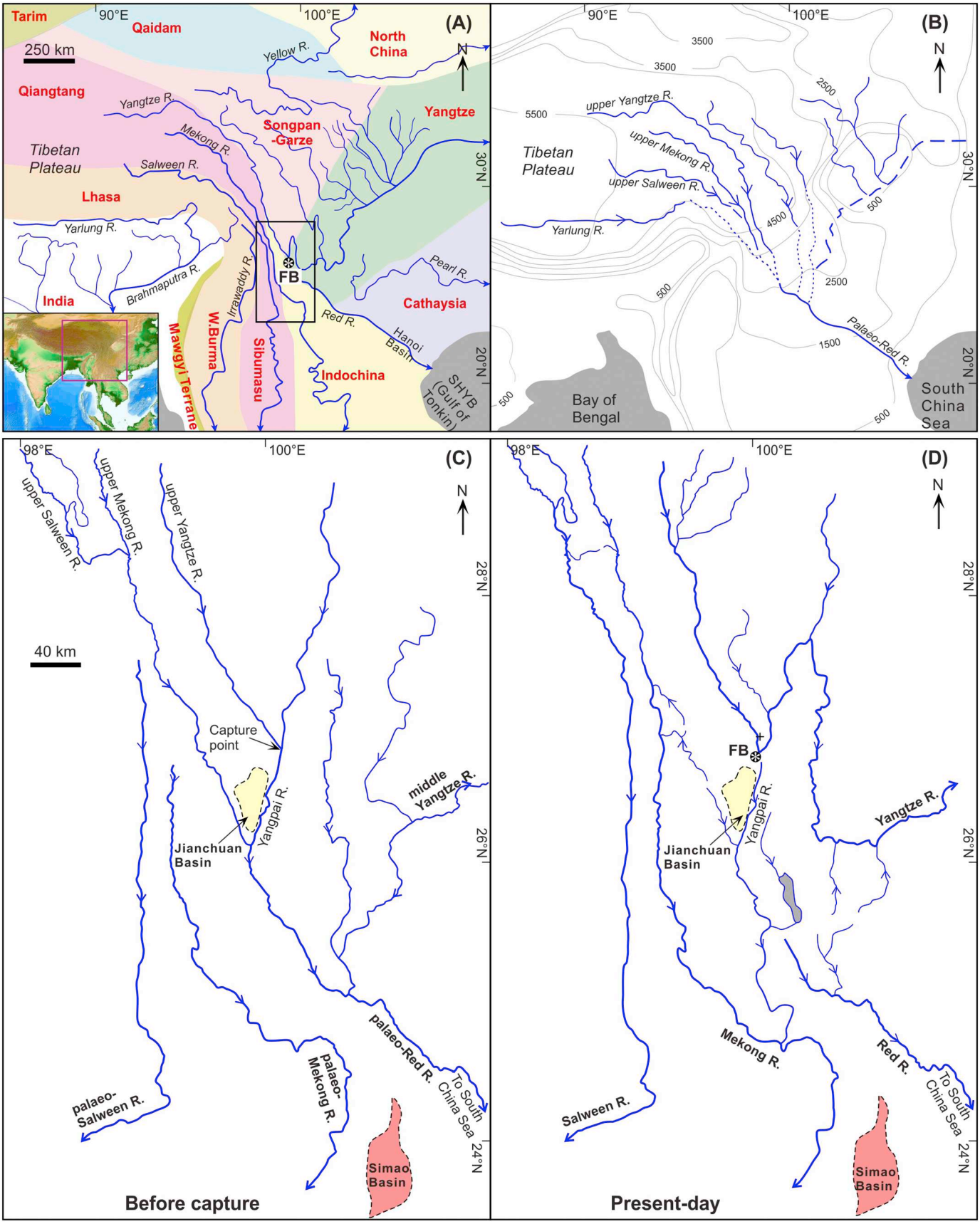

(caption on next page)

Fig. 1. (A) Modern day drainage of East Asia showing the unusually closely-spaced geometry of the Yangtze, Salween and Mekong in their middle reaches, superimposed on the tectonic units of the region. Contours are in metres. Figure modified from Clark et al. (2004) with tectonic unit boundaries compiled from a number of sources, including Zhang et al. (1985), Metcalfe (1996), and Pan et al. (2012). Box shows the location of Fig. 1C. (B) Proposed reconstructed drainage, from Clark et al. (2004), with the upper reaches of the Yangtze, Salween, Mekong, Irrawaddy headwaters and Yarlung flowing into the palaeo-Red River, forming a continental-scale drainage network. (C-D) Detail of the proposed river capture and drainage reversal at the "First Bend" in the Yangtze. FB = First Bend; SHYB = Song Hong-Yinggehai Basin.

detrital zircon U-Pb analyses to detect changes in provenance, alongside some use of Pb isotopes in K-feldspar. Later work saw a plethora of papers focussed on the use of detrital zircon U-Pb ages, as summarised by Wissink et al. (2016).

3.1.1. The proposed upper Yangtze to palaeo-Red River connection

Provenance evidence from the offshore repository of the Song Hong-Yinggehai Basin (SHYB, also known as the Gulf of Tonkin; Fig. 1A), into which the Red River debouches, takes the form of detrital zircon U-Pb ages, K-feldspar Pb isotope data, and bulk rock Sm-Nd analyses.

Away from the influence of Hainan Island (e.g. Yan et al., 2011), detrital zircon U-Pb age spectra from the western SHYB Miocene-Quaternary samples show, for the most part, good similarity to the modern Red River (e.g. Wang et al., 2014a, 2016, 2019; Cao et al., 2015; Xie et al., 2016a) (Fig. 4). This led Wang et al. (2014a) to consider that if capture of the upper Yangtze away from the Red River ever occurred it must have taken place prior to the Miocene which is the oldest sample analysed. However, Fig. 4B shows that some western SHYB samples show greater similarity to the upper Yangtze. Furthermore, a mixture between an upper Yangtze signature and a lower Red River signature, which would provide a more realistic signal for an ancient connected upper Yangtze–Red River at its river mouth, will plot between these two end members, directly comparable to the majority of the western SHYB samples. Therefore, we do not consider the conclusion of Wang et al. (2014a) to be robust.

Clift et al. (2004) carried out detrital K-feldspar Pb isotopes analyses and bulk rock Sm-Nd analyses from Eocene samples from the SHYB. They reported two K-feldspar grains from the Eocene sedimentary rocks with signatures that were unlike any known from the modern Red River drainage. Additionally, by comparing their εNd data from the Eocene samples with modern day εNd values from the Red River, they showed that Eocene values were less negative compared to the Red River today. From this information they interpreted that the palaeo-Red River was previously connected to a drainage basin which included a region with more juvenile younger crust, in the Eocene. However, later work from the Hanoi Basin (Fig. 1A) onshore Red River sediment repository contrasts with this work: Clift et al. (2008) and Zhang et al. (2017a) compared detrital K-feldspar Pb isotope data from Eocene-Miocene rocks of the Hanoi Basin with data from modern sediments from rivers that are proposed to have once drained into the palaeo-Red River. Based on the partial lack of overlap of signature between the modern upper Yangtze River and the palaeo-Red River sedimentary rocks (the region outlined by the dashed line ovals in Fig. 5), both studies concluded that there was no connection between the upper Yangtze, and the palaeo-Red River, from Eocene times onward. Furthermore, Clift et al. (2008) noted the occurrence of rare grains in an Eocene sample with signatures that would be consistent with Yangtze Craton bedrock over which the middle Yangtze flows. Whilst Clift et al. (2008) interpreted these data to suggest a connection between the palaeo-Red River and the middle Yangtze in the Eocene, those authors also note that grains of such signature are also found in the modern Red River, making the interpretation non-unique.

Clift et al. (2006a) also analysed mudstones from the Hanoi Basin for Sm-Nd. Their work showed a shift to less negative εNd values between ~25–35 Ma (Fig. 6) which they interpreted as due to loss of the contribution of the older cratonic middle Yangtze drainage to the Red River basin due to river capture and drainage reversal (Fig. 1). The apparent dichotomy with Clift et al. (2004) (see above) can be explained by the fact that the earlier paper made the comparison utilising modern Red River samples from sites considerably further upstream than the 2006 sites, and the values evolve to a less negative signal downstream. Thus, in fact, there is no difference in εNd values between the modern downstream Red River sediments and the Eocene sedimentary rocks from the SHYB. Since this calls into question the interpretation of Clift et al. (2004), we focus on the shift in εNd values observed by Clift et al. (2006a) between ~25 and 35 Ma in the Hanoi Basin, which they interpret as the timing when the middle Yangtze reversed its flow away from the Red River. We note that there is a significant difference between the εNd values of coeval (Eocene) samples in the Hanoi Basin and SHYB, suggesting a non-identical provenance. This might be explained by the significant and spatially variable additional input to the SHYB (Wissink et al., 2016) from sources such as Hainan Island and the Vietnam coastal regions (Yan et al., 2011; Wang et al., 2014a, 2016, 2019; Cao et al., 2015; Zhao et al., 2015; Jonell et al., 2017), as discussed above and illustrated in Fig. 4B and Fig. SI of Supplementary material 1, making the sedimentary record of this offshore basin much more complex to interpret.

Considering further the onshore repositories, Hoang et al. (2009) considered that the zircon U-Pb with Hf data from the tentatively dated upper Miocene sandstones from the Red River catchment of the Hanoi Basin strongly resembled the signature from the modern Red River (Fig. 4C, panel III). This would indicate that the river was largely in its modern form by the Late Miocene, assuming depositional ages are correct. However, comparison of the modern upper Yangtze field with the modern lower Red River field (Fig. 4C, panel I) shows a good degree of similarity, and it could be considered that the degree of overlap between the upper Miocene Hanoi Basin palaeo-Red River sedimentary rocks and the modern upper Yangtze field (Fig. 4C, panel II), is similar to the degree of similarity between the Hanoi Basin upper Miocene sedimentary rocks and the modern Red River (Fig. 4C, panel III). Comparison of U-Pb ages alone, for which there are more data, is more instructive. The MDS plot (Fig. 4B), which shows the upper Miocene Hanoi Basin palaeo-Red River data plotting closer to the modern Red River than to the upper Yangtze or any upper Yangtze-Red River composite, is consistent with the proposition of Hoang et al. (2009).

Further upstream, Yan et al. (2012) analysed detrital zircons from the Jianchuan Basin that lies just downstream of the Yangtze's First Bend (Fig. 1C and D). This basin is considered to be the region through which the upper Yangtze would have flowed during the period of its proposed connection with the palaeo-Red River (Clark et al., 2004). The Jianchuan Basin sedimentary rocks were previously considered to span from Paleocene to Pliocene, but recent work shows that the bulk of the rocks extend no younger than the Eocene (Gourbet et al., 2017). Reassessment of previous interpretations is therefore provided below in light of these new age constraints. Clark et al. (2004) considered that the facies of the Eocene Baoxiangsi Formation represented a major fluvial environment, thus potentially an ancient connected upper Yangtze-Red River. The Baoxiangsi Formation is now constrained to > 35 Ma from U-Pb zircon dating of a cross-cutting dyke (Gourbet et al., 2017). Yan et al. (2012), noted a change in the zircon U-Pb detrital age spectrum between the lower Baoxiangsi Formation (sample JSJ15 on Fig. 7), and the overlying units (JSJ18, JC13, JC18 of Fig. 7), now dated at Middle Eocene (ca. 35 Ma, on the basis of interstratified tuffs or volcaniclastics; Gourbet et al., 2017). Based on the similarity of the detrital zircons age spectrum of the Baoxiangsi Formation sample with that of the Songpan-Garze bedrock, Yan et al. (2012) interpreted

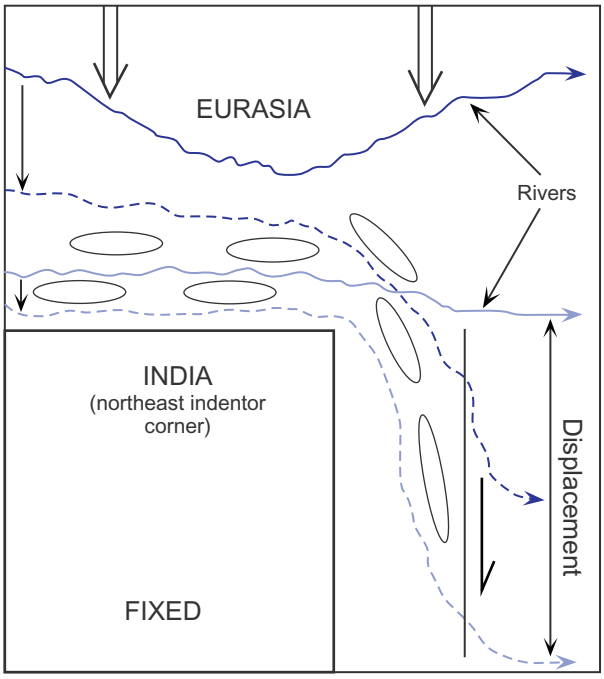

Fig. 2. Schematic representation of the hypothesis of Hallet and Molnar (2001), fixed relative to India, showing that for a parcel of crust just north of the Eastern Himalayan syntaxis, the dominant strains will first be largely compressive, in a direction radial to the syntaxis and then display roughly north-south right-lateral shear as it moves south of the syntaxis. Initial and final positions of the rivers are shown as solid and dotted lines, respectively. Ellipses represent the magnitude and direction of the crustal strains.

the Baoxiangsi Formation fluvial facies as derived from a major river draining the Songpan-Garze terrain to the NE (Fig. 1A); they did not however consider this river to be the upper Yangtze headwaters, since they considered that the Baoxiangsi Formation zircon age spectrum was a better match to the Songpan-Garze bedrock spectrum rather than to the upper Yangtze spectrum (Fig. 7A). Up-section, they interpreted the shift in provenance (Fig. 7B) as due to drainage reorganisation and influx of material from the Yangtze Craton. Additional data from Wissink et al. (2016) also recorded this provenance change (Fig. 7).

However, in contrast to the interpretation of Yan et al. (2012), Gourbet et al. (2017) noted the similarity in timing of this provenance shift with the 25–35 Ma change in εNd values in the Hanoi Basin, as described above, and therefore considered that the change in detrital zircon provenance by ~35 Ma in the Jianchuan Basin might indeed relate to beheading of the upper Yangtze from the palaeo-Red drainage, with locally-derived material deposited in the basin thereafter. A visual comparison of the data illustrated in Fig. 7A agrees more with Yan et al. (2012); the lower Baoxiangsi Formation sample displays a greater similarity with Songpan-Garze bedrock rather than with the upper Yangtze both in terms of its pronounced 1900 Ma peak and lack of grains dated < 200 Ma. Fig. 7B is equivocal in this respect. Thus, a shift from a major axial river to locally-derived facies by 35 Ma is concurred, but whether this represents river capture of the upper Yangtze remains disputed.

Downstream from the Jianchuan Basin, some of the Paleocene-upper Eocene deposits of the Denghei Formation of the Simao Basin (Fig. 1C and D), provide a better match to the upper Yangtze (Fig. 7B), particularly in terms of the lack of pronounced ~1900 Ma peak and presence of grains < 200 Ma. Chen et al. (2017) made a composite spectrum from three samples from Denghei Formation of braided fluvial facies, and a second composite spectrum from three samples from the overlying upper Eocene – Oligocene Mengla Formation of alluvial fan and braided facies. Comparing these spectra with each other, and from

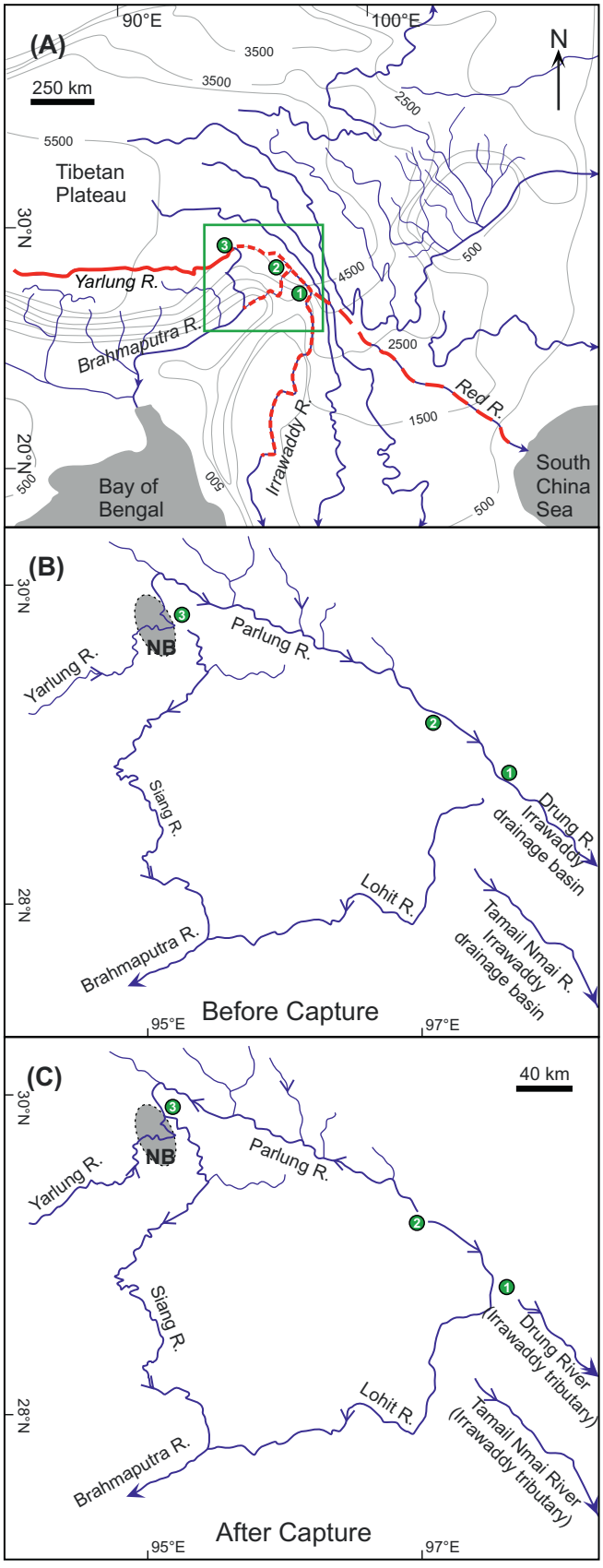

(caption on next page)

Fig. 3. Proposed reconstruction of the Yarlung-Irrawaddy-Red river palaeo-drainage (after Clark et al., 2004): (A) Overview of the suggested successive captures and reversals (circles labelled 1–3) of the Yarlung River from the palaeo-Red River by the Irrawaddy River, and most recently by the Brahmaputra River via the Lohit and then Siang Rivers, in the area of the Eastern Himalayan syntaxis. Red dashed line indicates the original path of the Yarlung River into the Red River; red dotted line indicates the path of the Yarlung River into the Irrawaddy drainage. Green box in panel A shows location of figures in panel B and C. (B) and (C) gives detail of the final major capture: prior to capture (B), the palaeo-Yarlung River flowed into the Irrawaddy River through the Parlung (shaded area represents the topographic expression of the Namche Barwa massif (NB) of the Eastern Himalayan syntaxis); (C) the Yarlung River flows into the Brahmaputra, first via the Lohit and then via the Siang.

spectra from approximately coeval samples from the Jianchuan Basin and potential source regions, they suggested that a palaeo-Yangtze river flowed through both basins until ca. 35 Ma, after which time deposits were locally derived. Fig. 7B, in which the samples that comprised the compiled spectra are represented separately, verifies the provenance shift, although with some variation as to the degree to which samples both above and below the provenance shift resemble the upper Yangtze.

In order for the sedimentary repositories in both the Jianchuan and Simao basins to be used to their full potential and interpreted with more clarity, attention should be paid to: (1) further work to construct a more detailed determination of the formations' depositional ages, particularly for the Simao Basin; (2) collection of more detrital zircon U-Pb data from different facies within the formations, to determine the extent to which an axial river may still be in evidence, even when transverse input is recorded from samples (e.g. compare Jian-11-06 with Jian-11-18 in Fig. 7B, panel II) and (3) consideration of the extent to which natural variation and/or local tectonics may affect a river's characteristic signature, and thus (a) whether relatively small shifts in signal, as for example seen in the Simao Basin, do indeed reflect the end of the proposed flow of the ancient upper Yangtze through this region and (b) whether the degree of dissimilarity between the upper Yangtze and Songpan-Garze signatures is sufficient to discriminate between them, once natural variation is taken into account.

3.1.2. The proposed connection of the Salween and Mekong with the palaeo-Red River

Whilst the Yangtze, with its contorted drainage pattern, makes the most convincing candidate for capture from the palaeo-Red River, nevertheless the upper Salween and upper Mekong Rivers are proposed to be part of the original Mississippi-style continental drainage feeding into the palaeo-Red River, in the model of Clark et al. (2004) (Fig. 1B and C). In this model, those authors speculate that the upper Salween may have once been a tributary of the upper Mekong, which joined the palaeo-Red River in the region of the Yangtze's First Bend (Fig. 1C). The Salween and Mekong are therefore considered together below.

Fig. 5A shows that whilst the Salween is indistinguishable from the modern Red River in terms of Pb isotopic composition of K-feldspar, the modern Mekong has K-feldspars with Pb isotope characteristics more radiogenic than found in the modern day upper Yangtze, Red or Salween Rivers (Bodet and Schärer, 2001; Clift et al., 2008; Zhang et al., 2017a). The fact that such distinctive grains are not found in the Eocene-Miocene palaeo-Red River deposits of the Hanoi Basin (Fig. 5B), could be taken to indicate that the upper Mekong was not connected to the Red River during the Eocene-Miocene (see also discussion in Clift et al., 2008). Nevertheless, a strong reservation against this interpretation is that the location of the two modern Mekong samples used to characterise the river's headwater signature are downstream of the capture point (Fig. SI; Supplementary material 1) as proposed by Clark et al. (2004), and thus the distinctive radiogenic feldspars could conceivably have come from bedrock over which the river flowed in this downstream region, rather than in the upstream Mekong headwaters. If that were the case, an ancient connection of the upper Mekong to the

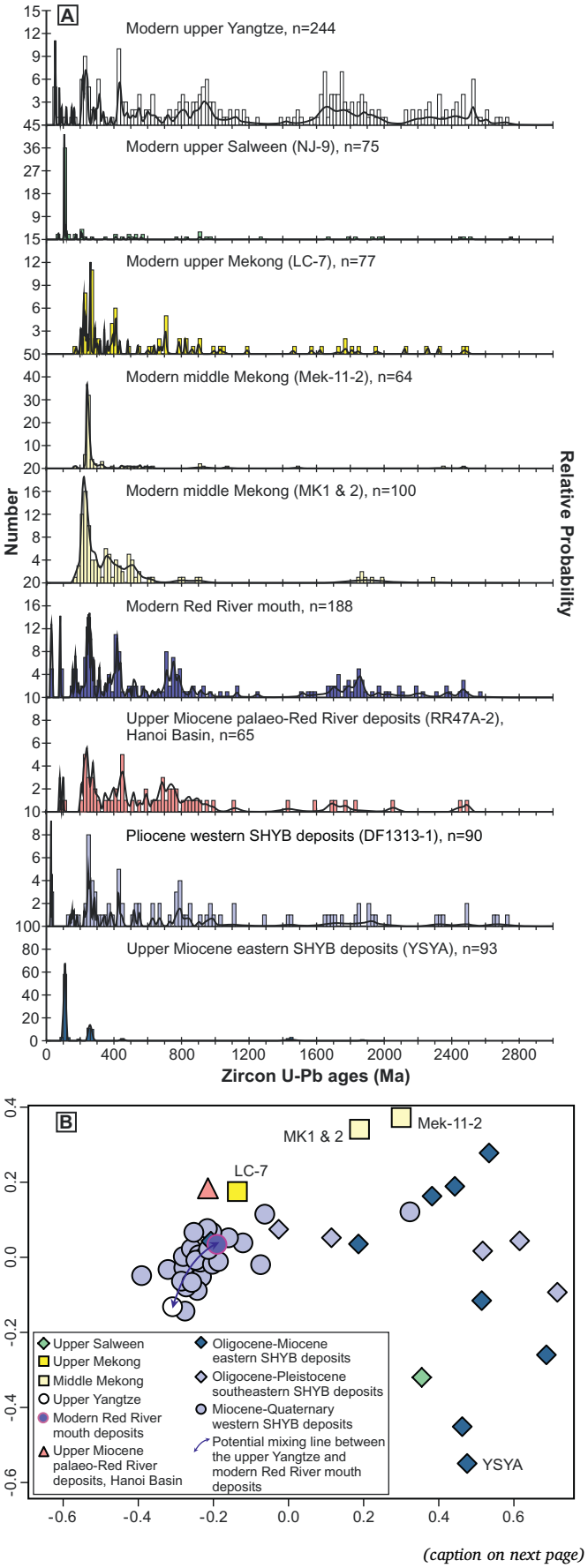

(caption on next page)

Fig. 4. Detrital zircon U-Pb data (A and B) and zircon U-Pb with Hf data (C), from onshore (Hanoi Basin) and offshore (Song Hong-Yinggehai Basin, SHYB) of the palaeo-Red River deposits compared to various modern rivers. Part label B shows that Cenozoic samples from the eastern and southeastern parts of the SHYB, which are close to Hainan Island, show little similarity to the modern Red River signature, but samples from the western part of the basin plot close to the modern Red River (geographical locations of the various samples in the SHYB are shown in Fig. SI of Supplementary materials 1). Nevertheless, some of these western SHYB samples plot close to the modern upper Yangtze, and most of the SHYB samples could be well described by a mix of these two endmember sources (mixing line shown by blue double sided arrow) which would well represent an ancient connected upper Yangtze-Red river signature at its mouth. See Section 3.1.1 for further discussion. All SHYB sample data are plotted on part label B, but only two representative samples, representing eastern and western SHYB are shown on part label A. Comparison is also made between the onshore and offshore palaeo-Red River deposits and the Mekong and Salween. Attendant discussion is given in Section 3.1.2. In panels IV and V of part label C, data from the modern Mekong and Salween below the proposed capture point (FB, "First Bend" of Fig. 1) are included, for the sake of completeness only. Such grains may not be derived from the headwaters and therefore cannot be considered to be characteristic of headwater signature, with certainty.
Data taken from Bao et al. (2015), Bodet and Schärer (2000), Cao et al. (2015), Chen et al. (2014), Chen (2015), Clift et al. (2006b), He et al. (2013), Hoang et al. (2009), Lin et al. (2017), Wang et al. (2014a, 2016, 2019), Wissink et al. (2016), Xie et al. (2016a), Yan et al. (2012) and Yang et al. (2012). Part label B was plotted using *IsoplotR* (Vermeesch, 2018).

Red River would not be detectable by this method in the palaeo-Red sedimentary record. The concern that these radiogenic feldspars are locally-sourced by rocks downstream of the proposed capture point is heightened by the fact that (1) the sample locations are downstream of the point where the river flows from the Qiangtang Block of its headwaters, to the Indochina Block (Fig. 1A) and thus this new terrain may be providing the source, and (2) of these two modern Mekong samples analysed, the more downstream sample is the only sample of the pair to contain these distinctive grains (Fig. 5A; compare "Mekong upstream" with "Mekong downstream" sample). Thus, there is a strong possibility that this signature is characteristic of the Indochina Block rather than the Qiangtang Block over which the Mekong headwaters flow.

Comparison of zircon U-Pb age spectra of the modern Mekong with the Miocene and modern Red River deposits, led Hoang et al. (2009) to suggest that the upper Mekong was not connected to the palaeo-Red River since the Miocene. This conclusion was based on their consideration that the 200–240 Ma zircon population in the Mekong samples is much less significant in the Red River deposits. However, the Mekong samples used by Hoang et al. (2009) were located considerably below the proposed capture point of the First Bend (samples MK1 and MK2 located in Fig. SI, Supplementary material 1). Since that publication was written, a sample from the upper Mekong, more appropriate for such a comparison, has been analysed (Fig. 4). A Mekong sample taken from just above the First Bend (LC-7, Chen et al., 2014) has a signature much more similar to the Miocene palaeo-Red River deposits (Fig. 4A and B). Therefore, in light of these new data, we consider Hoang et al.'s (2009) conclusion to be invalidated, and that more data are needed to better characterise the signal from the upstream Mekong before robust interpretations can be made. The same caveat applies to a comparison with the offshore palaeo-Red River deposits of the western SHYB; nevertheless, based on the available Mekong dataset, the majority of western SHYB samples plot closer to the modern Red River than the upper Mekong (Fig. 4B).

Zircon ages combined with Hf values are also ambiguous (Fig. 4C). Hoang et al. (2009) considered that the Miocene palaeo-Red River deposits lacked a match with the older components recorded in the Mekong (Fig. 4C, panel IV) and Salween (Fig. 4C, panel V) rivers, which could potentially be suggestive of a lack of Mekong/Salween-Red connection in the Miocene. We consider that the degree of proposed mismatch between the Miocene palaeo-Red River deposits and the Salween and Mekong, is similar to the degree of mismatch with the modern lower Red River, in terms of detrital zircon U-Pb versus Hf signature (Fig. 4C) and therefore no robust conclusions based on provenance discrimination can be drawn.

Sm-Nd analyses of samples which span the Neogene from the southwestern South China Sea show a shift in εNd values towards values similar to the modern Mekong at 8 Ma (Liu et al., 2017). Whilst it may be tempting to interpret the change at this time as the result of river capture away from the Mekong's previous drainage into the palaeo-Red, Liu et al. (2017) interpret the change to result from the river's avulsion away from the Gulf of Thailand at that time, consistent with seismic data from the region. Such an interpretation is in agreement with low-temperature thermochronological data that indicate that the upper to lower Mekong (and probably also the Salween) was in its current position since at least Mid Miocene times (Nie et al., 2018). Conversely, it is at variance with a provenance study that proposes the Mekong River propagated north-west since the Oligo-Miocene (Hennig et al., 2018); however, the study by Hennig et al. is based on a sediment record that, in view of the above-mentioned seismic evidence of only relatively recent avulsion of the Mekong to their study area, was likely not the palaeo-Mekong.

Summarising Sections 3.1.1 and 3.1.2, we concur with Wissink et al. (2016), who compiled a large body of detrital U-Pb data for the region, and concluded that "Without a definitive smoking gun, which includes detrital samples of the SHYB [Gulf of Tonkin] containing zircon or other geochemical signatures that can only be derived from outside of the modern Red River catchment, and contemporaneous, large-fluvial deposits of the SE margin containing the corresponding detrital signature, it is difficult to support the notion of a Yangtze-Red River connection". We agree with this assessment, for both the upper Yangtze, and the Mekong and Salween, yet Wissink et al.'s work mainly summarised detrital zircon U-Pb spectra. We posit that there is currently an over-reliance on provenance studies using detrital zircons to research the question. Other analytical techniques which may result in better discrimination between potential source areas might be more fruitful: The shift in εNd values recorded in the Hanoi Basin (Fig. 6), suggests drainage reorganisation involving the middle Yangtze may have begun in the latest Eocene-Oligocene. However, being a bulk rock technique, it suffers from dilution of signal downstream which can be difficult to deconvolve. A single grain technique such as Pb isotopes on feldspars, as recently demonstrated by Zhang et al., 2014b, Zhang et al., 2017a) may hold more clues.

3.2. Sedimentary repositories in the Central Myanmar Basin, Bengal Basin, and Bengal Fan

Whilst the upper Yangtze, upper Mekong and upper Salween proposed palaeo-tributaries of the palaeo-Red River today drain south and east to the South China, East China, and the Andaman Sea, the Yarlung Tsangpo proposed palaeo-tributary to the palaeo-Red River today drains south to the Bay of Bengal. The modern Yarlung Tsangpo flows east along the India–Asia Yarlung suture zone in southern Tibet, then abruptly bends southward across the Eastern Himalayan syntaxis before eventually draining into the Bay of Bengal (Fig. 1). According to Clark et al. (2004) it may have initially successively drained into the palaeo-Red River, palaeo-Irrawaddy drainage of the Central Myanmar Basin, and then finally into the Brahmaputra drainage, possibly routing first through the Lohit and then the Siang (Fig. 3).

3.2.1. Evidence for the Yarlung Tsangpo draining into the palaeo-Red River

Clark et al. (2004) proposed a possible palaeo-connection of both the Yarlung Tsangpo and the upper Irrawaddy headwaters, to the palaeo-Red River.

Clift et al. (2004) compared the εNd values from Eocene samples from the SHYB (average values ca. -10) to bedrock arc units of the Indus-Yarlung Suture Zone (positive values) and concluded from this

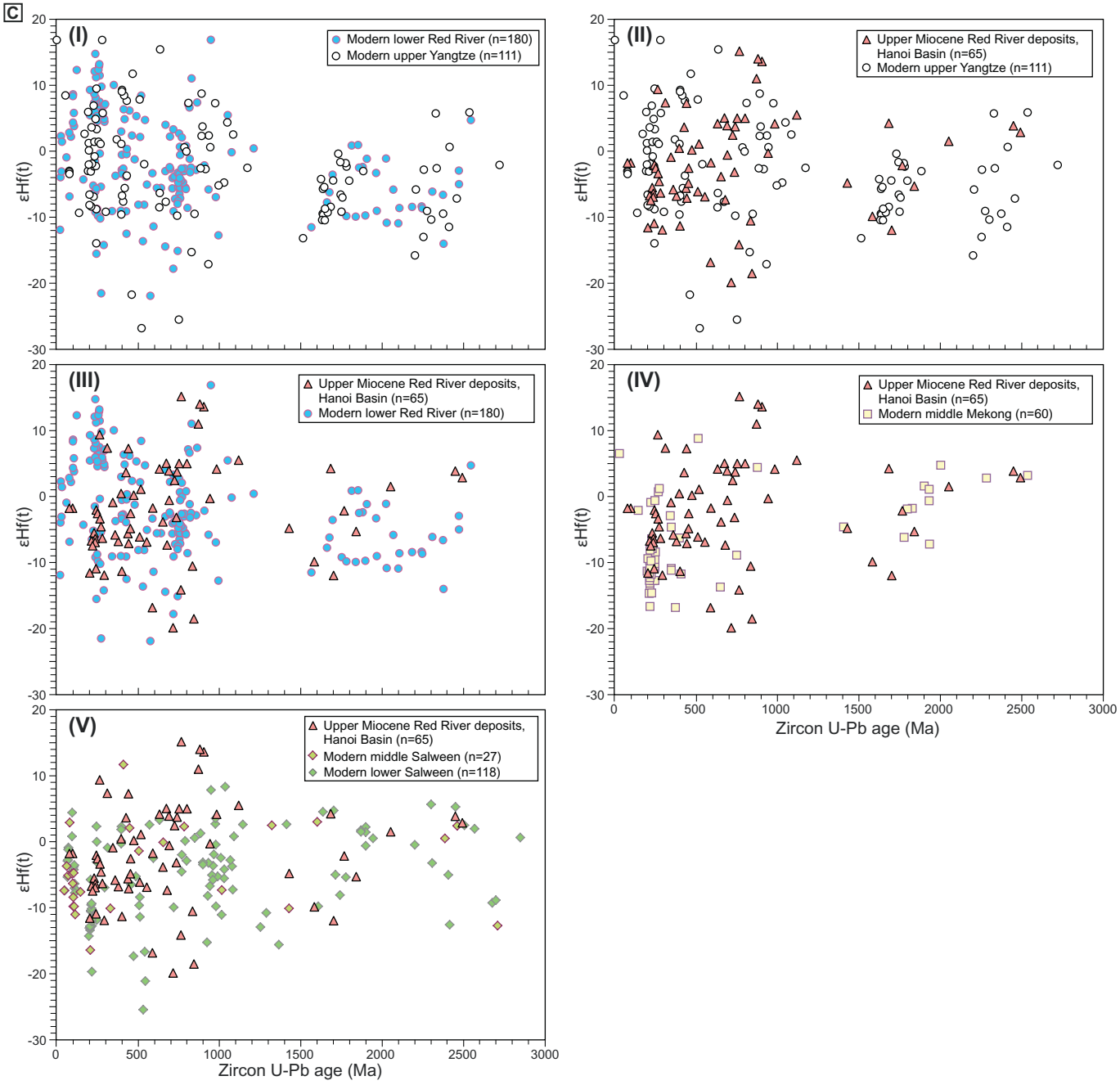

Fig. 4. (*continued*)

that the Yarlung Tsangpo did not flow into the palaeo-Red River, at least not during the Eocene. However, the positive values used for comparison by Clift et al. (2004) are not representative of the values of the Yarlung River, which is also fed by more crustal detritus from the Indian plate to the south of the suture zone as well as the Lhasa Block, to the north (Fig. 1A). εNd values from modern day sediment from the Yarlung Tsangpo are ca. -10 (Singh and France-Lanord, 2002), in fact very similar to Eocene values from the SHYB. However, as discussed in Section 3.1.1, εNd values between Eocene sedimentary rocks of the SHYB and onshore Hanoi Basin (εNd ca. -17; Fig. 6) are quite different, and those from the Hanoi Basin are likely to more faithfully represent the palaeo-Red River signature. εNd values from the Eocene Hanoi Basin deposits are more negative compared to those from the modern Yarlung Tsangpo. This difference does not necessarily negate the argument for a palaeo-connection however, since one might expect that downstream contribution from tributaries would affect a bulk rock signal; the lower reaches of the Red River flow along the boundary of the Indochina terrain (Fig. 1A) with εNd values which extend to ca. –20 (Clift et al., 2006a). Therefore, we do not consider the comparison robustly negates or confirms a possible connection between the Yarlung Tsangpo and the palaeo-Red River in the Eocene.

Use of a single grain technique, where a characteristic upstream signature is easier to recognise in a diluted downstream repository, proves more instructive. Hoang et al. (2009) noted dissimilarity of signature between the upper Miocene palaeo-Red deposits of the Hanoi Basin and a modern Irrawaddy River sample collected from the river's middle reach, in terms of zircon U-Pb age versus εHf value. Taking the middle Irrawaddy River sample's signature as characteristic of the Irrawaddy headwaters, they therefore interpreted that the headwaters did not drain into the palaeo-Red River during this period. We built on this approach to include data now available from the Irrawaddy headwaters, which make a more appropriate comparison, and data

from the source regions of the Yarlung Tsangpo. Fig. 8A shows that the ~50 Ma zircon U-Pb age peak typical of the Yarlung Tsangpo and Irrawaddy headwaters is not present in the upper Miocene palaeo-Red River deposits of the Hanoi Basin, indicating that a connection was not present at that time. Zircons aged ~50 Ma are also uncommon in the Neogene sedimentary rocks of the western SHYB (Section 3.1.1; Fig. 4A). Furthermore, whilst the depositional age of the Paleocene-Eocene sedimentary rocks of the proposed palaeo-Red sedimentary rocks of the Jianchuan and Simao Basins (Section 3.1.1) precludes them containing ~50 Ma zircons, these deposits also show a lack of grains dated back to 100 Ma, which is also typical of the Tsangpo and Irrawaddy headwaters (Fig. 8). Thus, in all studied potential palaeo-Red repositories, there is no evidence of a palaeo-Yarlung or upper Irrawaddy headwater connection with the palaeo-Red River.

3.2.2. *Evidence of the Yarlung Tsangpo draining into the palaeo-Irrawaddy River*

The Irrawaddy today flows along the Central Myanmar Basin (CMB) (Fig. 9). The CMB is a predominantly Cenozoic forearc-backarc basin, split by the Western Myanmar Arc (WMA) (Pivnik et al., 1998; Bertrand and Rangin, 2003). The basin is divided into a series of sub-basins, of which the main ones are the forearc Chindwin sub-basin in the north, forearc Minbu sub-basin to its south, and the Shwebo backarc sub-basin to the east (Fig. 9). The magmatic belt of the WMA is, today, largely buried beneath sedimentary rocks. Exposed are isolated volcanoes (e.g. Mt. Popa and Mt. Monywa), and the mid-Cretaceous–Eocene Wuntho batholith in the north (Barley et al., 2003; Gardiner et al., 2017) and the mid-Cretaceous Salingyi batholith in the south (Mitchell et al., 2012; Gardiner et al., 2017).

The CMB is bounded to the west by the Indo-Burman Ranges (IBR). The IBR consists of a series of west–vergent thrust packages of Triassic–Neogene turbidites and shallow marine facies, with minor low–grade metamorphic rocks and ophiolites (Bender, 1983; Maurin and Rangin, 2009). It is interpreted as an accretionary prism, with Paleogene rocks predominantly derived from the Burmese margin to the east, and Neogene rocks considered to be off−scraped from the Bengal Fan (Curray et al., 1979; Allen et al., 2008; Naing et al., 2014). Uplift of the IBR is a perquisite for formation of a through-going Irrawaddy River with the mountain range then acting as a barrier between the CMB and the Indian Ocean to the west. Timing of uplift of the IBR is poorly constrained (e.g. Maurin and Rangin, 2009; Zhang et al., 2017b); most workers believe that this event must have commenced no later than Miocene time (e.g. Licht et al., 2013, 2014), with recent work by Licht et al. (2018) proposing the age of initial emergence of the accretionary prism above sea level as late Middle Eocene.

The CMB's eastern side is constrained by the western margin of the Shan–Thai plateau, considered a ~Mesozoic palaeo–Andean continental arc margin. At its western margin, predominantly carbonates crop out, along with the thin southern extension of the Mogok Metamorphic Belt (MMB). The majority of the MMB crops out in the northern upper headwaters of the present day Irrawaddy drainage basin and consists of low– to high–grade metamorphic rocks, metamorphosed and subsequently exhumed between ~Eocene−Early Miocene (e.g. Bertrand et al., 2001; Barley et al., 2003; Wang et al., 2006; Searle et al., 2007; Lin et al., 2009; Mitchell et al., 2012; Xu et al., 2015), and Cretaceous-Paleogene granites of the Dianxi–Burma batholiths (e.g. Xie et al., 2016b and references therein; Zhao et al., 2016a,b, 2017). Slightly further north lie the similarly aged Bomi-Chayu batholiths (Booth et al., 2004; Liang et al., 2008; Chiu et al., 2009; Zhu et al., 2009).

There are two schools of thought regarding the palaeodrainage of this river. Some previous researchers (Brookfield, 1998; Clark et al., 2004; Liang et al., 2008; Robinson et al., 2014) have proposed that the Yarlung Tsangpo, prior to its capture by the Brahmaputra, was connected to the Irrawaddy, and was responsible for sedimentation in the CMB either in the Miocene (Liang et al., 2008) or from Eocene to Miocene (e.g. Robinson et al., 2014), after which time river capture of the Yarlung by the Brahmaputra occurred (Bracciali et al., 2015; Lang and Huntington, 2014). By contrast, other workers consider that there is no evidence for such an event (Licht et al., 2013, 2014; Wang et al.,

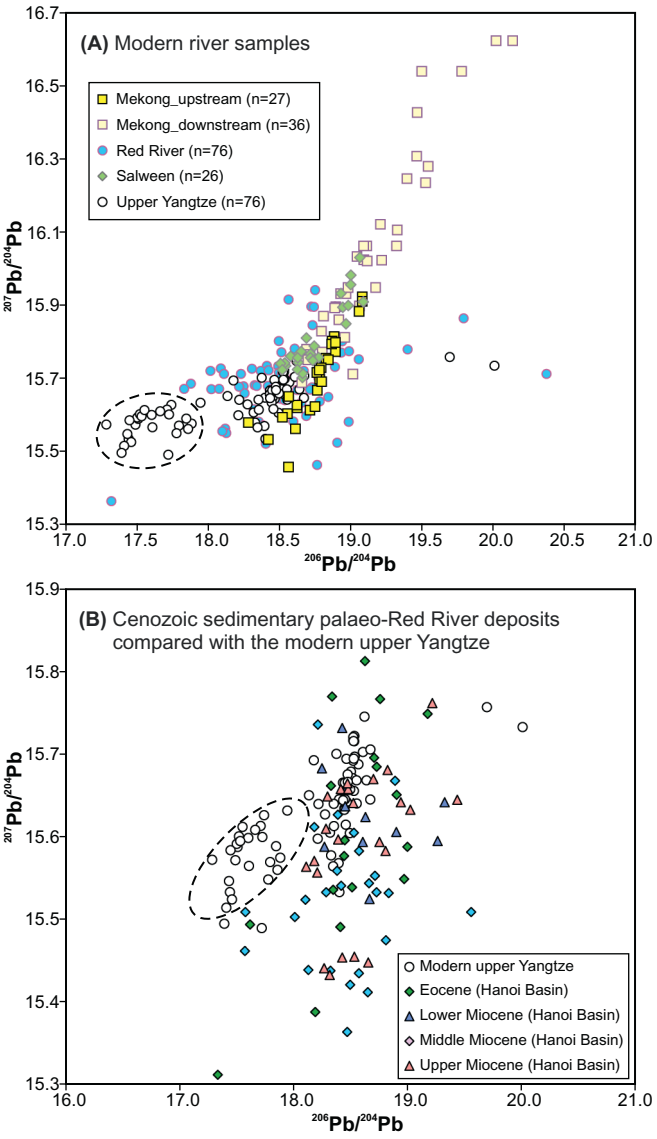

Fig. 5. (A) Pb isotopic compositions of detrital K-feldspar from modern river sediment of the upper Yangtze, Mekong, Salween, and Red Rivers shows that there is a field (outlined by dashed line circle) that differentiates the upper Yangtze from the other rivers (Zhang et al., 2017a). (B) Data from the Cenozoic sedimentary rocks of the Hanoi Basin (from Clift et al., 2008), a sedimentary repository of the Red River. From the partial lack of overlap of data between the distinctive part of the upper Yangtze signature (dashed line circle), and the Hanoi Basin sedimentary rocks, Zhang et al. (2017a) determined that there was no connection between the upper Yangtze and the Red River since Eocene times (see Section 3.1.1 for further discussion and note the contrast in interpretation with the data shown in Fig. 6). Data from the Cenozoic Hanoi Basin sedimentary rocks are also compared to fields from the Mekong and Salween to determine if these rivers may have previously fed into the palaeo-Red River. As discussed in Section 3.1.2, the highly radiogenic feldspars of the Mekong are only found in the downstream sample. These characteristic grains may therefore not be distinctive of the upper Mekong, and hence their absence in the palaeo-Red deposits cannot be taken as indicative of lack of a former connection. Data taken from Bodet and Schärer (2001), Clift et al. (2008) and Zhang et al. (2017a).

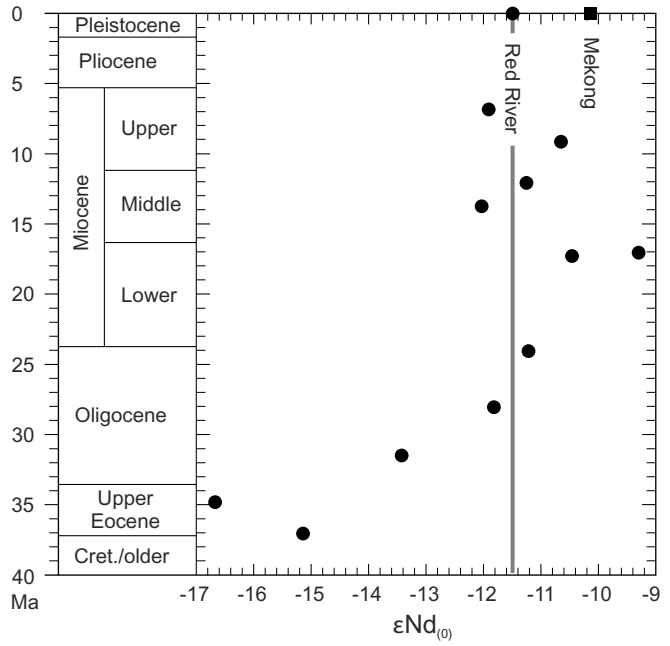

Fig. 6. Palaeo-Red repository of the Hanoi Basin showing changes in εNd values up-section, interpreted as the result of loss of the middle Yangtze, that flows over the Yangtze Craton (Fig. 1A) which has more negative εNd values (Clift et al., 2006a). Note that the depositional ages rely on unpublished oil company data. Grey vertical line shows the value of the modern Red River.

2014b; Zhang et al., 2017c) and that the Yarlung never flowed into the Irrawaddy drainage.

A locally–derived model for the CMB sediment provenance during the Middle to Late Eocene is proposed and/or interpreted on the following bases by the authors referenced below as follows: (1) west and west-southwest–directed palaeocurrents (Licht et al., 2013, 2018; Oo et al., 2015), (2) a quickly evolving river system with local catchments, as interpreted from disorganized stratigraphic shifts between marine and onshore fluvio–deltaic sediments, and from the presence of basal pebble lags (e.g. Licht et al., 2013; Oo et al., 2015), (3) the heterogeneity of Sr-Nd data which Licht et al. (2013, 2014) consider to indicate local derivation from the eastern Burmese margin (WMA and MMB), rather than from a homogenized source delivered by a south–-flowing trunk river before the uplift of the IBR, and (4) petrography and detrital zircon U-Pb ages which indicate overwhelming contribution from a volcanic arc (Oo et al., 2015; Licht et al., 2018); Licht et al. (2018) additionally record an increase in metamorphic detritus and zircons with old (Precambrian) U-Pb ages in the upper middle to upper Eocene rocks, although we note that there is variability in the record, with significant proportions of older grains also noted in some older middle Eocene samples (Fig. 10; Wang et al., 2014b). Licht et al. (2018) interpret this input as derived from the thin sliver of MMB to the east of the basin. Carrying out Hf isotopic characterization of the Mesozoic-Paleogene detrital zircons from these samples could allow this provenance interpretation to be verified, as explained further below (Fig. 11C).

In addition to the evidence outlined above, zircon U-Pb ages and Hf isotopes as well as bulk rock Nd data of the Eocene strata in the IBR are similar to those of the CMB (Allen et al., 2008; Naing et al., 2014). This suggests that, during much of the Eocene, the basin was open to the Indian Ocean and detrital materials were probably transported from the east to as far west as the Sunda Trench (Fig. 9).

Moving up-section, Licht et al. (2014) showed that εNd values in the CMB display a gradual decrease to more negative values from Eocene to Pliocene, stabilizing by the Neogene. Combined with a petrographic trend from predominantly magmatic arc-derived to predominantly orogenic-derived signature, those authors proposed a stable north-south drainage sourced from the Sino-Burmese Highlands, since the Neogene. They did not, however, exclude the possibility of an ephemeral or diluted contribution from a palaeo−Yarlung River but considered it unlikely before the Miocene. Their recent work (Licht et al., 2018) refined this model: in tandem with the provenance change described above, they proposed that a facies and palaeocurrent change between the upper middle Eocene Yaw Formation and the upper Oligocene (< 29 Ma) Letkat Formation represented a transition from estuarine conditions in a partially barrier-bound basin as the nascent IBR began to emerge, to a southward-directed braided fluvial environment after complete emergence of the IBR. The intervening time period is represented by a depositional hiatus in the Chindwin Basin area of study and thus it is not possible to determine with certainty when south-directed fluvial conditions initiated. Licht et al. (2018) surmise that the onset of may have been early in the intervening period in view of southward-directed palaeocurrents recorded in lower Oligocene deltaic strata in the Minbu Basin to the south (Gough and Hall, 2017) (Fig. 9).

By contrast, Robinson et al. (2014) interpreted a prominent change in εHf values of zircons from the CMB from Miocene times as evidence of a major palaeodrainage change. As discussed in more detail below, in the southern Lhasa terrane of the Tibetan Plateau, the Jurassic–Paleogene Gangdese arc (Fig. 9), exposed along the length of the Yarlung Tsangpo drainage, is characterized by zircons aged ~200–40 Ma (Fig. 10C) with positive zircon εHf values (Fig. 11, Column) (e.g. Chu et al., 2006; Ji et al., 2009; Guo et al., 2013; Robinson et al., 2014 and references therein; Meng et al., 2016, 2017). By contrast, similar aged zircons from the granites in the easternmost Lhasa terrane (Bomi-Chayu batholiths) and in the MMB in western Yunnan and central Myanmar (Dianxi-Burma batholiths) (Fig. 10C) show predominately negative εHf values (Fig. 11, Column) (e.g. Liang et al., 2008; Chiu et al., 2009; Robinson et al., 2014 and references therein; Chen et al., 2016; Gardiner et al., 2017, 2018). Both Liang et al. (2008) and Robinson et al. (2014) therefore used the similarity between detrital zircon ages and Hf signatures of the CMB and those of zircons from the Gangdese Transhimalaya of the Yarlung Tsangpo drainage, to propose that the Yarlung Tsangpo drainage sourced the CMB downstream prior to the Yarlung's capture by the Brahmaputra. However, Wang et al. (2014b) suggested that such zircons, with positive εHf values in the CMB might have been locally sourced, from the now buried WMA. Dating and isotopic characterization of these WMA granites (Fig. 10C; Fig. 11 Column) (Zhang et al., 2017c; Gardiner et al., 2017, 2018) showed that the locally–derived model of Wang et al. (2014a,b,c) is viable. Thus, long–distance input to the CMB is now no longer required to explain the CMB detrital data of Liang et al. (2008) and Robinson et al. (2014). Yet in such a scenario, in which material is locally-derived, how can the major influx of Mesozoic-Paleogene zircons with negative εHf values, by middle Oligocene times, be interpreted in terms of the palaeodrainage history of the basin? And when did the locally-derived detritus as, for example, interpreted by Licht et al. (2013, 2014, 2018) become replaced by material from a major through-going river with its headwaters in the northern MMB, when the Irrawaddy was born? Below, we integrate these disparate datasets with our own new data, to provide a palaeodrainage model consistent with all new and published datasets, in order to conclude the likelihood as to whether the Yarlung ever flowed into the Irrawaddy.

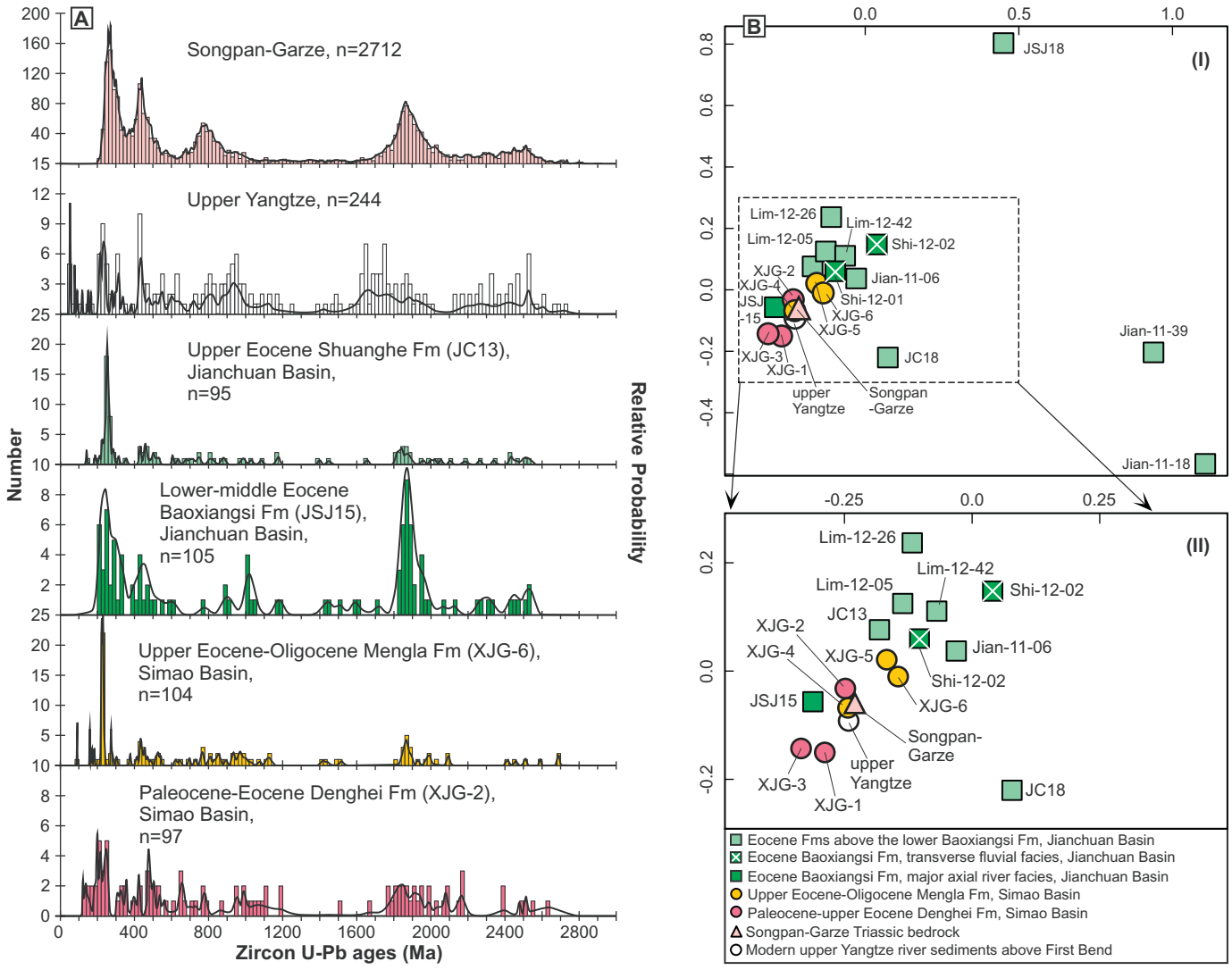

Fig. 7. Comparison of detrital zircon U-Pb data (presented as probability density plots with histograms (A) and a Multidimensional Scaling Plot (B)) from Songpan-Garze and Yangtze headwater potential source regions, with data from the Jianchuan and Simao Basins, considered to be the locations through which the upper Yangtze would have flowed if it ever previously flowed into the palaeo-Red River (Fig. 1B). Part label B, panel II, shows an expanded version of that part of B, panel I, highlighted by the box. The data from the Jianchuan Basin show a shift in provenance above the Baoxiangsi Formation at ca. 35 Ma, and an approximately coeval shift in the Simao Basin. This shift is interpreted as a change from deposition by a major river, debatably the upper Yangtze, to locally-derived deposits (see Section 3.1.1). Data for the Jianchuan Basin are from Yan et al. (2012) and Wissink et al. (2016) redated with the revised stratigraphy of Gourbet et al. (2017); data from the Simao Basin are from Chen et al. (2017). Data from the Songpan-Garze taken from Bruguier et al. (1997), Weislogel et al. (2006), Ding et al. (2013), Zhang et al. (2014a), and Tang et al. (2018). Data for the upper Yangtze are from Hoang et al. (2009), Yang et al. (2012), He et al. (2013), and Chen (2015). All available samples from the basins are plotted on B, apart from those from Gourbet et al. (2017) since for those samples grain numbers/sample was < 50. Baoxiangsi Formation analyses undertaken on samples interpreted as deposited by local transverse rather than axial rivers, on the basis of lithofacies, are marked (Wissink et al., 2016). Only an example representative sample from each basin below and above the provenance change is plotted in A. Part label B was made using *IsoplotR* (Vermeesch, 2018).

3.2.2.1. Description and integration of provenance datasets from the CMB

Our summary of the data in this section integrates both previously published data and our new data combined, from the Cenozoic sedimentary rocks of the CMB, the stratigraphy of which is summarised in Table 1. Previous work is differentiated from new work, and referenced, in the accompanying figures. Previous published analyses on surface outcrop samples from the CMB are restricted to zircon U-Pb with Hf, bulk rock Sm-Nd, and petrography (Liang et al., 2008; Licht et al., 2013, 2014, 2018; Wang et al., 2014b; Robinson et al., 2014; Oo et al., 2015) and the unpublished PhD data from Brezina (2014) which also includes mica Ar-Ar and zircon fission track analyses. For surface outcrop samples, we undertook new analyses where there were gaps in the time ranges analysed in published work, whilst for new analysis types (rutile U-Pb) we undertook analyses for the complete Cenozoic basin stratigraphy. Added to this, we have included our new data from the first subsurface core samples analysed from the CMB, made available to us by China National Offshore Oil Corporation (CNOOC). Depositional ages for subsurface core samples utilise seismic sequences, with dating

based on correlation to surface exposures and biostratigraphy (Li et al., 2013; Zhang et al., 2017c). Supplementary materials give details of our sampling approach and sample locations with respect to the published basin stratigraphy (Supplementary material 2), analytical methods (Supplementary material 3) and full results (Supplementary material 4).

3.2.2.1a. Zircon U-Pb ages and Hf signatures. U-Pb ages in zircon record the time of zircon growth in a magma, or less commonly, of new zircon growth during metamorphism. The hafnium isotope composition of the zircon can be used to evaluate the relative contributions from mafic and more evolved crustal sources to the magma within which the zircon grew.

All detrital samples are dominated by Mesozoic–Cenozoic grains (Fig. 10A and B). A ~100–80 Ma population is prevalent in Paleocene – Eocene samples, becoming less prominent in Oligocene samples, and subordinate by Miocene times. This ~100–80 Ma population is replaced in prevalence up-section by a ~50–75 Ma population and a younger population to ~20 Ma. Modern Irrawaddy River sands closely resemble the middle Miocene – Pliocene Irrawaddy Formation in terms of zircon U–Pb spectra, with a greater proportion of grains in the 100–150 Ma part of the spectrum, compared to older samples.

Hf analyses on Mesozoic–Cenozoic detrital zircons of both surface outcrop and subsurface samples show a major change between Eocene and Miocene samples: the Mesozoic–Cenozoic detrital zircons in the rocks of Eocene age and older are almost entirely of positive εHf values, whilst Miocene samples have a substantial additional population of grains with negative εHf values (Fig. 11A and B). The intervening Oligocene is a time of transition with the middle Oligocene surface outcrop samples and the upper Oligocene subsurface sample showing increasing proportions of grains with negative εHf values.

3.2.2.1b. Zircon fission track data and double dated ZFT and U-Pb with Hf characterization. ZFT ages represent a closure temperature between 290 and 320 °C for cooling rates between 1 and 10 °C/Myr but the presence of radiation damage may lower these values by 50 °C (Rahn et al., 2004). For detrital studies, unless the detrital material has been buried to depths sufficient to heat the rock above the closure temperature, the age approximates to the time that the mineral cooled through this temperature in its original igneous or metamorphic host rock. Double dating with U-Pb can be undertaken to identify volcanic-sourced grains, since these rapidly cooled grains have the same U-Pb and ZFT age.

The Eocene and Oligocene samples have a late Early Cretaceous ZFT population, and a mid Late Cretaceous population is present in some Neogene samples. Cenozoic populations dominate from Oligocene times onwards, with a Paleogene aged population in the Oligocene rock, and Neogene populations prevalent in Miocene samples. The dominant and youngest population of the middle Miocene-Pliocene sample is Paleogene. Results are displayed in Fig. 12.

The U-Pb ages of the youngest ZFT population of the Oligocene sample (30 Ma ZFT population), are in the range of 50–60 Ma and most grains have positive εHf values (Fig. 13). For two Miocene samples, youngest ZFT populations of Neogene age (18–20 Ma) have corresponding U-Pb ages ca. 20–55 Ma and εHf values are overwhelmingly negative. In the third Miocene sample the 18 Ma ZFT population has a somewhat older range of U-Pb ages from ca. 45–65 Ma, with mixed positive and negative εHf values (Fig. 13). These values and U-Pb ages are similar in the Paleogene ZFT population also documented in this sample.

3.2.2.1c. Rutile U-Pb ages. Rutile is a common accessory mineral in low- to high-grade metamorphic rocks, and its closure temperature in the U-Pb system is in the range of 640–~490 °C (e.g. Kooijman et al., 2010). Rutile U-Pb dating therefore can be used to constrain the thermal evolution of metamorphic terranes.

Detrital rutiles (Fig. 14) from Paleocene – Eocene samples show main populations between ~400 and 600 Ma and at ~100 Ma, the latter being a peak which is not recorded again after the Eocene. A modest number of grains between 40 and 80 Ma are recorded in the middle Oligocene surface outcrop sample, with the ~40 Ma peak dominating by the time of deposition of the subsurface upper Oligocene sample. This ~40 Ma population, and subsequently in the Neogene samples a ~20 Ma age peak, then dominate to the top of the succession.

3.2.2.1d. Ar-Ar mica dating. White micas occur in both igneous and metamorphic rocks. The closure temperature for white mica for the Ar-

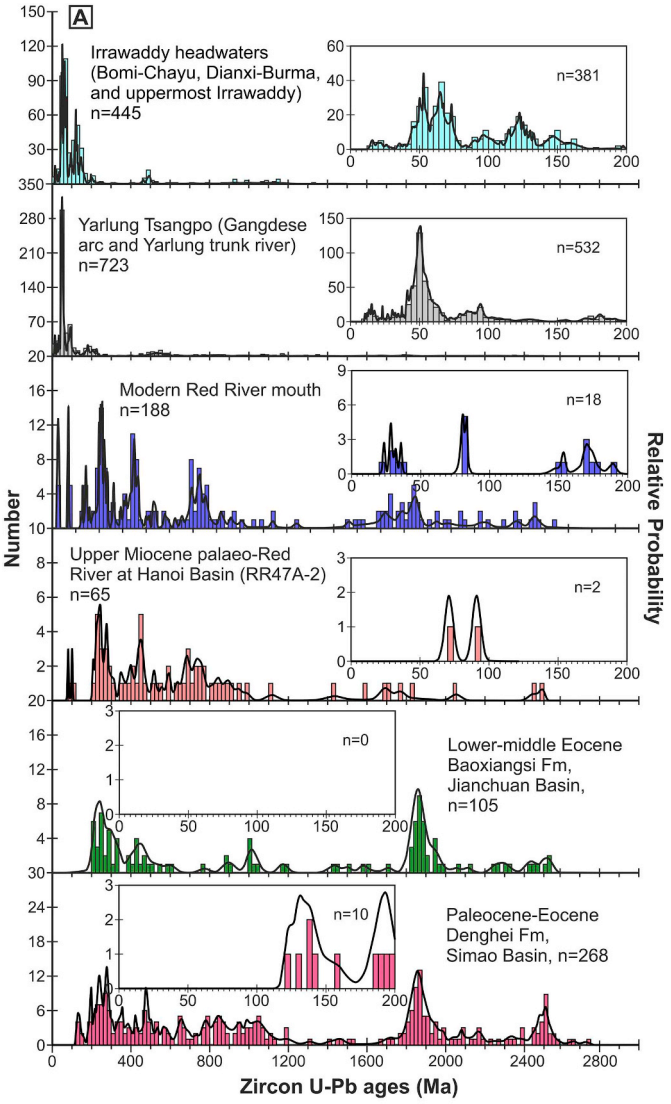

(caption on next page)

Fig. 8. Zircon U-Pb ages (as probability density plots; panel A) and versus Hf isotopic compositions (panel B) comparing the upper Miocene interpreted palaeo-Red River deposits (RR47A-2) and modern Red River data (Hoang et al., 2009; Wang et al., 2019) with data from the Yarlung drainage, including modern Yarlung trunk river (Cina et al., 2009; Zhang et al., 2012) and bedrock of the Gangdese arc from the Yarlung catchment (Chu et al., 2006; Wen et al., 2008; Ji et al., 2009; Zhu et al., 2011; Guo et al., 2013; Meng et al., 2016, 2017), as well as the Bomi-Chayu (Liang et al., 2008; Chiu et al., 2009; Zhu et al., 2009) and Dianxi-Burma (Xie et al., 2016b and references therein; Zhao et al., 2016a, 2016b, 2017) batholiths of the Irrawaddy headwaters through which the palaeo-Yarlung may have flowed if it had once drained into the palaeo-Red River. Detrital data from the uppermost Irrawaddy headwaters are also included (from Garzanti et al., 2016). No similarity is seen between the upper Miocene palaeo-Red River rocks and the rocks that comprise or contribute to the Yarlung palaeodrainage, particularly with respect to the characteristic 50 Ma peak of the Yarlung and Irrawaddy headwater catchments being absent in the palaeo-Red and modern Red River deposits.

Ar technique is ~400–450 °C (e.g. Harrison et al., 2009).

Detrital micas from middle Oligocene surface outcrop samples display a dominant peak at ~65 Ma with a subordinate population aged ~130 Ma (Fig. 15). By contrast, detrital micas from five early Miocene surface outcrop samples display a dominant peak at ~35 Ma, with a modest number of grains to 80 Ma and few older.

3.2.2.1e. Bulk rock Sr-Nd isotopic compositions. Sr and Nd isotope compositions of bulk-rock samples can be used to evaluate the relative contributions to a sedimentary unit from mafic and more evolved crustal sources. The Nd isotope composition is commonly represented as εNd, the deviation in parts per 10,000 from a model chondritic reservoir (CHUR).

Y3–84 is an igneous WMA sample from well Y3 (Fig. 9), and is characterized by moderately radiogenic $^{87}Sr/^{86}Sr_{(t)}$ ratios (0.7054) and $\varepsilon Nd_{(t)}$ values (+0.88). Eight mudstone subsurface core samples of Paleocene to Eocene age show similar Nd isotopic compositions ($\varepsilon Nd_{(t)} = -0.23$ to $+0.91$), of juvenile character and close to $\varepsilon Nd_{(t)}$ values of the WMA (Fig. 16). Coeval sediments for surface outcrop samples show more varied and, in general, more evolved values; this difference may reflect the position of the subsurface core samples directly overlying the arc versus the surface outcrop samples in their forearc positions. By contrast, Oligocene and Neogene samples overall exhibit higher radiogenic $^{87}Sr/^{86}Sr$ ratios and lower εNd values, typical of a greater input from a crustal component, and similar to values from the MMB and the modern Irrawaddy (Fig. 16). Our new data resemble those of published samples from the CMB (Licht et al., 2013, 2014), which demonstrate a significant change between the Eocene and Miocene.

3.2.2.1f. Petrography. Similar to the study of Licht et al. (2014, 2018) we record a trend from Eocene through Mio-Pliocene of increased feldspar and quartz at the expense of lithics in the QFL plot (Fig. 17), traditionally considered to be a change from “Arc” to “Recycled Orogen” provenance of Dickinson (1985), and a trend in the composition of lithics from predominantly volcanic, to metasedimentary and metamorphic. We note that the subsurface core samples (collected from well AZY-1, Shwebo backarc subbasin; Fig. 9) have less volcanic and more metasedimentary and metamorphic lithics and/or show higher metamorphic grade of lithic grains, compared to coeval surface outcrop samples, throughout the succession. This we attribute to the more northward location of the subsurface core samples, closer to the metamorphic source. Such a spatial variation in metamorphic grade of eroded detritus is mirrored in the present day setting, where the upstream Irrawaddy is much richer in metamorphic detritus compared to downstream reaches (Garzanti et al., 2016) (Fig. 17).

3.2.2.2. Towards a palaeodrainage model for the CMB and wider region. This section documents the birth and evolution of the Irrawaddy River and its relationship to the Yarlung Tsangpo.

A strong change in petrographic and isotopic signature is observed between Eocene and Miocene sedimentary rocks in the CMB. Paleocene and Eocene rocks have a petrographic signature of arc–affinity (Licht et al., 2013, 2014, 2018; this study) (Fig. 17), Mesozoic and Paleogene zircons with near–exclusively positive εHf values (Robinson et al., 2014; Wang et al., 2014b; this study) (Fig. 11), late Proterozoic–Cambrian and Cretaceous rutiles (this study) (Fig. 14), relatively juvenile Sr–Nd bulk signatures (Licht et al., 2013, 2014; this study) (Fig. 16) and exclusively Cretaceous zircon fission track ages (Brezina, 2014) (Fig. 12). By contrast, Miocene and younger rocks have a petrographic signature of recycled–orogen affinity, Mesozoic–Cenozoic zircons have shifted from being entirely of positive εHf signature as they were in the Eocene rocks, to having a substantial proportion of grains showing negative εHf values, rutiles have shifted from being entirely pre-Cenozoic aged as they were in the Eocene rocks, to having a dominant Cenozoic population, ZFT ages show dominant Neogene populations, and the Miocene rocks have a more evolved, crustal, Sr–Nd bulk signature (references and new work as per Eocene rocks, described above).

The Oligocene was a time of transition, with characteristics between those of the Eocene and Miocene rocks. Petrographic and bulk rock Sr–Nd characteristics are intermediate between the values of the Eocene and Miocene formations. Zircons from Oligocene samples have a Mesozoic–Cenozoic population with negative εHf values, the population becoming more significant through time, from the middle Oligocene surface outcrop sample to the upper Oligocene subsurface core sample. This trend is mirrored in the rutile data, where the Cenozoic rutile population distinctive of the Neogene samples is significant in the upper Oligocene subsurface core sample, and weakly represented, by a few grains, in the middle Oligocene surface outcrop sample. ZFT data from the Oligocene surface outcrop sample (no subsurface core data available) show a dominant Paleogene peak, unlike the Cretaceous dominance in the Eocene sample below and the Neogene dominant peak in the Miocene samples above. Mica Ar–Ar data from surface outcrop samples (no subsurface core data available) show a significant difference between the middle Oligocene rocks (peaks around 65 Ma and a diffuse population around 120–200 Ma) and the lower Miocene and younger rocks (peaks around 35 Ma).

Thus, in summary, there appears to be a significant provenance shift between Eocene and Miocene times, with first influx from this new provenance source observed in the middle Oligocene rocks. Since we have no samples from the Late Eocene or Early Oligocene, we conclude that the shift occurred sometime within this time interval, consistent with the data from Licht et al. (2018) as summarised in Section 3.2.2.

We discuss this change below.

As summarised in Section 3.2.2, a key question regarding the palaeodrainage of the Irrawaddy River is whether the palaeo–Irrawaddy drainage basin (CMB) previously contained the palaeo–Yarlung River, prior to its capture by the Brahmaputra. If it did not, then when did the palaeo-Irrawaddy River begin? Whilst Robinson et al. (2014) proposed that zircons of Mesozoic–Paleogene age with positive εHf values indicated derivation of detritus from the Gangdese arc of the Yarlung Tsangpo suture zone drainage (Fig. 11C), Wang et al. (2014b) argued that derivation of such detritus could have been from the proximal

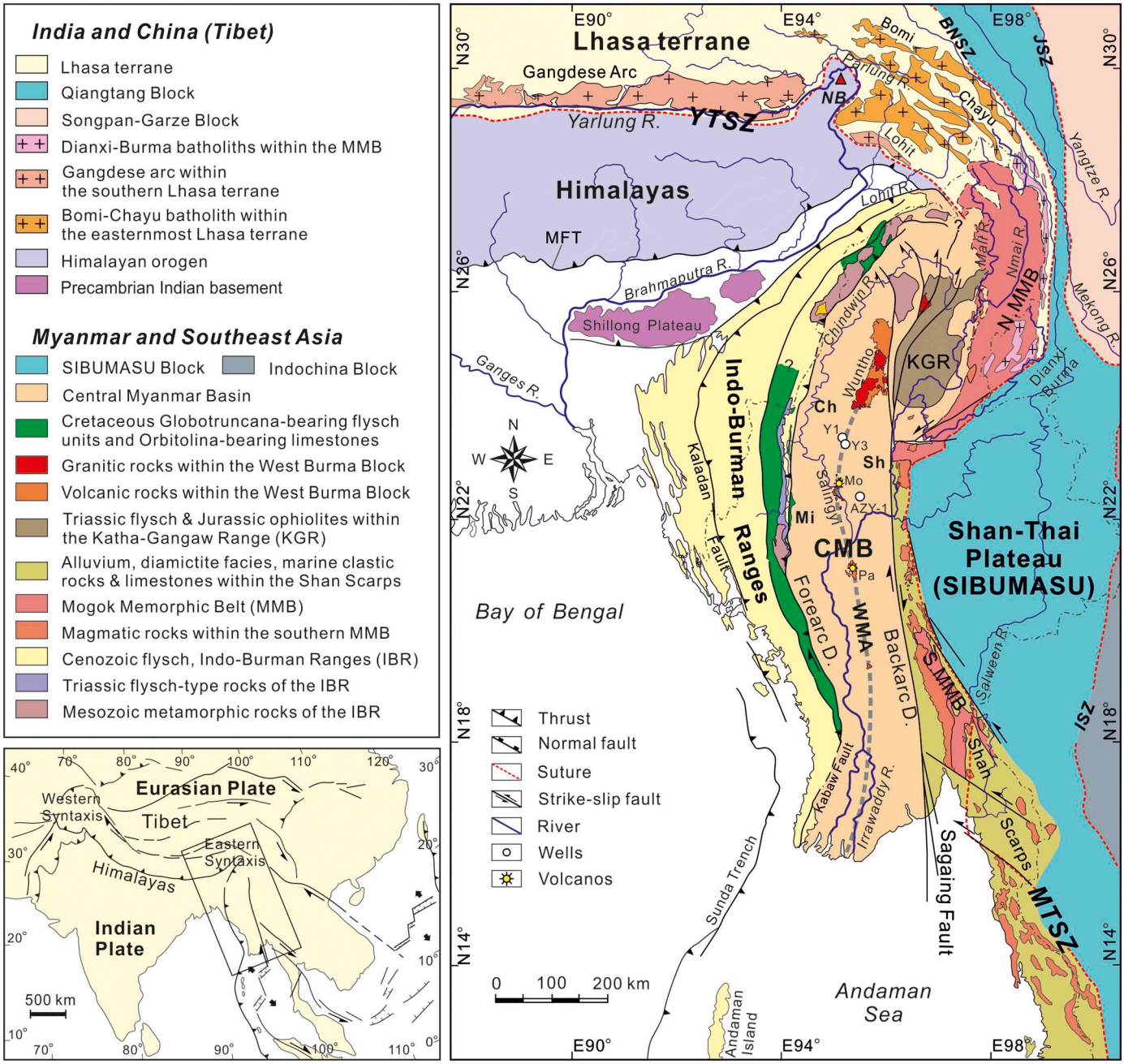

Fig. 9. Simplified geological map of Myanmar and the Eastern Himalayan syntaxis, showing major terranes, terrane boundaries, geological units and major modern rivers (modified after Mitchell et al., 2012 and Robinson et al., 2014). YTSZ, Yarlung–Tsangpo Suture Zone; BNSZ, Bangong–Nujiang Suture Zone; JSZ, Jinsha Suture Zone; ISZ, Inthanon Suture Zone; MTSZ, Meso–Tethys Suture Zone; NB, Namche Barwa; STD, South Tibet Detachment; MCT, Main Central Thrust; MBT, Main Boundary Thrust; MFT, Main Frontal Thrust; Sh, Shwebo subbasin; Ch, Chindwin subbasin; Mi, Minbu subbasin; CMB, Central Myanmar Basin; WMA, Western Myanmar Arc; Pa, Mt. Popa; Mo, Mt. Monywa. White circles show the wells we refer to in the text; Y1, Y3 and AZY–1 are the primary wells from which our samples were taken. Inset map shows the location of this figure (after Tapponnier et al., 1982).

WMA (Fig. 11C), although at that time such an interpretation was speculative since the Hf isotopic signature of zircons from this magmatic arc was unknown. Subsequent analysis on igneous bedrock samples from the WMA by Zhang et al. (2017c) and Gardiner et al. (2017) showed that the Mesozoic–Cenozoic zircons from the WMA were characterized by positive εHf values (Fig. 11C), indicating that Wang's proposition was viable. But in this case, how can the major change in εHf values of the Mesozoic-Paleogene zircons during the Late Eocene to Early Oligocene interval (Wang et al., 2014b; Robinson et al., 2014; this study), be explained? We provide a palaeodrainage model consistent with these data, below.

The detrital data for the Paleocene and Eocene CMB samples closely

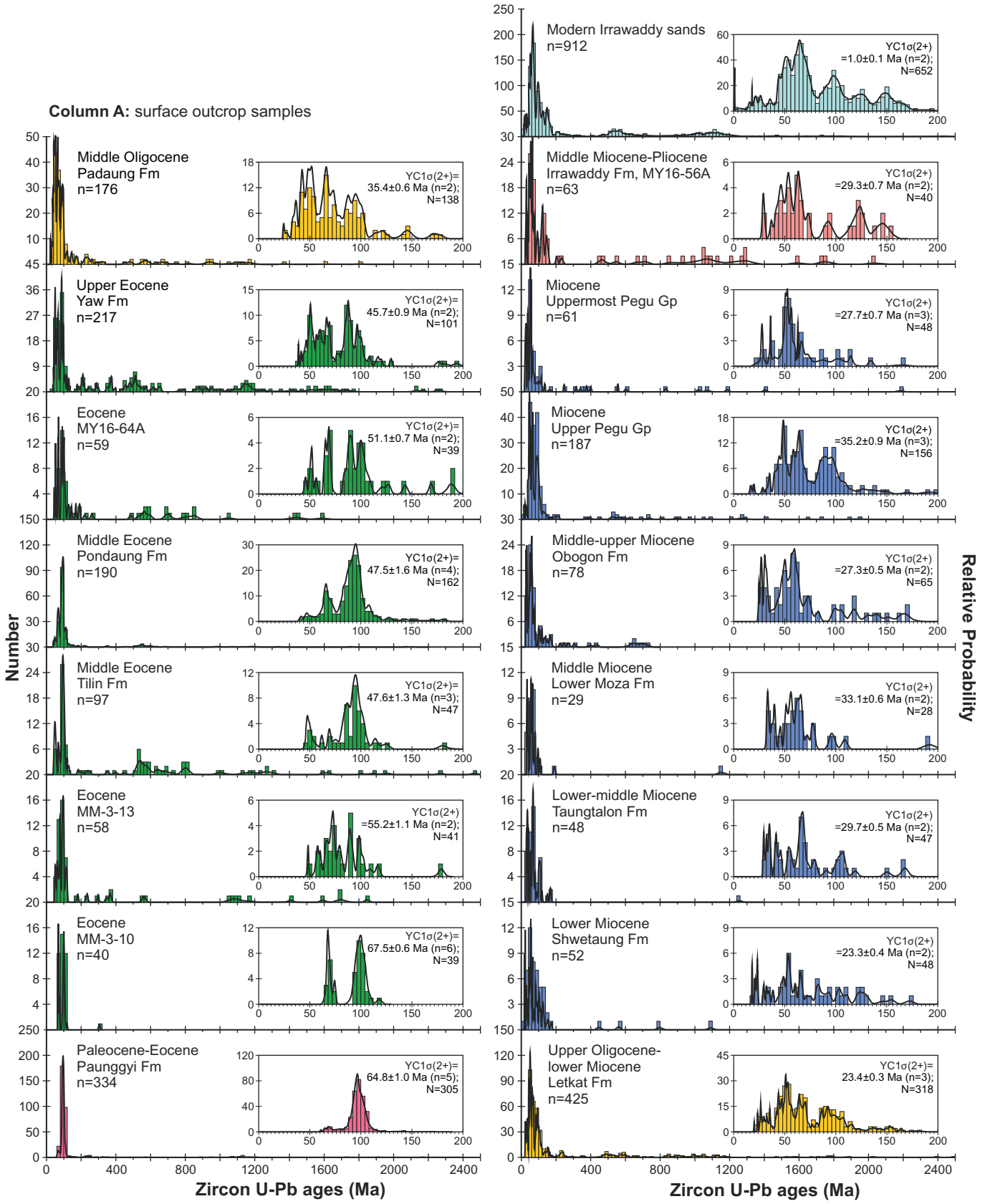

(caption on next page)

Fig. 10. U-Pb data of detrital zircons, from surface outcrop (A) and subsurface core (B) samples of the Central Myanmar Basin plotted as relative probability and frequency plots. Insets display detailed U-Pb age spectra in the range of 0–200 Ma (N–numbers of zircon < 200 Ma). All youngest population ages quoted here are derived using the weighted average $^{206}Pb/^{238}U$ age for the youngest group of at least two grains (n) overlapping within error at the 1 – sigma level; (YC1σ(2+); Dickinson and Gehrels (2009)). The subsurface data (Column B) are our own new analyses. In the surface outcrop samples (A) data are from our own samples (MM3–10, MM3–13, MY16-64A, MY16-56A) and published sources as follows: (1) Paleocene–Eocene Paunggyi Formation, middle Eocene Tilin Formation, middle Eocene Pondaung Formation and Miocene upper Pegu Group are from Wang et al. (2014b); (2) upper Eocene Yaw Formation and upper Oligocene-lower Miocene Letkat Formation are from Licht et al. (2018). (3) middle Oligocene Padaung Formation, Miocene Shwetaung, Taungtalon, Lower Moza and Obogon Formations are from Robinson et al. (2014); (4) Miocene uppermost Pegu Group is from Liang et al. (2008); (5) modern Irrawaddy sands are from Bodet and Schärer (2000), and Garzanti et al. (2016). Note that the Padaung Formation samples of Robinson et al. (2014) have been reassigned an age from previously Late Oligocene, to middle Oligocene, based on our dating of a tuff (27.0 ± 1.0 Ma from zircon U-Pb data; see Fig. TSM1C in Supplementary material 4) located in close proximity to these sample locations.

Column C provides data on potential source regions, discussed in Section 3.2.2. Data from the Western Myanmar Arc are from Zhang et al. (2017c) and references therein, and Gardiner et al. (2017); data from the Yarlung Tsangpo trunk river are from Cina et al. (2009) and Zhang et al. (2012); data from the Gangdese arc bedrock of the Yarlung Tsangpo catchment are from Chu et al. (2006), Wen et al. (2008), Ji et al. (2009), Zhu et al. (2011), Guo et al. (2013), Wang et al. (2015a,b), and Meng et al. (2016, 2017); data from the Dianxi-Burma and Bomi-Chayu batholiths which are exposed in the catchment of the modern Irrawaddy's headwaters are from Xie et al. (2016a,b) and references therein, Zhao et al., 2016a, 2016b, Zhao et al., 2017); Chiu et al. (2009) and references therein; and detrital data from the uppermost Irrawaddy headwaters are from Garzanti et al. (2016).

match the signature of the WMA in zircon U-Pb and Hf characteristics, as well as bulk rock Sr-Nd signature (the latter particularly for subsurface core samples), and therefore, as previously proposed by Wang et al. (2014b), no input from the Yarlung Tsangpo catchment is required to explain the provenance of these CMB sedimentary rocks. Furthermore, Mesozoic detrital zircons with positive εHf values have also been recorded in sedimentary rocks of the upper Cretaceous Kabaw Formation (Wang et al., 2014b). The age of these rocks indicates that they were deposited before India-Asia collision and by inference before initiation of the Yarlung Tsangpo along the India-Asia suture zone; occurrence of zircons of such signature found in Cretaceous rocks of the CMB therefore cannot have been delivered by a palaeo–Yarlung, thus supporting the proposal of the presence of a source local to the CMB. This conclusion is supported by the observations of Licht et al. (2013) who noted that mid-Eocene aged samples have a relatively heterogeneous Sr-Nd isotopic signature, which they considered indicated that these rocks were sourced by short–stem rivers of heterogeneous catchment rather than by a trunk river. A local rather than long–-distance provenance for the Paleocene–Eocene period is also consistent with petrographic data documenting arc–affinity (Licht et al., 2013, 2014, 2018) (Fig. 17) and with the interpretation of Licht et al. (2018) as summarised in Section 3.2.2. In this locally-sourced scenario, the older rutile populations (400–600 Ma) (Fig. 14) are presumably derived from Burmese basement, a proposal that is supported both by those more negative εNd analyses which indicate a contribution from crustal sources, and by the presence of a metamorphic and sedimentary contribution as determined from petrography. As regards the younger rutile population (~100 Ma), Searle et al. (2017) consider that this time period was one of quiescence in both the Himalaya–Tibet region and in Myanmar, where the MMB records no evidence of metamorphism of this age. Thus a local source is likely for the rutiles, perhaps related to metamorphism which might be associated with collision of the Mawgyi arc (Figs. 1A and 9) to the Burmese margin debatably around that time (Morley, 2012), or associated with subduction and WMA pluton intrusion (Mitchell et al., 2012; Zhang et al., 2017c).

In summary, all Eocene data are consistent with a WMA source. The double dated ZFT and U-Pb with Hf data from the Oligocene CMB surface outcrop samples show that the 30 Ma ZFT population is WMA-derived in view of its overwhelmingly positive εHf signature (Fig. 13). Thus we show that the WMA experienced a period of exhumation around 30 Ma. This period of exhumation is in agreement with the work of Li et al. (2013) and Zhang et al. (2017c) and may explain the lack of lower Oligocene sedimentary rocks preserved in parts of the CMB, reported by some authors, e.g. Bertrand and Rangin (2003), Zhang et al. (2017c), and Licht et al. (2018) (Table 1).

The middle Oligocene Padaung Formation records the first evidence of a new source contribution to the basin, which becomes more prominent into the upper Oligocene and Neogene samples. The new source is characterized by Jurassic–Cenozoic zircons with negative εHf values, Cenozoic rutiles and micas, and Sr-Nd values with a stronger crustal signature. Potential source regions hosting zircons with such signatures near the CMB are the Bomi-Chayu batholiths and Dianxi-Burma MMB batholiths of the Irrawaddy headwater drainage north of the CMB, as well as granites found in the thin southern sliver of MMB located adjacent to the Sagaing fault east of the CMB (Figs. 9 and 11C). In the MMB, there are widespread and exposed low– to high–grade metamorphic rocks which were metamorphosed and subsequently exhumed in Eocene–Oligocene times (Bertrand et al., 2001; Barley et al., 2003; Wang et al., 2006; Mitchell et al., 2012; Searle et al., 2007, 2017; Xu et al., 2015). The age of these metamorphic events is consistent with rutile and mica Cenozoic ages from the CMB samples (Figs. 14 and 15) and also with the youngest ZFT population, which has negative εHf values (Figs. 12 and 13), consistent with this MMB source. Furthermore, the increasing input from this source, and the decreasing age of the youngest rutile peak from Paleogene to Neogene aged, up-section, would be consistent with progressive exhumation of the source region. Bulk rock Sr-Nd data (Fig. 16) and petrographic data (Fig. 17) are also consistent with a MMB source. Thus, we propose that the MMB Dianxi-Burma and Bomi-Chayu granites were a significant new source region providing detritus to the CMB.

We consider that the region of the MMB contributing the detritus was likely the northern MMB (located in the current headwaters of the Irrawaddy drainage basin), rather than the southern sliver of MMB located east of the CMB since (1) the majority of the MMB outcrops in the north; (2) the U-Pb ages of zircons analysed in the southern MMB do not extend as young as those recorded in the northern MMB and in the CMB Miocene detrital samples (Fig. 11) although we acknowledge this may simply be the result of a data gap; and (3) the southern MMB outcrops are associated with significant carbonates of the Shan-Thai Plateau, yet no carbonate lithics are recorded in the Oligo-Miocene petrography (Fig. 17), although the possible effects of dissolution must also be considered. Thus we consider that the northern MMB started to deliver detritus to the CMB through establishment of a palaeo–Irrawaddy trunk river by middle Oligocene times.

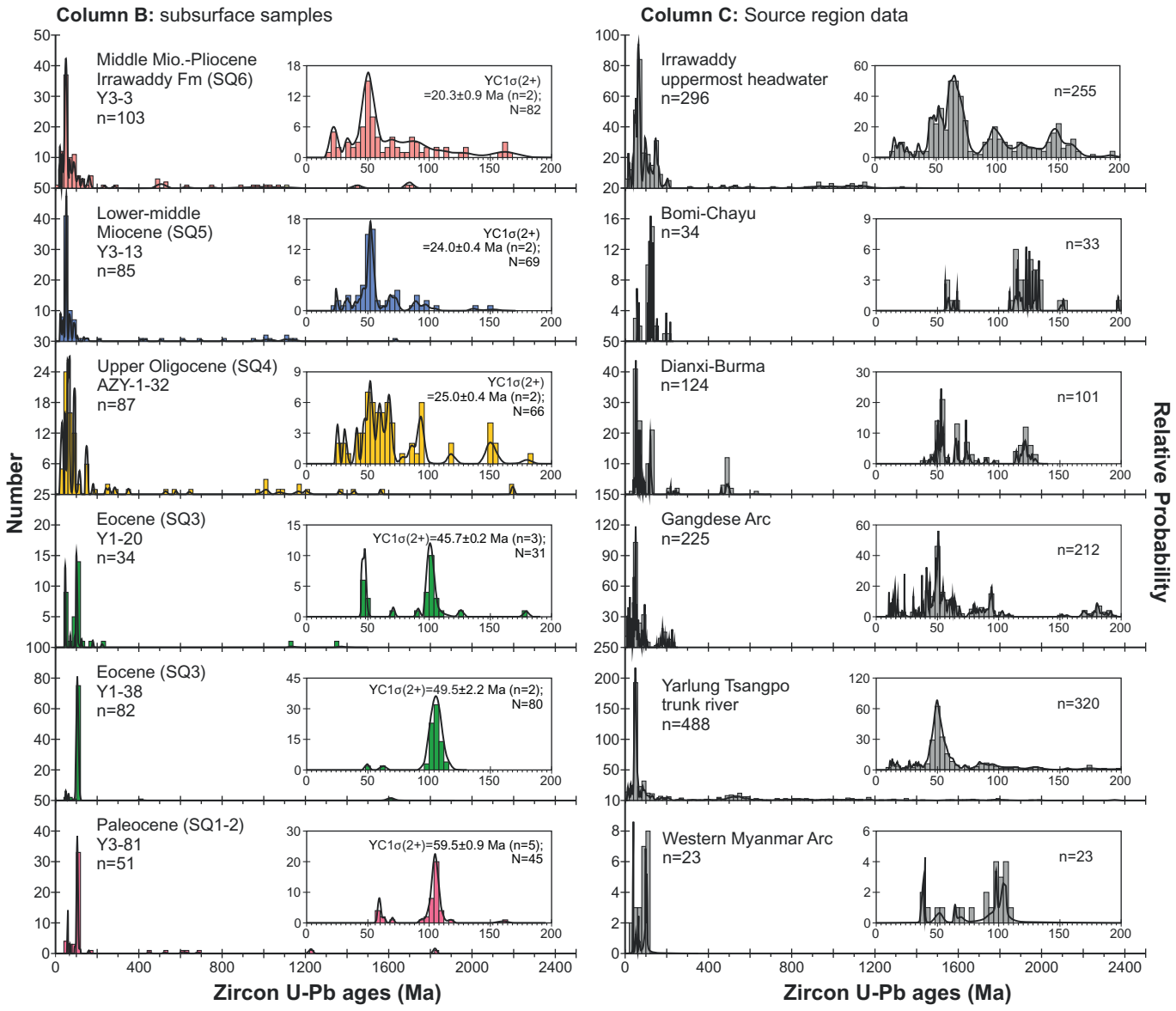

Fig. 10. (*continued*)

Whilst it is not possible to pinpoint the first arrival of this MMB-derived detritus to the basin more tightly, due to our data gap covering the Late Eocene and Early Oligocene, we note that Licht et al. (2018) consider initiation would have been closer to the start of our data gap, based on southerly-directed palaeocurrents recorded in the lower Oligocene deltaic strata of the Minbu sub-basin to the south (Gough and Hall, 2017). We concur with Licht et al. (2018) that initiation may have occurred closer to the start of the data gap, if the south-directed palaeocurrents are interpreted as representing through drainage from headwaters in Northern Myanmar, rather than from local drainage with headwaters in the palaeo-high which separated the Minbu and Chindwin basins into separate pull-apart basins by this time (Licht et al., 2018). Provenance data similar to that which is described above, is critical for the Minbu basin.

From Late Oligocene times onwards, the MMB was a dominant influx to the basin, as evidenced by, for example, the rutile data. By the Miocene, the last major shifts in provenance as, for example, illustrated by the change in mica Ar-Ar age spectra, and the combined ZFT with U-Pb with Hf data, between Oligocene and Miocene samples, had occurred. From Neogene times onwards a stable provenance, broadly similar to present day, is recorded.

We suggest that the establishment of the palaeo–Irrawaddy as a through–going river was likely driven by gradual headward erosion of its northern tributaries as the MMB exhumed to the north. We tentatively suggest that the progressive nature of this northward cutback may be evidenced by the greater proportion of zircons in the range 100–150 Ma in the upper Miocene to modern day samples; such zircons are more characteristic of the Bomi-Chayu batholiths in the far northern

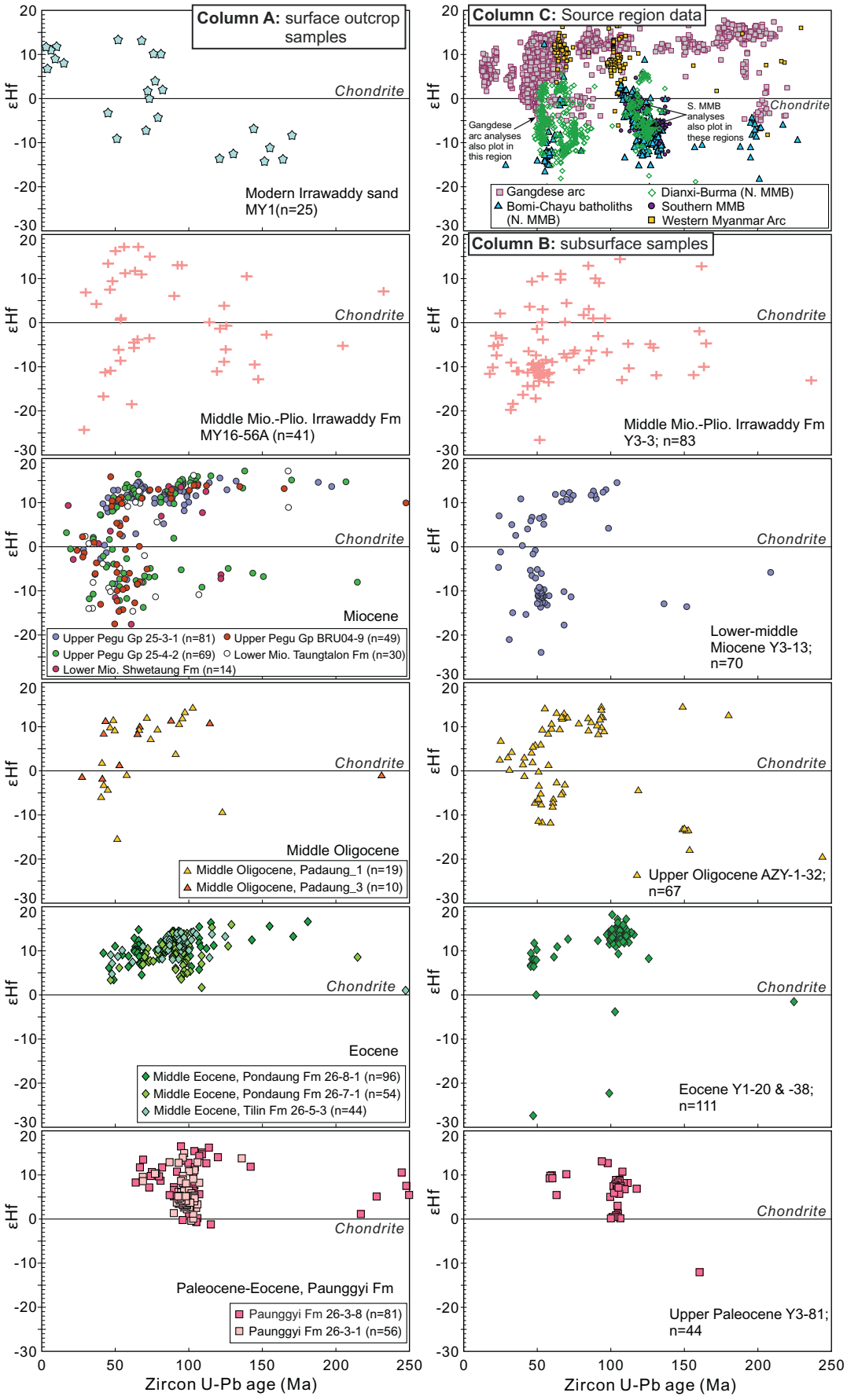

(caption on next page)

Fig. 11. εHf(t) values versus $^{206}Pb/^{238}U$ zircon ages (Ma) for detrital zircons from sedimentary rocks in the Central Myanmar Basin. Data plotted in Column A (left column) are our new analysed surface outcrop sample (MY16 – 56A, with published outcrop data (Bodet and Schärer, 2000; Liang et al., 2008; Wang et al., 2014b; Robinson et al., 2014). Data plotted in Column B (right column) are our new subsurface core sample data. Data shown in Plot C are time–corrected εHf values versus $^{206}Pb/^{238}U$ zircon ages (Ma) for igneous zircons from batholiths within the Gangdese arc of the Yarlung catchment, the Bomi–Chayu batholiths and northern Mogok Metamorphic Belt (Dianxi–Burma batholiths) of the Irrawaddy headwaters, the southern sliver of Mogok Metamorphic Belt (Southern MMB; see Fig. 1 location) and Western Myanmar Arc; data are modified after Robinson et al. (2014) and references therein, Chen et al., 2016, Zhang et al. (2017c), and Gardiner et al. (2017).

Table 1
Summarised stratigraphy of the Central Myanmar Basin. The left panel summarises the formation names, facies, and lithologies as traditionally depicted using lithostratigraphy (after Bender, 1983; Pivnik et al., 1998; Licht et al., 2013), corroborated and/or updated with recent data as discussed in text. No published facies for backarc. The right hand panel shows the more recent seismic stratigraphy (after Li et al., 2013; Zhang et al., 2017c). SQs = Seismic Sequences, Tx = reflector boundaries.

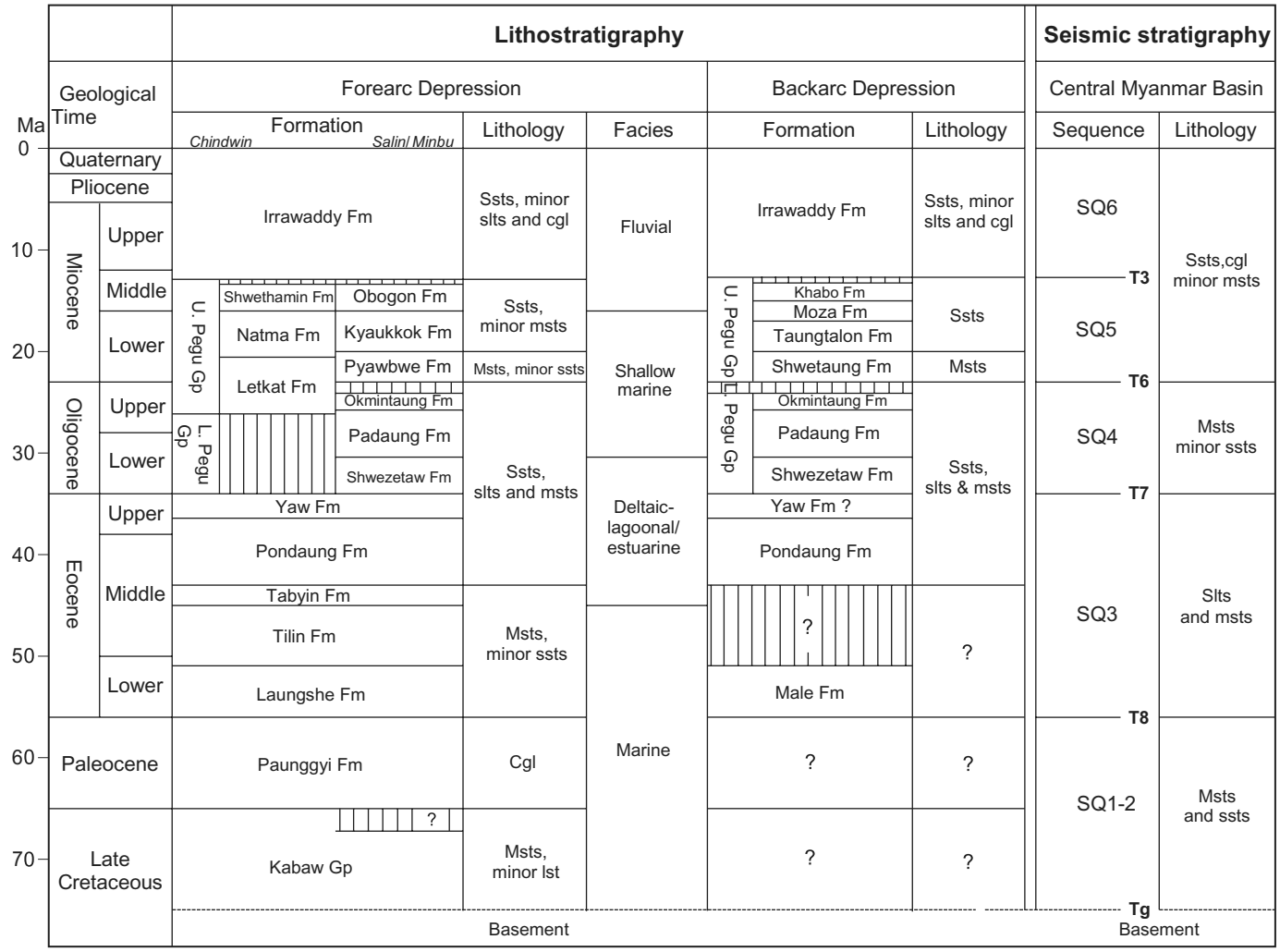

region compared to the Dianxi-Burma batholiths located more southward in the MMB Highlands (Figs. 9 and 11C).

With this palaeodrainage reconstruction, it is hard to envision a time when the palaeo–Yarlung might have flowed into the Irrawaddy drainage. From the CMB data, we deduce that drainage of the palaeo-Yarlung into the Irrawaddy could only have been viable between Late Eocene to Early Miocene times: Early Eocene zircons with negative εHf values, characteristic of the region through which the palaeo-Yarlung would have flowed if it had once drained into the Irrawaddy (Fig. 11C) are not observed in the Middle Eocene CMB record, precluding any drainage from a palaeo-Yarlung into the CMB during the Mid Eocene; and by (at least) 18 Ma, Yarlung detritus is already found in the Bengal Fan and Bengal Basin and capture of the Yarlung by the Brahmaputra had occurred (Bracciali et al., 2015; Blum et al., 2018), as described in Section 3.2.3, below. Yet between the Late Eocene and Early Miocene, petrography and Sr – Nd data from Licht et al. (2013, 2014) show a

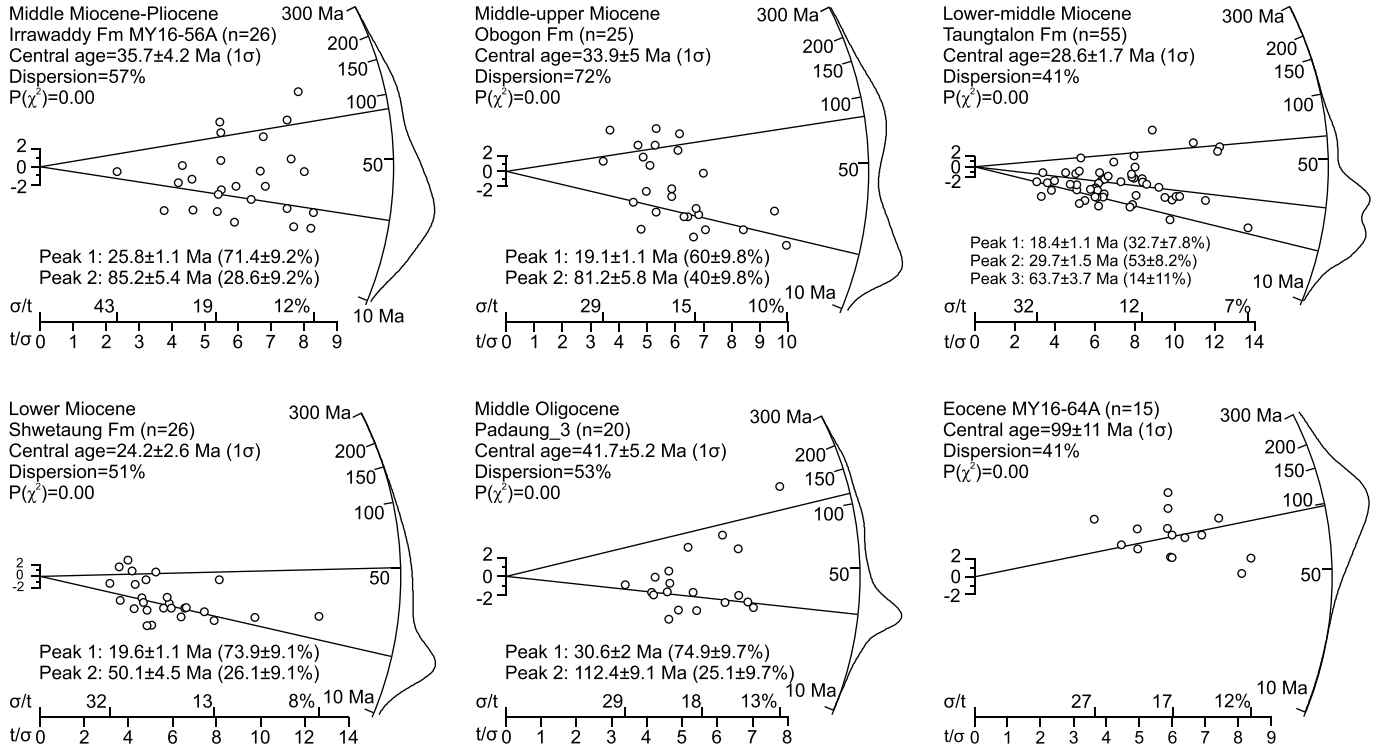

Fig. 12. Detrital zircon fission track data from surface outcrop samples of the Central Myanmar Basin, shown on radial plots. Data from the unpublished PhD thesis of Brezina (2014), and our new data (MY16-64A and MY16-56A). The plots were made using *RadialPlotter* (Vermeesch (2009).

gradual temporal trend to stabilization, not easily reconcilable with the arrival and subsequent disappearance of a major river (Fig. 16). Furthermore, we note the absence of a zircon population of ~190–220 Ma with negative εHf values in the sedimentary rocks of the CMB (Figs. 10 and 11). Such grains are typical of the Northern/Central Lhasa magmatic belts and are found in the Paleogene and early Neogene sedimentary rocks of the Yarlung Tsangpo suture zone (Wang et al., 2010; Hu et al., 2012; Leary et al., 2016a). Such zircons might also be expected in co-eval sedimentary rocks of the CMB if they were the deposits of a palaeo-Yarlung, although the effects of dilution should also be considered.

In summary, we propose that the palaeo–Yarlung never drained into the palaeo–Irrawaddy. The palaeo-Irrawaddy, with its headwaters in the MMB of northern Myanmar, initiated sometime between the Late Eocene and Early Oligocene, and was established as a major through–going river in the CMB with stable provenance similar to present day by the Early Miocene.

3.2.3. When the Yarlung Tsangpo first drained into the Bengal Basin and Bay of Bengal

Prior to the routing of the palaeo-Yarlung into the Brahmaputra drainage, the palaeo-Brahmaputra drained only the southern Himalayan slopes, with a small input of material from the Indo-Burman Ranges to the east. The southern slopes of the Himalaya are comprised of Indian plate material, and zircons are overwhelmingly of Palaeozoic-Precambrian age (e.g. Cina et al., 2009). Thus, leaving aside a minority of Mesozoic grains that are transported to the Bengal Basin from the Paleogene Indo-Burman Ranges (e.g. Allen et al., 2008; Naing et al., 2014), the first major influx of Mesozoic zircons reflects input from the Transhimalayan Gangdese batholiths of the Yarlung Tsangpo suture zone (Fig. 10C), along which the Yarlung river flows (Fig. 9).

In the easternmost part of the Himalayan foreland basin, through which the Brahmaputra river flows, Transhimalayan detritus has been recorded from the base of the studied sedimentary succession of the Siwalik Group (Lang and Huntington, 2014), dated at ~8 Ma (Lang et al., 2016), thus providing a minimum age to the time when the Yarlung flowed into the Bengal Basin. In the Bengal remnant ocean basin, where the sediment record extends older, Transhimalayan material has been documented from Early Miocene times (Fig. 18) (Bracciali et al., 2015). In the Bengal Fan, Transhimalayan zircons have been found from the base of the fan, dated at 18 Ma at that location (Blum et al., 2018). Thus we can be confident that the Yarlung Tsangpo routed to the Bengal Basin by Early Miocene times.

Further consideration of the zircon data allows the details of the routing to be established, specifically with respect to the route that the Yarlung took to join with the Brahmaputra. Whilst today the Yarlung flows through the Siang across the rapidly exhuming Eastern Himalayan Namche Barwa syntaxis, previous routings through the Parlung and Lohit have been proposed (Figs. 3 and 19). Govin et al. (2018), studied a Siwalik sedimentary succession in the easternmost Himalayan foreland, combining it with the work of Lang and Huntington (2014) downstream, in order to interpret the palaeo-drainage reproduced in Fig. 19. These authors noted that they cannot determine when the Siang connection commenced due to lack of an appropriately old sedimentary record (Fig. 19A). They note that by the Late Miocene, short lag times indicative of derivation from the syntaxis, recorded by Lang and Huntington (2014), indicate that the Yarlung was routing via the Siang (Fig. 19B). Early Cretaceous grains are more

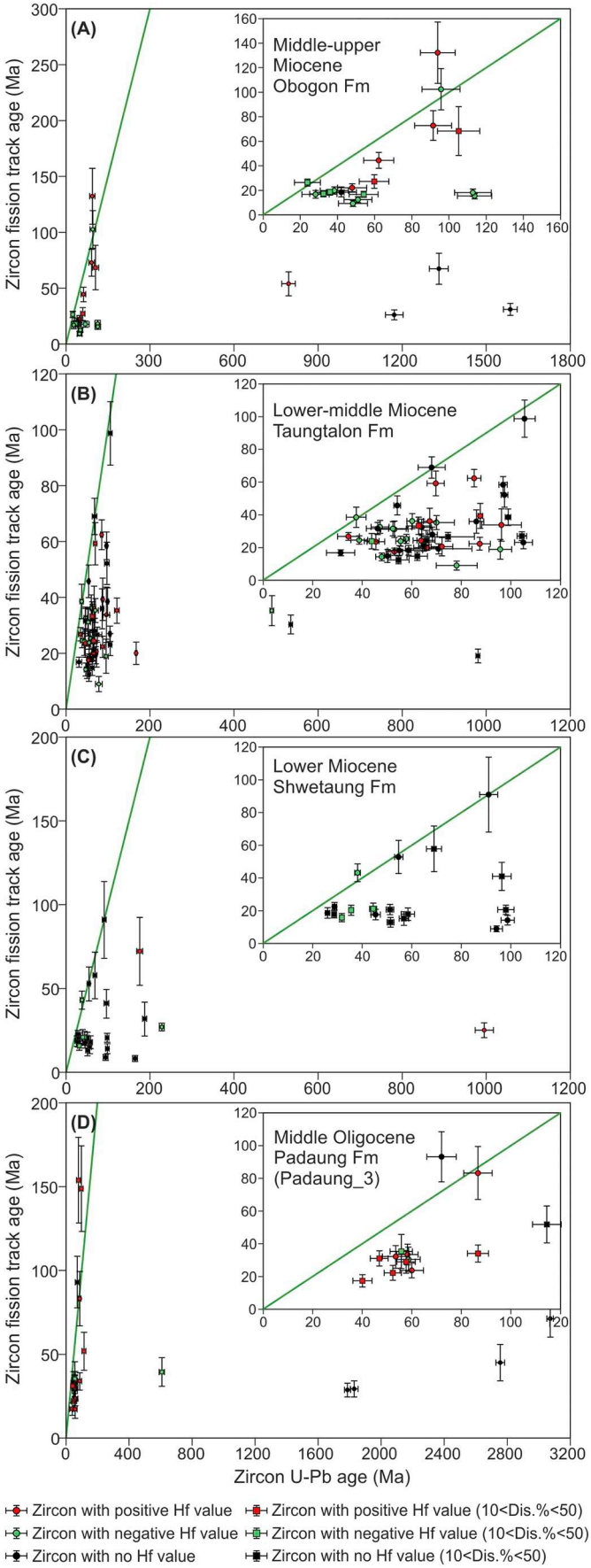

Fig. 13. Zircons, double dated with fission track and U-Pb techniques. Hf analyses were also carried out on these grains. We only discriminate between positive (red symbols) and negative (green symbols) values here, since this is the point of interest in this study. Absolute values can be found in Table TSM3 in Supplementary material 4. Data are from the unpublished thesis of Brezina (2014).

typical of the Bomi-Chayu batholiths than the Gangdese Transhimalaya (Figs. 9, 10C and 20, basal panel). Lang and Huntington (2014) suggested that the time of increase of such a population could date the timing of reversal of the Parlung River that drains the Bomi-Chayu region. Govin et al. (2018) recorded a major increase in the Early Cretaceous population between the top of their studied section at ca. 800 ka, and the modern Siang River (Fig. 20). They therefore proposed that the proposed Parlung-Siang drainage reversal occurred after 800 ka.

3.2.4. *The palaeodrainage of the Yarlung Tsangpo*

In Section 3.2.3, we summarised the evidence that the Yarlung Tsangpo did not flow into the Bay of Bengal prior to Miocene times (Bracciali et al., 2015). We have made the argument, above (Section 3.2.2), that the Yarlung Tsangpo did not flow into the Irrawaddy. Therefore, what was the drainage route of the Yarlung Tsangpo during the Paleogene, prior to its routing into the Bay of Bengal?

Due to the lack of Paleogene deposits preserved in the Yarlung suture zone, it is difficult to speculate on the Paleogene palaeodrainage of the basin. Unlike some previous workers (see Sections 3.1 and 3.2.1), we do not believe that there is strong evidence to refute the hypothesis of Clark et al. (2004) that the Yarlung Tsangpo once drained into the palaeo-Red River, potentially via a connected palaeo-Mekong / Salween. Available data provide no evidence, but such data are very limited. Likewise, the likelihood that the Yarlung Tsangpo previously connected to the palaeo-Mekong and/or palaeo-Salween Rivers unconnected to a palaeo-Red River is difficult to assess due to lack of data. One potential palaeo-Mekong repository has been identified in the Jinggu Basin (Wissink et al., 2016). Here, Cenozoic sedimentary rocks with poor age constraint but believed to stretch from Eocene to Miocene, show no evidence of detrital zircons, which is distinctive of the modern Yarlung Tsangpo (Fig. 10C). Clark et al. (2004), speculate that the upper Salween may have been a tributary to the upper Mekong, and in such a scenario, the data from the Jinggu Basin would therefore rule out a Yarlung-Mekong/Salween connection.

An alternative palaeodrainage scenario (Fig. 21), that we favour in view of (1) the published geology of the Yarlung Tsangpo suture zone, and (2) the lack of evidence that the Yarlung ever flowed into the palaeo-Red/Mekong/Salween, is that during the Paleogene the Indus–Yarlung Suture Zone, which is today the upland drainage of the Yarlung Tsangpo, was an internally drained basin between the Himalayas and the Gangdese arc (Fig. 21A and B). Such an internal basin model has already, debatably (Clift et al., 2001; Najman, 2006; Wu et al., 2007) been proposed for the palaeo–Indus River in the equivalent suture zone in the western Himalayas (Sinclair and Jaffey, 2001; Henderson et al., 2010); Sinclair and Jaffey (2001) and Henderson et al. (2010) proposed initial development of an axial Indus River not until post–Late Oligocene–earliest Miocene (< 24 Ma). For the upper Oligocene-Miocene conglomerates that extend along the Yarlung Tsangpo suture zone in the east, most workers (e.g. Carrapa et al., 2014, DeCelles et al., 2011, Leary et al., 2016a, 2016b; Li et al., 2017) interpret an internally drained basin for the early deposits, debatably passing up into axial eastward-draining fluvial facies up-section (Fig. 21C); the outlier is Wang et al. (2013) who propose that the early drainage initially flowed west, but their palaeocurrent data is incorporated into an overall eastward-draining axial river model by Leary et al. (2016b), who also caution on the use of palaeocurrent indicators in that highly deformed location. Such a through–going axial river was

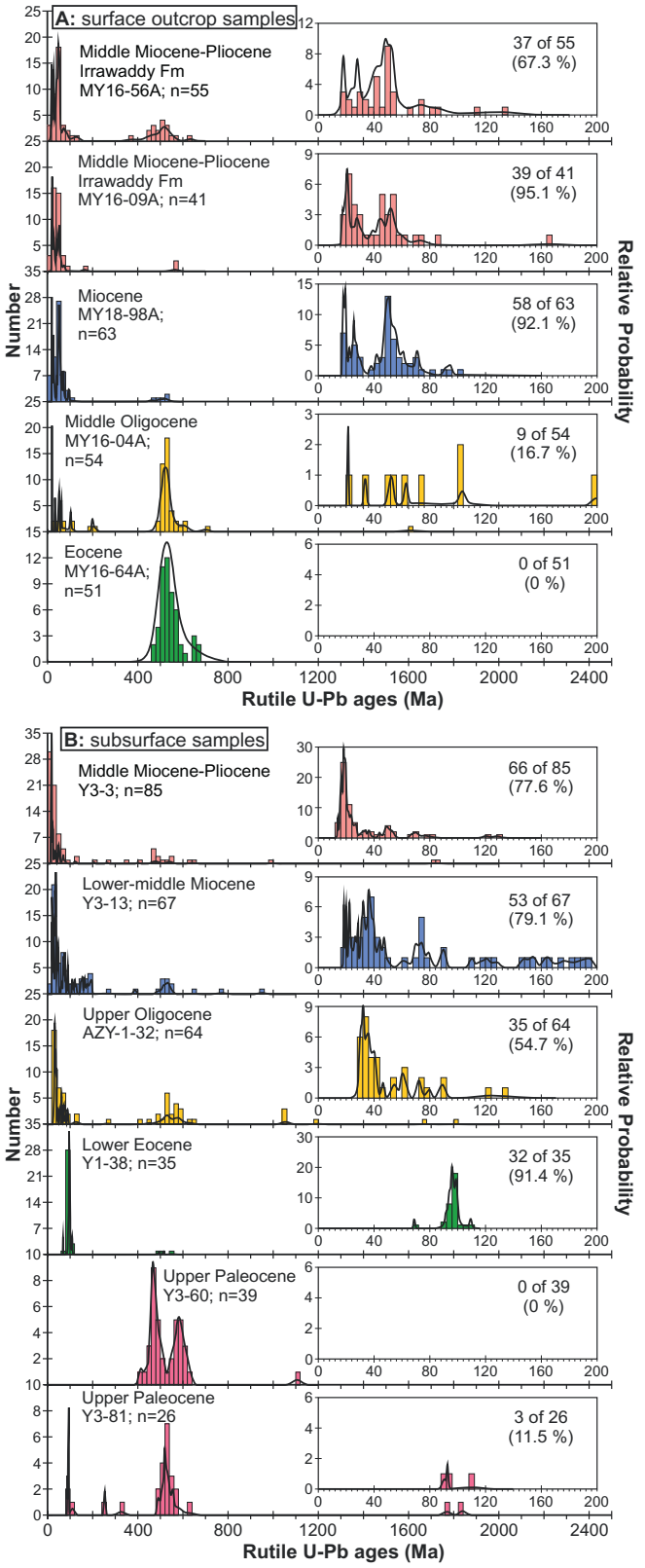

Fig. 14. U-Pb data of detrital rutile from surface outcrop (A) and subsurface (B) samples from the Central Myanmar Basin plotted as relative probability and frequency plots. Insets display detailed U-Pb age spectra in the range of 0–200 Ma. The age assignments are further constrained by the zircon U-Pb data in Fig. 10B. The age of the Oligocene outcrop sample is further constrained by the nearby tuff (see Figure caption 10 for detail).

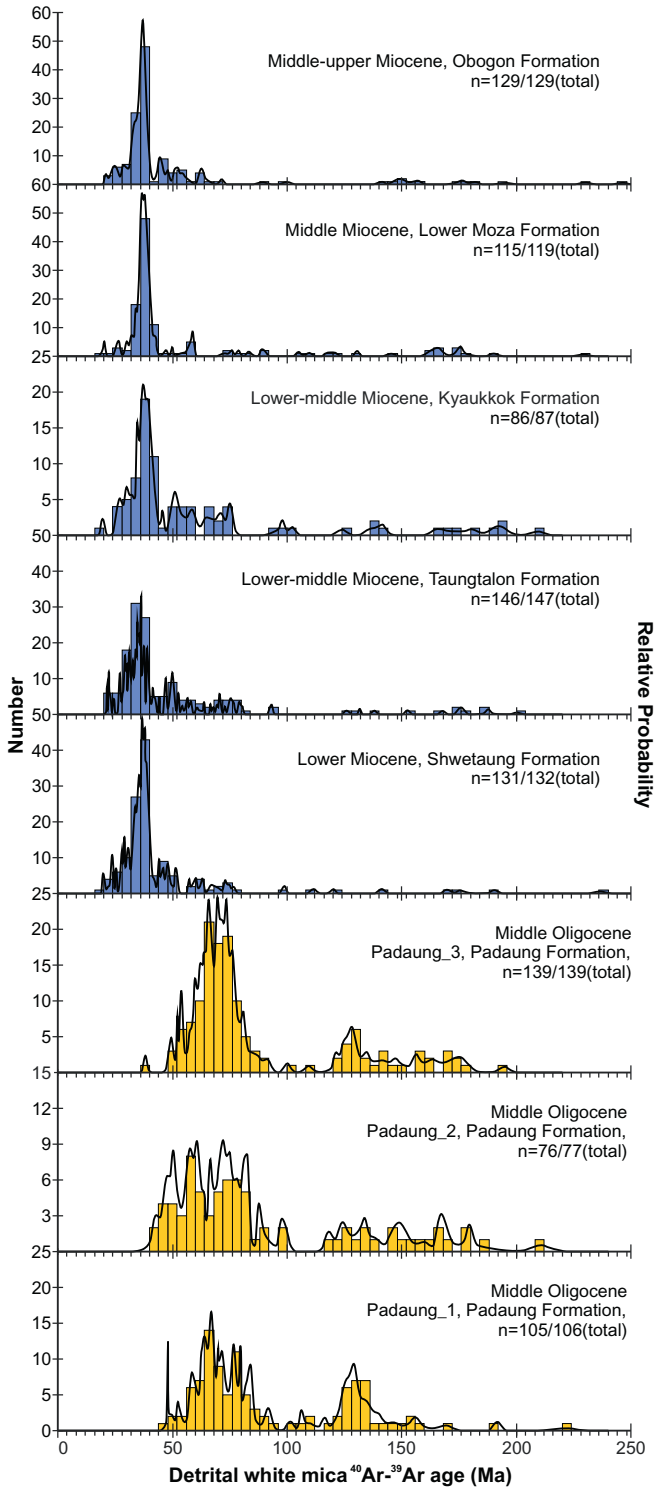

Fig. 15. ^{40}Ar–^{39}Ar data (< 250 Ma) of detrital mica samples from Central Myanmar Basin plotted as relative probability and frequency plots. Data are reproduced from the unpublished PhD thesis of Brezina (2014).

proposed to be established in the Miocene as a response to development of the Himalayan Great Counter Thrust (Wang et al., 2013; Li et al., 2017), and/or to uplift and exhumation of the India–Asia suture zone after Indian slab break–off (DeCelles et al., 2011; Carrapa et al., 2014; Leary et al., 2016a,b). The first arrival of palaeo-Yarlung–derived sediments documented in the eastern Himalayan foreland in the Early Miocene (e.g. Bracciali et al., 2015), is broadly compatible with the

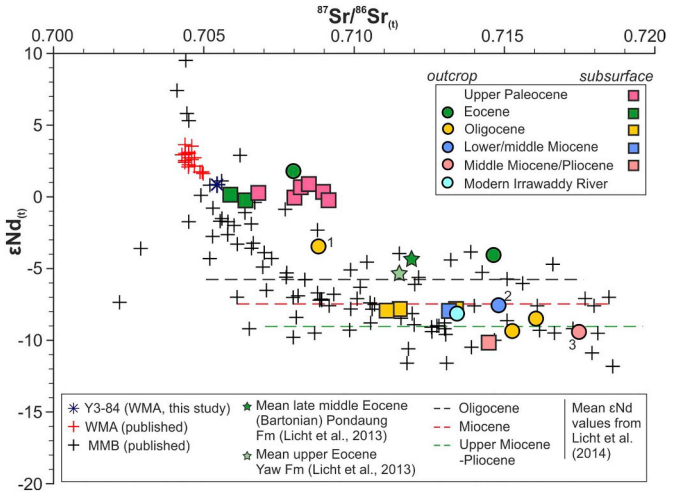

Fig. 16. Neodymium (εNd) and strontium ($^{87}Sr/^{86}Sr$) data for surface outcrop (at t = 0) and subsurface (at t = time of deposition) for mudstones from the Central Myanmar Basin. End members shown are data from sample Y3–84 from WMA igneous bedrock (this study) and published $\varepsilon Nd_{(t)}$ and $^{87}Sr/^{86}Sr_{(t)}$ values from the WMA (Mitchell et al., 2012 and Lee et al., 2016); data of the MMB are from Yang et al. (2006, 2009), Xu et al. (2008), Zhu et al. (2009), Lin et al. (2012), Mitchell et al. (2012), Wang et al. (2014c, 2015a, 2015b), Ma et al. (2014), Zhao et al. (2016a,b, 2017); values are plotted for the time of emplacement. The average values for late middle Eocene (Bartonian) Pondaung Fm and upper Eocene Yaw Fm (Licht et al., 2013) are marked. Note that the depositional ages of surface outcrop samples marked with numbers are from Licht et al. (2014): 1–lower Oligocene Shwezataw Fm; 2–lower Miocene Pyawbwe Fm; and 3–middle to upper Miocene lower Irrawaddy Fm. Dashed lines have been used to convey the data of Licht et al. (2014) as no Sr data are available.

onset of eastward–flowing through–drainage of the palaeo–Yarlung River since the Early–Middle Miocene.

4. Synthesis of the current "state of the art", and looking ahead

Use of a proposed major drainage reorganisation within the region encompassing the catchments of the major East Asian Rivers, to constrain the tectonics of the eastern Tibet margin (Clark et al., 2004), is an attractive approach. Nevertheless, alternatives exist to explain the unusual drainage configuration which focus more on horizontal shear rather than uplift and drainage captures as a mechanism to explain the geomorphology (e.g. Hallet and Molnar, 2001); furthermore, there is some debate as to whether it is a necessity that the high-elevation low-relief landscape formed prior to uplift (e.g. Yang et al., 2015; Cao et al., 2018).

Testing the drainage capture model, by proving the existence of the proposed river captures using sedimentary provenance studies, is an approach advocated by Clark et al. (2004). The above paper is a summary of the "state of the art" in this respect.

Provenance studies in the region of study are hampered by the paucity of well-dated sedimentary records of the palaeo-Red River. Offshore records are typically complex to interpret due to the potential of mixed source region input. The onshore records are fragmentary (e.g. Hoang et al., 2009), poorly dated, and particularly lacking for the all-important Paleogene time period. The Hanoi Basin, with its near complete Cenozoic sedimentary record, seems to be the perfect palaeo-Red River repository for further work, and the one study that has managed to access subsurface outcrop samples from this region shows a change at the end of Eocene which would be consistent with a river capture of middle Yangtze away from a previously-larger palaeo-Red River (Clift et al., 2006a). Yet further access to similar samples has so far, unfortunately, not been possible and is an avenue that would be

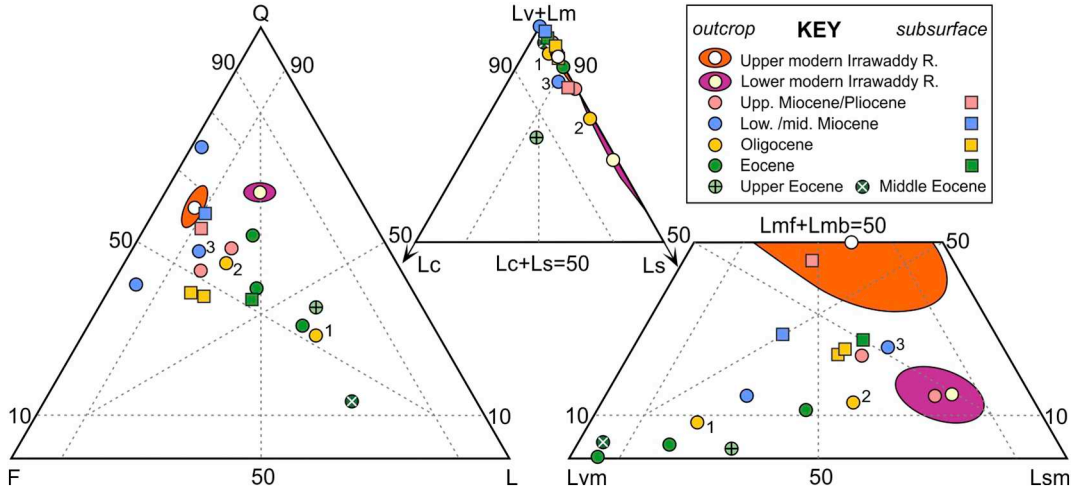

Fig. 17. Petrography of samples from the Central Myanmar Basin. Modern Irrawaddy River data are from Garzanti et al. (2016). Q = quartz, F-feldspar, L = total lithic fragments, Lc = carbonate lithic fragments, Lv = volcanic lithic fragments, Lm = metamorphic lithic fragments, Ls = sedimentary clastic (non-carbonate) lithic fragments, Lvm = volcanic + low metamorphic grade metavolcanic lithics, Lsm = sedimentary + low-metamorphic grade metasedimentary lithics, Lmf = high metamorphic grade felsic lithic fragments, Lmb = high metamorphic grade mafic lithic fragments. Note that the depositional ages of surface outcrop samples marked with numbers are made with reference to Licht et al. (2014): 1-lower Oligocene Shwezataw Fm; 2-upper Oligocene Okmintaung Fm; 3-lower Miocene Pyawbwe Fm.

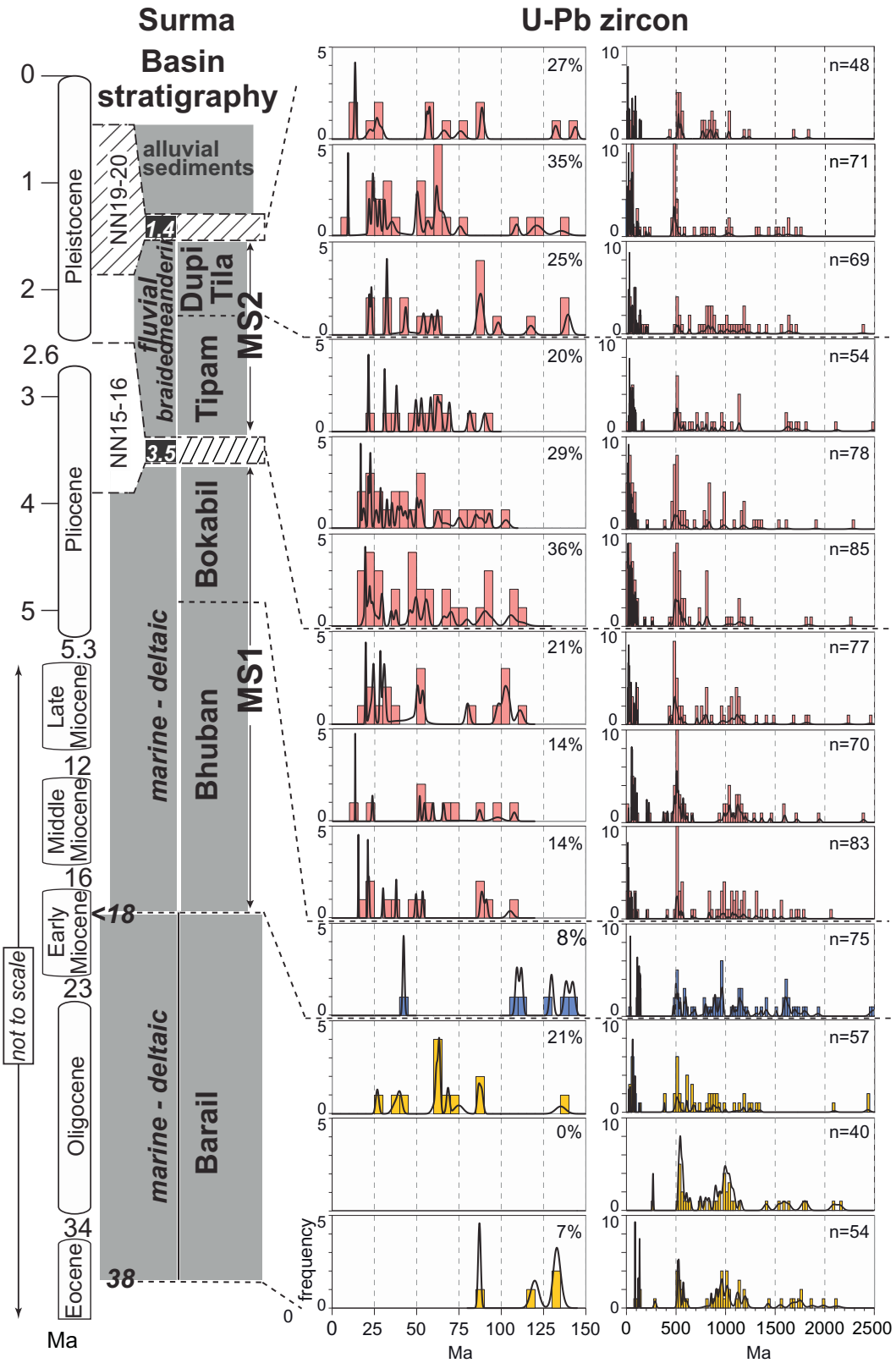

Fig. 18. In the Bengal Basin, documentation of a significant population of zircons of Cretaceous-Paleogene age, derived from the Transhimalaya, in sedimentary rocks of early Miocene age, records the time that the palaeo-Yarlung first flowed into the Brahmaputra in the Bay of Bengal. Figure modified from Bracciali et al. (2015).

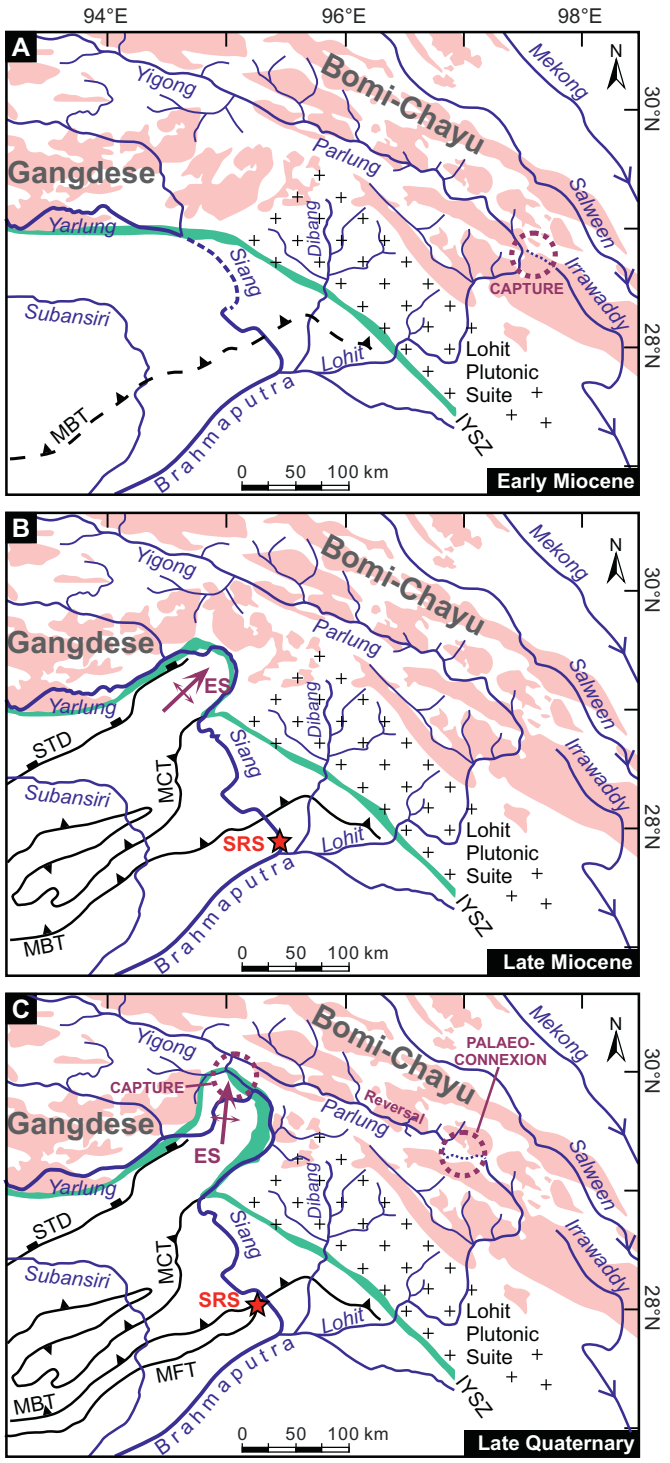

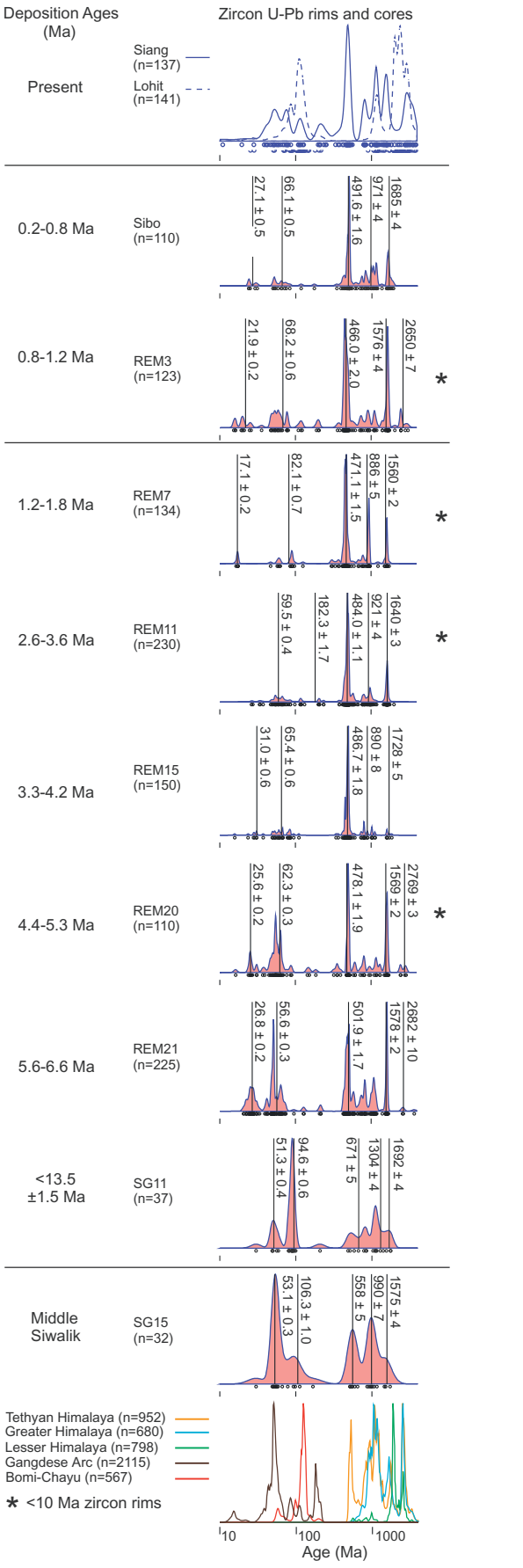

Fig. 19. Proposed palaeodrainage scenario showing the details of the routing by which the Yarlung Tsangpo entered the Himalayan foreland. ES = Eastern Himalayan Syntaxis; MBT = Main Boundary Thrust; STD = South Tibetan Detachment; MFT = Main Frontal Thrust; IYSZ = Indus-Yarlung Suture Zone; SRS shows the location of the studied rocks at the Sibo, Remi and Siang localities. Modified from Govin et al. (2018).

(caption on next page)

Fig. 20. Detrital zircon U-Pb data from the Siwalik sedimentary record in the easternmost region of the Himalayan foreland basin. The increase in Bomi-Chayu-derived Early Cretaceous grains between the uppermost Siwalik sample and the modern day Siang indicates that the Parlung River drainage reversal into the Siang occurred after ca. 800 ka. Modified from Govin et al. (2018).

very fruitful to explore, should access to more samples and detailed information on depositional age data be granted.

Keeping in mind the above limitations, there seems little non-contradictory sedimentary provenance evidence to support a palaeo-Red River of continental dimensions, from research undertaken so far:

- Some studies, particularly, but not only, using the detrital zircon U-Pb technique, have proposed palaeo-connections between the upper Yangtze/Salween/Mekong and the palaeo-Red River. However, seen in the broader context, the evidence does not seem strong (e.g. Wissink et al., 2016). We conclude that the limited data from the Hanoi Basin, showing a provenance change which may be related to middle Yangtze river flow reversal at the end of the Eocene (Clift et al., 2006a), is the strongest line of evidence to date.
- Likewise, the Yarlung-Irrawaddy-Red River branch of the system shows little evidence of a prior connection. It is now well-established that in the early Miocene the Yarlung started to flow into the Bay of Bengal (Bracciali et al., 2015). In this paper we integrate our new data with previous data to construct a palaeodrainage model, consistent with all available data, in which the Yarlung did not flow into the Irrawaddy prior to the start of its drainage into the Bay of Bengal. Instead we propose that (1) the Yarlung suture zone along which the river flows was an internally-drained basin in the Paleogene and (2) the Central Myanmar Basin along which the Irrawaddy River flows today consisted of locally-derived sediments in the Eocene, with a through-flowing Irrawaddy river draining from the Mogok Metamorphic Belt to the north, initiated some time in the Late Eocene to Early Oligocene, establishing itself as a river of stable provenance, similar to present day, by the start of the Miocene. Currently there is no evidence that the palaeo-Yarlung flowed into the palaeo-Red, but this comment relies only on comparisons with a very limited dataset from the palaeo-Red River sediment repositories, as discussed above.

In summary, we consider there is currently insufficient sedimentary evidence to be confident of the hypothesis that a palaeo-Red River of continental proportions previously existed. With some exceptions (e.g. Kong et al., 2012), a number of researchers consider that if a palaeo-Red River of continental proportions ever existed at all, it must have fragmented early in the Cenozoic. This would be consistent with the growing body of evidence that suggests that parts of eastern Tibet were uplifted by Paleocene-Eocene times (Hoke et al., 2014; Li et al., 2015). Nevertheless, if river reorganisations occurred post-uplift (Yang et al., 2015) later captures would be equally plausible. Furthermore, if drainage reorganisation did occur, and took place early in the Cenozoic, prior to or synchronous with uplift, what is the relationship between these events and regional river incision, which is documented, predominantly (e.g. Clark et al., 2005; Ouimet et al., 2010; Tian et al., 2015), as occurring in Miocene times? These questions, and the mechanisms responsible for these events, remain debated (e.g. Liu-Zeng et al., 2018).

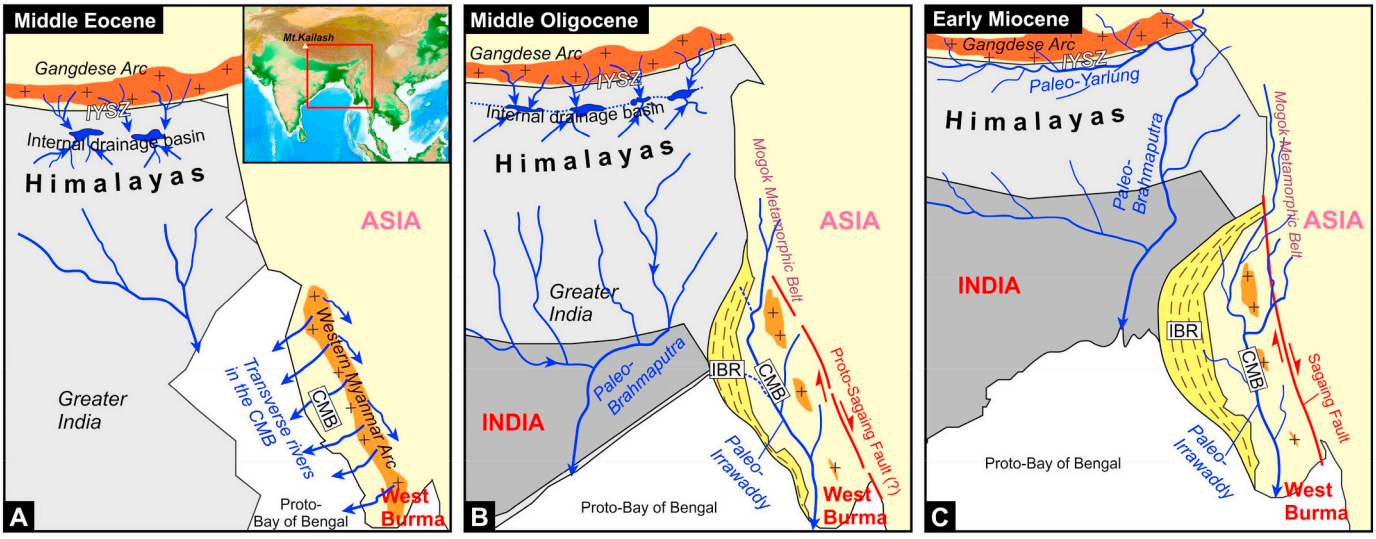

Fig. 21. Schematic reconstruction of palaeo–drainage in Myanmar and the India–Asian collision zone for the Cenozoic. (A) The Indus-Yarlung Suture Zone basin is internally-drained and the Central Myanmar Basin is filled with WMA arc-derived deposits and is open to the ocean to the west. The Brahmaputra drains only the Indian plate southern slopes of the Himalaya. (B) By this time, the Indo-Burman Ranges have risen to create a valley side for the CMB, and the Irrawaddy River has initiated, draining from the Mogok Metamorphic Belt and Bomi-Chayu granites to the north. (C) The Yarlung Tsangpo becomes a through-flowing river, connecting via the Brahmaputra to the Bay of Bengal; the Irrawaddy attains a stable palaeodrainage pattern similar to present day. IYSZ, Indus–Yarlung Suture Zone; CMB, Central Myanmar Basin; IBR, Indo-Burman Ranges. Tectonic reconstructions of Myanmar and the Indian Plate are based on Hall (2012).

Supplementary data to this article can be found online at https://doi.org/10.1016/j.earscirev.2019.02.003.

Acknowledgements

This work was financially supported by the National Science and Technology Major Project of China (2011ZX05030-002-003 and 2016ZX05026-003-001), an Open Research Foundation of KLTPR (grant TPR–2016–20 to PZ) and a Funding Program of International Exchanges and Cooperation for Graduate Students at CUG awarded to PZ. Hf analyses at Bristol were funded by NERC grant NE/K008862/1 to BD. Lancaster University is thanked for their support during the one year exchange programme. Thanks are due to Vassil Karloukovski (Lancaster University) for sample preparation, to Angus Calder (St Andrews University) for mudstone ICP–MS analysis and to Ruth Robinson for discussion on Brezina's PhD thesis. Santa Maria Travels and Tours, Mya Min Din and Zaw Win Htwe, are thanked for logistical assistance in Myanmar. We thank Editor Shuhab Khan and reviewers Peter Clift and Joel Saylor, for detailed and constructive comments which improved the quality of this manuscript.

References

Allen, R., Najman, Y., Carter, A., Barfod, D., Bickle, M.J., Chapman, H.J., Garzanti, E., Vezzoli, G., Andò, S., Parrish, R., 2008. Provenance of the tertiary sedimentary rocks of the Indo–Burman Ranges, Burma (Myanmar): Burman arc or Himalayan–derived? J. Geol. Soc. 165, 1045–1057. https://doi.org/10.1144/0016-76492007-143.

Bao, C., Chen, Y.L., Bu, X.F., Chen, X., Li, D.P., 2015. LA-ICP-MS U-Pb ages and Hf isotopic compositions of detrital zircons in the sediments of the Nujiang River, Yunnan Province, and their geological significance. Geol. Bull. China 34, 1413–1425 (in Chinese with English abstract).

Barley, M.E., Pichard, A.L., Khin, Zaw., Pak, P., Doyle, M.G., 2003. Jurassic to Miocene magmatism and metamorphism in the Mogok metamorphic belt and the India–Eurasia collision in Myanmar. Tectonics 22 (1019). https://doi.org/10.1029/2002TC001398.

Bender, F., 1983. Geology of Burma. Borntraeger, Berlin. (293 pp.).

Bertrand, G., Rangin, C., 2003. Tectonics of the western margin of the Shan plateau (Central Myanmar): implication for the India–Indochina oblique convergence since the Oligocene. J. Asian Earth Sci. 21, 1139–1157. https://doi.org/10.1016/S1367-9120(02)00183–9.

Bertrand, G., Rangin, C., Maluski, H., Bellon, H., Scientific Party, G.I.A.C., 2001. Diachronous cooling along the Mogok Metamorphic Belt (Shan scarp, Myanmar): the trace of the northward migration of the Indian syntaxis. J. Asian Earth Sci. 19, 649–659. https://doi.org/10.1016/S1367-9120(00)00061-4.

Blum, M., Rogers, K., Gleason, J., Najman, Y., Cruz, J., Fox, L., 2018. Allogenic and autogenic controls in the stratigraphic record of the Deep-Sea Bengal Fan. Sci. Rep. 8 (7973). https://doi.org/10.1038/s41598-018-25819-5.

Bodet, F., Schärer, U., 2000. Evolution of the SE–Asian continent from U–Pb and Hf isotopes in single grains of zircon and baddeleyite from large rivers. Geochim. Cosmochim. Acta 64, 2067–2091. https://doi.org/10.1016/S0016-7073(00)00352-5.

Bodet, F., Schärer, U., 2001. Pb isotope systematics and time-integrated Th-U of SE-Asian continental crust recorded by single K-feldspar grains in large rivers. Chem. Geol. 177, 265–285. https://doi.org/10.1016/S0009-2541(00)00413-7.

Booth, A.L., Zeitler, P.K., Kidd, W.S.F., Wooden, J., Liu, Y.P., Idleman, B., Hren, M., Chamberlain, C.P., 2004. U-Pb zircon constraints on the tectonic evolution of southeastern Tibet, Namche Barwa Area. Am. J. Sci. 304, 889–929. https://doi.org/10.2475/ajs.304.10.889.

Bracciali, L., Najman, Y., Parrish, R.R., Akhter, S.H., Millar, I., 2015. The Brahmaputra tale of tectonics and erosion: Early Miocene river capture in the Eastern Himalaya. Earth Planet. Sci. Lett. 415, 25–37. https://doi.org/10.1016/j.epsl.2015.01.022.

Brezina, C.A., 2014. The Detrital Mineral Record of Cenozoic Sedimentary Rocks in the Central Burma Basin: Implications for the Evolution of the Eastern Himalayan Orogen and Timing of Large Scale River Capture. Unpublished PhD thesis. St Andrews University, UK.

Brookfield, M.E., 1998. The evolution of the great river systems of southern Asia during the Cenozoic India–Asia collision: rivers draining southwards. Geomorphology 22, 285–312. https://doi.org/10.1016/S0169-555X(97)00082-2.

Bruguier, O., Lancelot, J.R., Malavieille, J., 1997. U-Pb dating on single detrital zircon grains from the Triassic Songpan-Ganze flysch (Central China): provenance and tectonic correlations. Earth Planet. Sci. Lett. 152, 217–231. https://doi.org/10.1016/S0012-821X(97)00138-6.

Cao, L.C., Jiang, T., Wang, Z.F., Zhang, Y.Z., Sun, H., 2015. Provenance of Upper Miocene sediments in the Yinggehai and Qiongdongnan basins, northwestern South China Sea: evidence from REE, heavy minerals and zircon U-Pb ages. Mar. Geol. 361, 136–146. https://doi.org/10.1016/j.margeo.2015.01.007.

Cao, L.C., Shao, L., Qiao, P.J., Zhao, Z.G., van Hinsbergen, D.J.J., 2018. Early Miocene birth of modern Pearl River recorded low-relief, high-elevation surface formation of SE Tibetan Plateau. Earth Planet. Sci. Lett. 496, 120–131. https://doi.org/10.1016/j.epsl.2018.05.039.

Carrapa, B., Orme, D.A., DeCelles, P.G., Kapp, P., Cosca, M.A., Waldrip, R., 2014. Miocene burial and exhumation of the India–Asia collision zone in southern Tibet: response to slab dynamics and erosion. Geology 42, 443–446. https://doi.org/10.1130/G35350.1.

Castelltort, S., Goren, L., Willett, S.D., Champagnac, J.D., Herman, F., Braun, J., 2012. River drainage patterns in the New Zealand Alps primarily controlled by plate tectonic strain. Nat. Geosci. 5, 744–748. https://doi.org/10.1038/NGEO1582.

Chen, X., 2015. U-Pb Dating and Hf Isotopic Composition of Detrital Zircons in the Sediments from Three Rivers in Southwestern China and its Geological Significance. Master Degree Thesis. China University of Geosciences, China.

Chen, X., Chen, Y.L., Bao, C., Li, G.Q., Yan, J.P., Li, D.P., 2014. U-Pb dating and Hf isotopic composition of detrital zircons in the sediments from the Lancang River and its geological significance. Geoscience 28, 1170–1182 (in Chinese with English abstract).

Chen, X.J., Xu, Z.Q., Sein, Kyaing, Meng, Y.K., Cai, Z.H., 2016. The Early Cretaceous tectonic magmatism in the Mogok District, Central Myanmar, and its implication for the Evolution of. Tethys. Acta Geol. Sin. 90, 3060–3080 (in Chinese with English abstract).

Chen, Y., Yana, M.D., Fang, X.M., Song, C.H., Zhang, W.L., Zan, J.B., Zhang, Z.G., Li, B.S., Yang, Y.P., Zhang, D.W., 2017. Detrital zircon U–Pb geochronological and sedimentological study of the Simao Basin, Yunnan: Implications for the Early Cenozoic evolution of the Red River. Earth Planet. Sci. Lett. 476, 22–33. https://doi.org/10.1016/j.epsl.2017.07.025.

Chiu, H.Y., Chung, S.L., Wu, F.Y., Liu, D., Liang, Y.H., Lin, I.J., Iizuka, Y., Xie, L.W., Wang, Y., Chu, M.F., 2009. Zircon U–Pb and Hf isotopic constraints from eastern Transhimalayan batholiths on the precollisional magmatic and tectonic evolution in southern Tibet. Tectonophysics 477, 3–19. https://doi.org/10.1016/j.tecto.2009.02.034.

Chu, M.F., Chung, S.L., Song, B., Liu, D.Y., O'Reilly, S.Y., Pearson, N.J., Ji, J.Q., Wen, D.R., 2006. Zircon U–Pb and Hf isotope constraints on the Mesozoic tectonics and crustal evolution of southern Tibet. Geology 34, 745–748. https://doi.org/10.1130/G22725.1.

Cina, S.E., Yin, A., Grove, M., Dubey, C.S., Shukla, D.P., Lovera, O.M., Kelty, T.K., Gehrels, G.E., Foster, D.A., 2009. Gangdese arc detritus within the eastern Himalayan Neogene foreland basin: Implications for the Neogene evolution of the Yalu–Brahmaputra River system. Earth Planet. Sci. Lett. 285, 150–162. https://doi.org/10.1016/j.epsl.2009.06.005.

Clark, M.K., Schoenbohm, L.M., Royden, L.H., Whipple, K.X., Burchfiel, B.C., Zhang, X., Tang, W., Wang, E., Chen, L., 2004. Surface uplift, tectonics, and erosion of eastern Tibet from large–scale drainage patterns. Tectonics 23https://doi.org/10.1029/2002TC001402.. TC1006.

Clark, M.K., House, M.A., Royden, L.H., Whipple, K., Burchfiel, B.C., Zhang, X., Tang, T., 2005. Late Cenozoic uplift of southeastern Tibet. Geology 33, 525–558. https://doi.org/10.1130/G21265.1.

Clift, P.D., Shimizu, N., Layne, G.D., Blusztajn, J., 2001. Tracing patterns of erosion and drainage in the Paleogene Himalaya through ion probe Pb isotope analysis of detrital K-feldspars in the Indus Molasse, India. Earth Planet. Sci. Lett. 188, 475–491. https://doi.org/10.1016/S0012-821X(01)00346-6.

Clift, P.D., Layne, G.D., Blusztajn, J., 2004. Marine sedimentary evidence for monsoon strengthening, Tibetan uplift and drainage evolution in East Asia. In: Clift, P.D., Kuknt, W., Wang, P.X., Hayes, D. (Eds.), Continent-Ocean Interactions within East Asian Marginal Seas. American Geophysical Union, Geophysical Monograph, vol. 149. pp. 255–282.

Clift, P.D., Blusztain, J., Duc, N.A., 2006a. Large-scale drainage capture and surface uplift in eastern Tibet-SW China before 24 Ma inferred from sediments of the Hanoi Basin, Vietnam. Geophys. Res. Lett. 33https://doi.org/10.1029/2006GL027772. L19403.

Clift, P.D., Carter, A., Campbell, H.I., Pringle, M.S., Lap, N.V., Allen, C.M., Hodges, K.V., Tan, M.H., 2006b. Thermochronology of mineral grains in the Red and Mekong Rivers, Vietnam: provenance and exhumation implications for Southeast Asia. Geochem. Geophys. Geosyst. 7https://doi.org/10.1029/2006GC001336. Q10005.

Clift, P.D., van Long, H., Hinton, R., Ellam, R.M., Hannigan, R., Tan, M.T., Blusztajn, J., Duc, N.A., 2008. Evolving East Asian river systems reconstructed by trace element and Pb and Nd isotope variations in modern and ancient Red River-Song Hong sediments. Geochem. Geophys. Geosyst. 9https://doi.org/10.1029/2007GC001867. Q04039.

Curray, J.R., Moore, D.G., Lawver, L.A., Emmel, F.J., Raitt, R.W., Henry, M., Kieckhefer, R., 1979. Tectonics of the Andaman Sea and Burma. In: Watkins, J., Montadert, L., Dickerson, P.W. (Eds.), Geological and geophysical investigations of continental margins. American Association of Petroleum Geologists, Memoirs, vol. 29. pp. 189–198.

Davis, S.J., Dickinson, W.R., Gehrels, G.E., Spencer, J.E., Lawton, T.F., Carroll, A.R., 2010. The Paleogene California River: evidence of Mojave-Uinta paleodrainage from U-Pb ages of detrital zircons. Geology 38, 31–934. https://doi.org/10.1130/G31250.1.

DeCelles, P.G., Kapp, P., Quade, J., Gehrels, G.E., 2011. Oligocene–Miocene Kailas basin, southwestern Tibet: record of postcollisional upper–plate extension in the Indus–Yarlung suture zone. Geol. Soc. Am. Bull. 123, 1337–1362. https://doi.org/10.1130/B30258.1.

Dickinson, W.R., 1985. Interpreting provenance relations from detrital modes of sandstones. In: Zuffa, G.G. (Ed.), Provenance of Arenites. Reidel Publishing Company, Boston, pp. 333–361. https://doi.org/10.1007/978-94-017-2809-6_15.

Dickinson, W.R., Gehrels, G.E., 2009. Use of U–Pb ages of detrital zircons to infer maximum depositional ages of strata: a test against a Colorado Plateau Mesozoic database. Earth Planet. Sci. Lett. 288, 115–125. https://doi.org/10.1016/j.epsl.2009.09.013.

Ding, L., Yang, D., Cai, F.L., Pullen, A., Kapp, P., Gehrels, G.E., Zhang, L.Y., Zhang, Q.H., Lai, Q.Z., Yue, Y.H., Shi, R.D., 2013. Provenance analysis of the Mesozoic Hoh-Xil-Songpan-Ganzi turbidites in northern Tibet: Implications for the tectonic evolution of the eastern Paleo-Tethys Ocean. Tectonics 32, 34–48. https://doi.org/10.1002/tect.20013.

Gardiner, N.J., Hawkesworth, C.J., Robb, L.J., Whitehouse, M.J., Roberts, N.M.W., Kirkland, C.L., Evans, N.J., 2017. Contrasting granite metallogeny through the zircon record: a case study from Myanmar. Sci. Rep. 7 (748). https://doi.org/10.1038/s41598-017-00832-2.

Gardiner, N.J., Searle, M.P., Morley, C.K., Robb, L.J., Whitehouse, M.J., Roberts, N.M.W., Kirkland, C.I., Spencer, C.J., 2018. The crustal architecture of Myanmar imaged through zircon U-Pb, Lu-Hf and O isotopes: Tectonic and metallogenic implications. Gondwana Res. 62, 27–60. https://doi.org/10.1016/j.gr.2018.02.008.

Garzanti, E., Wang, J.G., Vezzoli, G., Limonta, M., 2016. Tracing provenance and sediment fluxes in the Irrawaddy River basin (Myanmar). Chem. Geol. 440, 73–90. https://doi.org/10.1016/j.chemgeo.2016.06.010.

Gough, A., Hall, R., 2017. Oligocene fluvio-deltaic depositional environments Salin Sub-Basin, Central Myanmar. In: American Geophysical Union Fall Meeting 2017, New Orleans, Abstract #EP21F-1904.

Gourbet, L., Leloup, P.H., Paquette, J.L., Sorrel, P., Maheo, G., Wang, G.C., Xu, Y.D., Cao, K., Antoine, P.O., Eymard, I., Liu, W., Lu, H.J., Replumaz, A., Chevalier, M.L., Zhang, K.X., Wu, J., Shen, T.Y., 2017. Reappraisal of the Jianchuan Cenozoic basin stratigraphy and its implications on the SE Tibetan plateau evolution. Tectonophysics 700-701, 162–179. https://doi.org/10.1016/j.tecto.2017.02.007.

Govin, G., Najman, Y., Dupont-Nivet, G., Millar, I., van der Beek, P., Huyghe, P., O'Sullivan, P., Mark, C., Vögell, N., 2018. The tectonics and paleo-drainage of the easternmost Himalaya (Arunachal Pradesh, India) recorded in the Siwalik rocks of the foreland basin. Am. J. Sci. 318, 764–798. https://doi.org/10.2475/07.2018.02.

Guo, L.S., Liu, Y.L., Liu, S.W., Cawood, P.A., Wang, Z.H., Liu, H.F., 2013. Petrogenesis of Early to Middle Jurassic granitoid rocks from the Gangdese belt, Southern Tibet: Implications for early history of the Neo-Tethys. Lithos 179, 320–333. https://doi.org/10.1016/j.lithos.2013.06.011.

Hall, R., 2012. Late Jurassic–Cenozoic reconstructions of the Indonesian region and the Indian Ocean. Tectonophysics 570–571, 1–41. https://doi.org/10.1016/j.tecto.2012.04.021.

Hallet, B., Molnar, P., 2001. Distorted drainage basins as markers of crustal strain east of the Himalaya. J. Geophys. Res. Solid Earth 106, 13697–13709. https://doi.org/10.1029/2000JB900335.

Harrison, T.M., Célérier, J., Aikman, A.B., Hermann, J., Heizler, M.T., 2009. Diffusion of ^{40}Ar in muscovite. Geochim. Cosmochim. Acta 73, 1039–1051. https://doi.org/10.1016/j.gca.2008.09.038.

He, M.Y., Zheng, H.B., Clift, P.D., 2013. Zircon U-Pb geochronology and Hf isotope data from the Yangtze River sands: implications for major magmatic events and crustal evolution in Central China. Chem. Geol. 360-361, 186–203. https://doi.org/10.1016/j.chemgeo.2013.10.020.

Henderson, A.L., Najman, Y., Parrish, R., BouDagher-Fadel, M., Barford, D., Garzanti, E., Andò, S., 2010. Geology of the Cenozoic Indus Basin sedimentary rocks: paleoenvironmental interpretation of sedimentation from the western Himalaya during the early phases of India–Eurasia collision. Tectonics 29https://doi.org/10.1029/2009TC002651. TC6015.

Hennig, J., Breitfeld, H.T., Gough, A., Hall, R., Long, T.V., Kim, V.M., Quang, S.D., 2018. U-Pb zircon ages and provenance of upper Cenozoic sediments from the Da Lat Zone, SE Vietnam: Implications for an intra-Miocene unconformity and paleo-drainage of the proto–Mekong River. J. Sediment. Res. 88, 495–515. https://doi.org/10.2110/jsr.2018.26.

Hoang, L.V., Wu, F.Y., Clift, P.D., Wysocka, A., Swierczewska, A., 2009. Evaluating the evolution of the Red River system based on in situ U–Pb dating and Hf isotope analysis of zircons. Geochem. Geophys. Geosyst. 10https://doi.org/10.1029/2009GC002819. Q11008.

Hoke, G.D., Liu-Zeng, J., Hren, M.T., Wissink, G.K., Garzione, C.N., 2014. Stable isotopes reveal high southeast Tibetan Plateau margin since the Paleogene. Earth Planet. Sci. Lett. 394, 270–278. https://doi.org/10.1016/j.epsl.2014.03.007.

Hu, X.M., Sinclair, H.D., Wang, J.G., Jiang, H.H., Wu, F.Y., 2012. Late Cretaceous-Paleogene stratigraphic and basin evolution in the Zhepure Mountains of southern Tibet: implications for the timing of India-Asia initial collision. Basin Res. 24, 1–24. https://doi.org/10.1111/j.1365-2117.2012.00543.

Ji, W.Q., Wu, F.Y., Chung, S.L., Li, J.X., Liu, C.Z., 2009. Zircon U–Pb geochronology and Hf isotopic constraints on petrogenesis of the Gangdese batholith, southern Tibet. Chem. Geol. 262, 229–245. https://doi.org/10.1016/j.chemgeo.2009.01.020.

Jonell, T.N., Clift, P.D., Hoang, L.V., Hoang, T., Carter, A., Wittmann, H., Böning, P., Pahnke, K., Rittenour, T., 2017. Controls on erosion patterns and sediment transport in amonsoonal, tectonically quiescent drainage, Song Gianh, Central Vietnam. Basin Res. 29, 659–683. https://doi.org/10.1111/bre.12199.

Kong, P., Zheng, Y., Caffee, M.W., 2012. Provenance and time constraints on the formation of the first bend of the Yangtze River. Geochem. Geophys. Geosyst. 13https://doi.org/10.1029/2012GC004140. Q06017.

Kooijman, E., Mezger, K., Berndt, J., 2010. Constraints on the U–Pb systematics of metamorphic rutile from in situ LA-ICP-MS analysis. Earth Planet. Sci. Lett. 293, 321–330. https://doi.org/10.1016/j.epsl.2010.02.047.

Lang, K.A., Huntington, K.W., 2014. Antecedence of the Yarlung–Siang–Brahmaputra River, eastern Himalaya. Earth Planet. Sci. Lett. 397, 145–158. https://doi.org/10.1016/j.epsl.2014.04.026.

Lang, K.A., Huntington, K.W., Burmester, R., Housen, B., 2016. Rapid exhumation of the eastern Himalayan syntaxis since the late Miocene. Geol. Soc. Am. Bull. 128, 1403–1422. https://doi.org/10.1130/B31419.1.

Leary, R.J., DeCelles, P.G., Quade, J., Gehrels, G.E., Waanders, G., 2016a. The Liuqu Conglomerate, southern Tibet: Early Miocene basin development related to deformation within the Great Counter Thrust system. Lithosphere 8, 427–450. https://doi.org/10.1130/L542.1.

Leary, R.J., Orme, D.A., Laskowski, A.K., DeCelles, P.G., Kapp, P., Carrapa, B., Dettinger, M., 2016b. Along-strike diachroneity in deposition of the Kailas Formation in central southern Tibet: implications for Indian slab dynamics. Geosphere 12, 1198–1223. https://doi.org/10.1130/GES01325.1.

Lee, H.Y., Chung, S.L., Yang, H.M., 2016. Late Cenozoic volcanism in Central Myanmar: Geochemical characteristics and geodynamic significance. Lithos 245, 174–190. https://doi.org/10.1016/j.lithos.2015.09.018.

Li, R.Y., Mei, L.F., Zhu, G.H., Zhao, R.M., Xu, X.M., Zhao, H.X., Zhang, P., Yin, Y.P., Ma, Y.X., 2013. Late Mesozoic to Cenozoic tectonic events in volcanic arc, West Burma Block: evidences from U–Pb zircon dating and apatite fission track data of granitoids. J. Earth Sci. 24, 553–568. https://doi.org/10.1007/s12583-013-0349-7.

Li, S.Y., Currie, B.S., Rowley, D.B., Ingalls, M., 2015. Cenozoic paleoaltimetry of the SE margin of the Tibetan Plateau: constraints on the tectonic evolution of the region. Earth Planet. Sci. Lett. 432, 415–424. https://doi.org/10.1016/j.epsl.2015.09.044.

Li, S., Ding, L., Xu, Q., Wang, H.Q., Yue, Y.H., Baral, U., 2017. The evolution of Yarlung Tsangpo River: constraints from the age and provenance of the Gangdese Conglomerates, southern Tibet. Gondwana Res. 41, 249–266. https://doi.org/10.1016/j.gr.2015.05.010.

Liang, Y.H., Chung, S.L., Liu, D.Y., Xu, Y.G., Wu, F.Y., Yang, J.H., Wang, Y., Lo, C.H., 2008. Detrital zircon evidence from Burma for reorganization of the eastern Himalayan river system. Am. J. Sci. 308, 618–638. https://doi.org/10.2475/04.2008.08.

Licht, A., France–Lanord, C., Reisberg, L., Fontaine, C., Soe, A.N., Jaeger, J.J., 2013. A palaeo Tibet–Myanmar connection? Reconstructing the Late Eocene drainage system of central Myanmar using a multi–proxy approach. J. Geol. Soc. 170, 929–939. https://doi.org/10.1144/jgs2012-126.

Licht, A., Reisberg, L., France–Lanord, C., Naing Soe, A., Jaeger, J.J., 2014. Cenozoic evolution of the central Myanmar drainage system: insights from sediment provenance in the Minbu Sub–Basin. Basin Res. 28, 237–251. https://doi.org/10.1111/bre.12108.

Licht, A., Dupont-Nivet, G., Win, Zaw, Swe, Hnin Hnin, Kaythi, Myat, Roperch, P., Ugrai, T., Littell, V., Park, D., Westerweel, J., Jones, D., Poblete, F., Aung, Day Wa, Huang, H.S., Hoorn, C., Sein, Kyaing, 2018. Paleogene evolution of the Burmese forearc basin and implications for the history of India-Asia convergence. Geol. Soc. Am. Bull. https://doi.org/10.1130/B35002.1.

Lin, T.H., Lo, C.H., Chung, S.L., Hsu, F.J., Yeh, M.W., Lee, T.Y., Ji, J.Q., Wang, Y.Z., Liu, D.Y., 2009. ^{40}Ar/^{39}Ar dating of the Jiali and Gaoligong shear zones: implications for crustal deformation around the Eastern Himalayan Syntaxis. J. Asian Earth Sci. 34, 674–685. https://doi.org/10.1016/j.jseaes.2008.10.009.

Lin, I.J., Chung, S.L., Chu, C.H., Lee, H.Y., Gallet, S., Wu, G.Y., Ji, J.Q., Zhang, Y.Q., 2012. Geochemical and Sr–Nd isotopic characteristics of Cretaceous to Paleocene granitoids and volcanic rocks, SE Tibet: petrogenesis and tectonic implications. J. Asian Earth Sci. 53, 131–150. https://doi.org/10.1016/j.jseaes.2012.03.010.

Lin, T.H., Chung, S.L., Tang, J.T., Oo, T., 2017. The delimitation between the mature and juvenile crustal provinces in SE Asia: insights from detrital zircon U-Pb and Hf isotopic data for the Salween drainage, Myanmar. J. Asian Earth Sci. 145, 641–651. https://doi.org/10.1016/j.jseaes.2017.06.018.

Liu, C., Clift, P.D., Murray, R.W., Blusztajn, J., Ireland, T., Wan, S.M., Ding, W.W., 2017. Geochemical evidence for initiation of the modern Mekong delta in the southwestern South China Sea after 8 Ma. Chem. Geol. 451, 38–54. https://doi.org/10.1016/j.chemgeo.2017.01.008.

Liu-Zeng, J., Zhang, J., McPhillips, D., Reiners, P., Wang, W., Pik, R., Zeng, L., Hoke, G., Xie, K., Xiao, P., Zheng, D., Ge, Y., 2018. Multiple episodes of fast exumation since Cretaceous in southeast Tibet, revealed by low-temperature thermochronology. Earth Planet. Sci. Lett. 490, 62–76. https://doi.org/10.1016/j.epsl.2018.03.011.

Ma, L.Y., Wang, Y.J., Fan, W.M., Geng, H.Y., Cai, Y.F., Zhong, H., Liu, H.C., Xing, X.W., 2014. Petrogenesis of the early Eocene I-type granites in west Yingjiang (SW Yunnan) and its implication for the eastern extension of the Gangdese batholiths. Gondwana Res. 25, 401–419. https://doi.org/10.1016/j.gr.2013.04.010.

Maurin, T., Rangin, C., 2009. Structure and kinematics of the Indo–Burmese wedge: recent and fast growth of the outer wedge. Tectonics 28https://doi.org/10.1029/2008TC002276. TC2010.

Meng, Y.K., Xu, Z.Q., Santosh, M., Ma, X.X., Chen, X.J., Guo, G.L., Liu, F., 2016. Late Triassic crustal growth in southern Tibet: evidence from the Gangdese magmatic belt. Gondwana Res. 37, 449–464. https://doi.org/10.1016/j.gr.2015.10.007.

Meng, Y.K., Dong, H.W., Cong, Y., Xu, Z.Q., Cao, H., 2017. The early-stage evolution of the Neo-Tethys Ocean: evidence from granitoids in the middle Gangdese batholith, southern Tibet. J. Geodyn. 94–95, 34–49. https://doi.org/10.1016/j.jog.2016.01.003.

Metcalfe, I., 1996. Pre-Cretaceous evolution of SE Asian terranes. Geol. Soc. Lond. Spec. Publ. 106, 97–122. https://doi.org/10.1144/GSL.SP.1996.106.01.09.

Mitchell, A., Chung, S.L., Oo, T., Lin, T.H., Hung, C.H., 2012. Zircon U–Pb ages in Myanmar: Magmatic–metamorphic events and the closure of a neo–Tethys ocean. J. Asian Earth Sci. 56, 1–23. https://doi.org/10.1016/j.jseaes.2012.04.019.

Morley, C.K., 2012. Late Cretaceous–Early Palaeogene tectonic development of SE Asia. Earth Sci. Rev. 115, 37–75. https://doi.org/10.1016/j.earscirev.2012.08.002.

Naing, T.T., Bussuen, D.A., Winkler, W.H., Nold, M., Von Quadt, A., 2014. Provenance study on Eocene–Miocene sandstones of the Rakhine Coastal Belt, Indo–Burman Ranges of Myanmar: geodynamic implications. Scott, R.A., Smyth, H.R., Morton, A. C., Richardson, N. (Eds.), Sediment Provenance Studies in Hydrocarbon Exploration and Production. Geological Society, London, Special Publications, vol. 386, pp. 195–216. doi:https://doi.org/10.1144/SP386.10.

Najman, Y., 2006. The detrital record of orogenesis: a review of approaches and

techniques used in the Himalayan sedimentary basins. Earth Sci. Rev. 74, 1–72. https://doi.org/10.1016/j.earscirev.2005.04.004.
Nie, J.S., Ruetenik, G., Gallagher, K., Hoke, G., Garzione, C.N., Wang, W.T., Stockli, D., Hu, X.F., Wang, Z., Wang, Y., Stevens, T., Danišík, M., Liu, S.P., 2018. Rapid incision of the Mekong River in the middle Miocene linked to monsoonal precipitation. Nat. Geosci. 11, 944–948. https://doi.org/10.1038/s41561-018-0244-z.
Oo, K.L., Zaw, K., Meffre, S., Aung, D.W., Lai, C.K., 2015. Provenance of the Eocene sandstones in the southern Chindwin Basin, Myanmar: implications for the unroofing history of the Cretaceous–Eocene magmatic arc. J. Asian Earth Sci. 107, 172–194. https://doi.org/10.1016/j.jseaes.2015.04.029.
Ouimet, W., Whipple, K., Royden, L., Reiners, P., Hodges, K., Pringle, M., 2010. Regional incision of the eastern margin of the Tibetan Plateau. Lithosphere 2, 50–63. https://doi.org/10.1130/L57.1.
Pan, G.T., Wang, L.Q., Li, R.S., Yuan, S.H., Ji, W.H., Yin, F.G., Zhang, W.P., Wang, B.D., 2012. Tectonic evolution of the Qinghai–Tibet plateau. J. Asian Earth Sci. 53, 3–14. https://doi.org/10.1016/j.jseaes.2011.12.018.
Pivnik, D.A., Nahm, J., Tucker, S., Smith, G.O., Nyein, K., Nyunt, M., Maung, P.H., 1998. Polyphase deformation in a fore–arc/back–arc basin, Salin Subbasin, Myanmar (Burma). Am. Assoc. Pet. Geol. Bull. 82, 1837–1856. https://doi.org/10.1306/1D9BD15F-172D-11D7-8645000102C1865D.
Rahn, M.K., Brandon, M.T., Batt, G.E., Garver, J.I., 2004. A zero-damage model for fission-track annealing in zircon. Am. Mineral. 89, 473–484. https://doi.org/10.2138/am-2004-0401.
Robinson, R.A.J., Brezina, C.A., Parrish, R.R., Horstwood, M.S.A., Oo, N.W., Bird, M.I., Thein, M., Walters, A.S., Oliver, G.J.H., Zaw, K., 2014. Large rivers and Orogens: the evolution of the Yarlung Tsangpo–Irrawaddy system and the eastern Himalayan syntaxis. Gondwana Res. 26, 112–121. https://doi.org/10.1016/j.gr.2013.07.002.
Searle, M.P., Noble, S.R., Cottle, J.M., Waters, D.J., Mitchell, A.H.G., Hlaing, Tin, Horstwood, M.S.A., 2007. Tectonic evolution of the Mogok metamorphic belt, Burma (Myanmar) constrained by U–Th–Pb dating of metamorphic and magmatic rocks. Tectonics 26https://doi.org/10.1029/2006TC002083. TC3014.
Searle, M.P., Morley, C.K., Waters, D.J., Gardiner, N.J., Kyi Htun, U., Than Than, Nu, Robb, L.J., 2017. Chapter 12: Tectonic and metamorphic evolution of the Mogok Metamorphic and Jade Mines belts and ophiolitic terranes of Burma (Myanmar). In: Barber, A.J., Zaw, Khin, Crow, M.J. (Eds.), Myanmar: Geology, Resources and Tectonics. vol. 48. Geological Society, London, Memoirs, pp. 261–293. https://doi.org/10.1144/M48.12.
Sinclair, H.D., Jaffey, N., 2001. Sedimentology of the Indus Group, Ladakh, northern India: implications for the timing of initiation of the palaeo–Indus River. J. Geol. Soc. 158, 151–162. https://doi.org/10.1144/jgs.158.1.151.
Singh, S.K., France-Lanord, C., 2002. Tracing the distribution of erosion in the Brahmaputra watershed from isotopic compositions of stream sediments. Earth Planet. Sci. Lett. 202, 645–662. https://doi.org/10.1016/S0012-821X(02)00822-1.
Tang, Y., Zhang, Y.P., Tong, L.L., 2018. Mesozoic-Cenozoic evolution of the Zoige depression in the Songpan-Ganzi flysch basin, eastern Tibetan Plateau: Constraints from detrital zircon U-Pb ages and fission-track ages of the Triassic sedimentary sequence. J. Asian Earth Sci. 151, 285–300. https://doi.org/10.1016/j.jseaes.2017.10.021.
Tapponnier, P., Peltzer, G., Le Dain, A.Y., Armijo, R., Cobbold, P., 1982. Propagating extrusion tectonics in Asia: new insights from simple experiments with plasticine. Geology 10, 611–616. https://doi.org/10.1130/0091-7613(1982)10<611:PETIAN>2.0.CO;2.
Tian, Y., Kohn, B.P., Hu, S., Gleadow, A.J.W., 2015. Synchronous fluvial response to surface uplift in the eastern Tibetan Plateau: implications for crustal dynamics. Geophys. Res. Lett. 42, 29–35 (doi:2014GL062383).
Vermeesch, P., 2009. RadialPlotter: a Java application for fission track, luminescence and other radial plots. Radiat. Meas. 44, 409–410. https://doi.org/10.1016/j.radmeas.2009.05.003.
Vermeesch, P., 2018. IsoplotR: a free and open toolbox for geochronology. Geosci. Front. 9, 1479–1493. https://doi.org/10.1016/j.gsf.2018.04.001.
Wang, Y.J., Fan, W.M., Zhang, Y.H., Peng, T.P., Chen, X.Y., Xu, Y.G., 2006. Kinematics and $^{40}Ar/^{39}Ar$ geochronology of the Gaoligong and Chongshan shear systems, western Yunnan, China: implications for early Oligocene tectonic extrusion of SE Asia. Tectonophysics 418, 235–254. https://doi.org/10.1016/j.tecto.2006.02.005.
Wang, J.G., Hu, X.M., Wu, F.Y., Jansa, L., 2010. Provenance of the Liuqu conglomerate in southern Tibet: a Paleogene erosional record of the Himalayan-Tibetan orogen. Sediment. Geol. 231, 74–84. https://doi.org/10.1016/j.sedgeo.2010.09.004.
Wang, J.G., Hu, X.M., Garzanti, E., Wu, F.Y., 2013. Upper Oligocene–Lower Miocene Gangrinboche Conglomerate in the Xigaze area, southern Tibet: implications for Himalayan uplift and paleo–Yarlung–Zangbo initiation. J. Geol. 121, 425–444. https://doi.org/10.1086/670722.
Wang, C., Liang, X.Q., Xie, H.Y., Tong, C.X., Pei, J.X., Zhou, Y., Jiang, Y., Fu, J.G., Dong, C.G., Liu, P., 2014a. Provenance of Upper Miocene to Quaternary sediments in the Yinggehai-Song Hong Basin, South China Sea: evidence from detrital zircon U–Pb ages. Mar. Geol. 355, 202–217. https://doi.org/10.1016/j.margeo.2014.06.004.
Wang, J.G., Wu, F.Y., Tan, X.C., Liu, C.Z., 2014b. Magmatic evolution of the Western Myanmar Arc documented by U–Pb and Hf isotopes in detrital zircon. Tectonophysics 612, 97–105. https://doi.org/10.1016/j.tecto.2013.11.039.
Wang, Y.J., Zhang, L.M., Cawood, P.A., Ma, L.Y., Fan, W.M., Zhang, A.M., Zhang, Y.Z., Bi, X.W., 2014c. Eocene supra-subduction zone mafic magmatism in the Sibumasu Block of SW Yunnan: Implications for Neotethyan subduction and India–Asia collision. Lithos 206-207, 384–399. https://doi.org/10.1016/j.lithos.2014.08.012.
Wang, R., Richards, J.P., Zhou, L.M., Hou, Z.Q., Stern, R.A., Creaser, R.A., Zhu, J.J., 2015a. The role of Indian and Tibetan lithosphere in spatial distribution of Cenozoic magmatism and porphyry Cu–Mo deposits in the Gangdese belt, southern Tibet. Earth Sci. Rev. 150, 68–94. https://doi.org/10.1016/j.earscirev.2015.07.003.
Wang, Y.J., Li, S.B., Ma, L.Y., Fan, W.M., Cai, Y.F., Zhang, Y.H., Zhang, F.F., 2015b. Geochronological and geochemical constraints on the petrogenesis of Early Eocene metagabbroic rocks in Nabang (SW Yunnan) and its implications on the Neotethyan slab subduction. Gondwana Res. 27, 1474–1486. https://doi.org/10.1016/j.gr.2014.01.007.
Wang, C., Liang, X., Foster, D.A., Xie, Y., Tong, C., Pei, J., Fu, J., Jiang, Y., Dong, C., Zhou, Y., 2016. Zircon U-Pb geochronology and heavy mineral composition constraints on the provenance of the middle Miocene deep-water reservoir sedimentary rocks in the Yinggehai–Song Hong Basin, South China Sea. Mar. Pet. Geol. 77, 819–834. https://doi.org/10.1016/j.marpetgeo.2016.05.009.
Wang, C., Liang, X.Q., Foster, D.A., Tong, C.X., Liu, P., Liang, X.R., Zhang, L., 2019. Linking source and sink: Detrital zircon provenance record of drainage systems in Vietnam and the Yinggehai–Song Hong Basin, South China Sea. Geol. Soc. Am. Bull. 131, 191–204. https://doi.org/10.1130/B32007.1.
Weislogel, A.L., Graham, S.A., Chang, E.Z., Wooden, J.L., Gehrels, G.L., Yang, H.S., 2006. Detrital zircon provenance of the Late Triassic Songpan-Ganzi complex: sedimentary record of collision of the North and South China blocks. Geology 34, 97–100. https://doi.org/10.1130/G21929.
Wen, D.R., Liu, D.Y., Chung, S.L., Chu, M.F., Ji, J.Q., Zhang, Q., Song, B., Lee, T.Y., Yeh, M.W., Lo, C.H., 2008. Zircon SHRIMP U–Pb ages of the Gangdese Batholith and implications for Neotethyan subduction in southern Tibet. Chem. Geol. 252, 191–201. https://doi.org/10.1016/j.chemgeo.2008.03.003.
Whipple, K.X., Tucker, G.E., 1999. Dynamics of the stream-power river incision model: Implications for height limits of mountain ranges, landscape response timescales, and research needs. J. Geophys. Res. Solid Earth 104, 661–674. https://doi.org/10.1029/1999JB900120.
Wissink, G.K., Hoke, G.D., Garzione, C.N., Liu-Zeng, J., 2016. Temporal and spatial patterns of sediment routing across the southeast margin of the Tibetan Plateau: Insights from detrital zircon. Tectonics 35, 2538–2563. https://doi.org/10.1002/2016TC004252.
Wu, F.Y., Clift, P.D., Yang, J.H., 2007. Zircon Hf isotopic constraints on the sources of the Indus Molasse, Ladakh Himalaya, India. Tectonics 26https://doi.org/10.1029/2006TC002051. TC2014.
Xie, Y.H., Tong, C.X., Pei, J.X., Liu, P., Liang, X.Q., Wang, C., Zhou, Y., Jiang, Y., Wen, S., Fu, J.G., Yu, S.H., Xiang, J.H., 2016a. Detrital zircon ages and reservoir source of the Second Member of the Huangliu Formation in the Yinggehai Basin. Geotectonic et Metallogenia 40, 517–530. https://doi.org/10.16539/j.ddgzyckx.2016.03.009. (in Chinese with English abstract).
Xie, J.C., Zhu, D.C., Dong, G.C., Zhao, Z.D., Wang, Q., Mo, X.X., 2016b. Linking the Tengchong Terrane in SW Yunnan with the Lhasa Terrane in southern Tibet through magmatic correlation. Gondwana Res. 39, 217–229. https://doi.org/10.1016/j.gr.2016.02.007.
Xu, Y.G., Lan, J.B., Yang, Q.J., Huang, X.L., Qiu, H.N., 2008. Eocene break-off of the Neo-Tethyan slab as inferred from intraplate-type mafic dykes in the Gaoligong orogenic belt, eastern Tibet. Chem. Geol. 255, 439–453. https://doi.org/10.1016/j.chemgeo.2008.07.016.
Xu, Z.Q., Wang, Q., Cai, Z.H., Dong, D.W., Li, H.Q., Chen, X.J., Duan, X.D., Cao, H., Li, J., Burg., J.P., 2015. Kinematics of the Tengchong Terrane in SE Tibet from the late Eocene to early Miocene: insights from coeval mid-crustal detachments and strike-slip shear zones. Tectonophysics 665, 127–148. doi:https://doi.org/10.1016/j.tecto.2015.09.033.
Yan, Y., Carter, A., Palk, C., Brichau, S., Hu, X.Q., 2011. Understanding sedimentation in the Song Hong–Yinggehai Basin, South China Sea. Geochem. Geophys. Geosyst. 12https://doi.org/10.1029/2011GC003533. Q06014.
Yan, Y., Carter, A., Huang, C.Y., Chan, L.S., Hu, X.Q., Lan, Q., 2012. Constraints on Cenozoic regional drainage evolution of SW China from the provenance of the Jianchuan Basin. Geochem. Geophys. Geosyst. 13https://doi.org/10.1029/2011gc003803. Q03001.
Yang, Q.J., Xu, Y.G., Huang, X.L., Luo, Z.Y., 2006. Geochronology and geochemistry of granites in the Gaoligong tectonic belt, western Yunnan: Tectonic implications. Acta Petrol. Sin. 817-834, 22 (In Chinese with English abstract).
Yang, Q.J., Xu, Y.G., Huang, X.L., Luo, Z.Y., Shi, Y.R., 2009. Geochronology and geochemistry of granites in the Tengliang area, western Yunnan: tectonic implication. Acta Petrol. Sin. 25, 1092–1104 (In Chinese with English abstract).
Yang, S.Y., Zhang, F., Wang, Z.B., 2012. Grain size distribution and age population of detrital zircons from the Changjiang (Yangtze) river system, China. Chem. Geol. 296–297, 26–38. https://doi.org/10.1016/j.chemgeo.2011.12.016.
Yang, R., Willett, S.D., Goren, L., 2015. In situ low-relief landscape formation as a result of river network disruption. Nature 520, 526–528. https://doi.org/10.1038/nature14354.
Yang, R., Fellin, M.G., Herman, F., Willett, S.D., Wang, W., 2016. Spatial and temporal pattern of erosion in the three Rivers Region, southeastern Tibet. Earth Planet. Sci. Lett. 433, 10–20. https://doi.org/10.1016/j.epsl.2015.10.032.
Zeitler, P.K., Meltzer, A.S., Koons, P.O., Craw, D., Hallet, B., Chamberlain, C.P., Kidd, W.S.F., Park, S., Seeber, L., Bishop, M.L., Shroder, J., 2001. Erosion, Himalayan geodynamics, and the geology of metamorphism. GSA Today 11, 4–8. https://doi.org/10.1130/1052-5173(2001)011<0004:EHGATG>2.0.CO;2.
Zhang, Z.M., Liou, J.G., Coleman, R.G., 1985. An outline of the plate tectonics of China. Geol. Soc. Am. Bull. 95, 295–312. https://doi.org/10.1130/0016-7606(1984)95<295:AOOTPT>2.0.CO;2.
Zhang, J.Y., Yin, A., Liu, W.C., Wu, F.Y., Lin, D., Grove, M., 2012. Coupled U-Pb dating and Hf isotopic analysis of detrital zircon of modern river sand from the Yalu River (Yarlung Tsangpo) drainage system in southern Tibet: Constraints on the transport processes and evolution of Himalayan rivers. Geol. Soc. Am. Bull. 124, 1449–1473. https://doi.org/10.1130/B30592.1.
Zhang, Y.X., Tang, X.C., Zhang, K.J., Zeng, L., Gao, C.L., 2014a. U-Pb and Lu-Hf isotope systematics of detrital zircons from the Songpan-Ganzi Triassic flysch, NE Tibetan

Plateau: implications for provenance and crustal growth. Int. Geol. Rev. 56, 29–56. https://doi.org/10.1080/00206814.2013.818754.
Zhang, Z.J., Tyrrell, S., Li, C.A., Daly, J.S., Sun, X.L., Li, Q.W., 2014b. Pb isotope compositions of detrital K-feldspar grains in the upper-middle Yangtze River system: implications for sediment provenance and drainage evolution. Geochem. Geophys. Geosyst. 15, 2765–2779. https://doi.org/10.1002/2014GC005391.
Zhang, Z.J., Daly, J.S., Li, C.A., Tyrrell, S., Sun, X.L., Yan, Y., 2017a. Sedimentary provenance constraints on drainage evolution models for SE Tibet: evidence from detrital K-feldspar. Geophys. Res. Lett. 44, 4064–4073. https://doi.org/10.1002/2017GL073185.
Zhang, J.E., Xiao, W.J., Windley, B.F., Cai, F.L., Sein, K., Naing, S., 2017b. Early Cretaceous wedge extrusion in the Indo–Burma Range accretionary complex: implications for the Mesozoic subduction of Neotethys in SE Asia. Int. J. Earth Sci. 106, 1391–1408. https://doi.org/10.1007/s00531-017-1468-7.
Zhang, P., Mei, L.F., Hu, X.L., Li, R.Y., Wu, L.L., Zhou, Z.C., Qiu, H.N., 2017c. Structures, uplift, and magmatism of the Western Myanmar Arc: constraints to mid–Cretaceous–Paleogene tectonic evolution of the western Myanmar continental margin. Gondwana Res. 52, 18–38. https://doi.org/10.1016/j.gr.2017.09.002.
Zhao, M., Shao, L., Liang, J.S., Li, Q.Y., 2015. No Red River capture since the late Oligocene: Geochemical evidence from the Northwestern South China Sea. Deep-Sea Res. II Top. Stud. Oceanogr. 122, 185–194. https://doi.org/10.1016/j.dsr2.2015.02.029.
Zhao, S.W., Lai, S.C., Qin, J.F., Zhu, R.Z., 2016a. Petrogenesis of Eocene granitoids and microgranular enclaves in the western Tengchong Block: constraints on eastward subduction of the Neo-Tethys. Lithos 264, 96–107. https://doi.org/10.1016/j.lithos.2016.08.025.
Zhao, S.W., Lai, S.C., Qin, J.F., Zhu, R.Z., 2016b. Tectono-magmatic evolution of the Gaoligong belt, southeastern margin of the Tibetan plateau: constraints from granitic gneisses and granitoid intrusions. Gondwana Res. 35, 238–256. https://doi.org/10.1016/j.gr.2015.05.007.
Zhao, S.W., Lai, S.C., Qin, J.F., Zhu, R.Z., Wang, J.B., 2017. Geochemical and geochronological characteristics of late cretaceous to early Paleocene granitoids in the Tengchong Block, Southwestern China: implications for crustal anatexis and thickness variations along the eastern Neo-Tethys subduction zone. Tectonophysics 694, 87–100. https://doi.org/10.1016/j.tecto.2016.11.038.
Zhu, D.C., Mo, X.X., Wang, L.Q., Zhao, Z.D., Niu, Y.L., Zhou, C.Y., Yang, Y.H., 2009. Petrogenesis of highly fractionated I-type granites in the Zayu area of eastern Gangdese, Tibet: constraints from zircon U-Pb geochronology, geochemistry and Sr-Nd-Hf isotopes. Sci. China Ser. D Earth Sci. 52, 1223–1239. https://doi.org/10.1007/s11430-009-0132-x.
Zhu, D.C., Zhao, Z.D., Niu, Y.L., Mo, X.X., Chung, S.L., Hou, Z.Q., Wang, L.Q., Wu, F.Y., 2011. The Lhasa Terrane: record of a microcontinent and its histories of drift and growth. Earth Planet. Sci. Lett. 301, 241–255. https://doi.org/10.1016/j.epsl.2010.11.005.